Preparation and physico-chemical properties of nickel nanostructured materials deposited in etched ion-track membrane

By

M.M. Nkosi

Submitted in fulfilment of the requirements for the degree of PhD in Chemistry in the Department of Chemistry, University of the Western Cape

Supervisor: Prof. V.M. Linkov November 2005

Co-supervisors: Dr. A. Nechaev and Dr. C.C. Theron

DECLARATION BY CANDIDATE

I declare that *Preparation and physico-chemical properties of nickel nanostructured materials deposited in etched ion-track membrane* is my own work, that it has not been submitted before for any degree or examination in any other university, that all the sources I have used or quoted have been indicated and acknowledged as complete references.

Mlungisi Moses Nkosi

Signed:…… Date:…….

ACKNOWLEDGEMENTS

My heartfelt gratitude goes first to The Almighty GOD in Heaven, without whom this work would have been a futile exercise.

I would like to express my great gratitude to my supervisor, Prof. Vladimir M. Linkov, for his constructive recommendations and suggestions during this study.

I would like to express the most profound and sincere gratitude to my co-supervisors, Dr. Alexander Nechaev and Dr. Chris C. Theron, for their constant encouragement, guidance, patience and invaluable instruction that contributed to the fulfillment of this work and my academic life throughout my research programme.

Thanks are due to all the members of the South African Institute of Advanced Materials Chemistry (SAIAMC) and the Department of Chemistry for their friendly support and help all round.

I would also like to express my sincere appreciation to the staff and students at the Materials Research Group, iThemba Laboratory for Accelerator Based Sciences (iThemba LABS), for their support.

Without the financial support of the National Research Foundation (NRF) this research project wouldn't have been possible.

I am extremely grateful to Nolan Botha, Miranda Waldron, Gerald Malgas and Basil Julies for the extensive help with SEM and EDS measurements.

I am also grateful to Tshepo Ntsoane for the extensive help with XRD analysis. Sincere gratitude to Lindiwe Khotseng for help with the use of the Scanning Electrochemical Microscope (SECM).

Grateful thanks are also due to Barbara Rogers and Amanda Foster for their role in keeping the laboratory organized and always being helpful.

I am also grateful to the staff of the technical and electronic workshop for their assistance in manufacturing various devices and repairing instruments.

To past and present members of the Cape Town Church of Christ, UWC Ministry, Sandro, Mmalewane, Oladele, Wilson, Palesa, Malibongwe, Minah, I express my deepest gratitude.

Huge thanks are given to my beloved family for their continuous support, understanding, encouragement and blessings; you'll never know how much your support has meant to me.

ABSTRACT

The development of finely dispersed powders and superfine-grained materials intended for application in various areas of science and engineering is one of the challenges facing modern nanotechnology. Thus, specific fundamental and applied research was required in order to consolidate advancement made in preparing nano- and submicron crystalline composite materials.

Useful templates for electrochemical deposition of nanowires include porous alumina films formed by anodic oxidation of aluminium, nuclear track-etched porous membranes, nanochannel array-glass and mesoporous channel hosts. The properties of the nanowires are directly related to the properties of the nanoporous templates such as, the relative pore orientations in the assembly, the pore size distribution, and the surface roughness of the pores. The template synthesis method, based on the use of porous polymeric and inorganic matrixes, is now actively used for synthesis of such composite materials. The method allows the chemical and/or electrochemical synthesis of nano- and microstructured tubes and wires consisting of conducting polymers, metals and semiconductors.

In this study various technological challenges relating to template synthesis and development of nickel nano- and microstructures on adequately strong and durable substrates were investigated. The two methods used were the electrochemical and chemical deposition. “Hard nickel” bath solution was used for optimal nickel deposition. This optimization included investigating variables such as the template structure, type of electrolyte and form of electrolytic deposition.

Scanning Electron Microscopy was used to investigate the structures of template matrixes and the resultant materials. The cyclic voltammetry method was applied for the analysis of electrochemical properties and hydrogen evaluation reaction of nano- and microstructured nickel based electrodes. The activity of composite nano- and microstructured materials in various configurations resulting from pore filling of template matrices by nickel was explored. Studies of the physical structure and chemical properties of the nanostructured materials included investigating the necessary parameters of template matrices. The optimum conditions of synthesis, which allowed development of materials with the highest catalytic activity, were determined. The effect of the template structure on microcrystallinity of the catalyst particles was established using the XRD

method. Different new types of non-commercial asymmetric ion track membranes has been tested for nanostructure preparation.

The catalytic activity of the new developed nanomaterials is higher as compared to materials using commercial templates. The procedures to modify the newly developed nickel catalyst with Pt, Pd and Pt-Pd alloy have been developed. The Pt and Pt-Pd alloy containing catalyst showed the best performance in water electrolysis. In this work, the promising role for specific application of the new materials in hydrogen economy has been demonstrated.

GLOSSARY OF TERMS

Alkali

A substance that creates a bitter taste and a slippery feel when dissolved in water and will turn red litmus paper blue. An alkali has a pH greater than seven and is the opposite of an acid. Highly alkaline waters tend to cause drying of the skin. Alkalis may include the soluble hydroxide, carbonate, and bicarbonate salts of calcium, magnesium, potassium and sodium. A hydroxide alkali may also be called a base.

Amperometry

An electroanalytical technique based upon the measurement of the current flowing through the working electrode of an electrochemical cell.

Anode

The electrode that has a positive potential relative to the other electrode. In an electrochemical cell this is the electrode where oxidation occurs. In a galvanic cell it is again the electrode with the highest positive potential. The current on the anode is considered a positive current according to international convention; however in electroanalytical chemistry the electron current is often used and then termed the anodic current.

Anion

A negatively charged ion.

Asymmetrical membrane

Membrane constituted of two or more structural planes of non-identical morphologies.

Cathode

The electrode that has a lower or negative potential relative to the other electrode. It is the electrode where reduction occurs in an electrochemical cell.

Cation

A positively charged ion.

Cell voltage

The electrical potential difference between two electrodes of an electrochemical cell. In case of a three-electrode cell, it is the potential difference between the working electrode and the counter electrode.

Chronoamperometry

An electrochemical measuring technique used for electrochemical analysis or for the determination of the kinetics and mechanism of electrode reactions. A fast-rising potential pulse is applied on the working electrode of an electrochemical cell and the current flowing through this electrode is measured as a function of time.

Current density

Current referred to the unit area of the electrode. Current divided by true electrode area.

Electrocatalysis

The phenomenon of increasing the rate of an electrode reaction by changing the electrode material. The rate of electrode reactions can strongly depend on the composition and morphological structure of the electrode surface. This is called the "electrocatalytic effect".

Electrochemical cell

A device that converts chemical energy into electrical energy (or vice versa) when a chemical reaction is occurring in the cell. Typically, it consists of two metal electrodes immersed into an aqueous solution (electrolyte) with electrode reactions occurring at the electrode-solution surfaces.

Electrochemical deposition

The electrodeposition process is defined as deposition in which electric current is carried across an electrolyte and a substance is deposited at one of the electrodes. It is a very powerful form of deposition which is capable of depositing over half the elements in the periodic table.

Electrochemistry

A science concerned with the properties of solutions of electrolytes and with processes occurring when electrodes are immersed in these solutions.

Electrolysis

A method by which chemical reactions are carried out by the passage of electric current through a solution of an electrolyte or through a molten salt.

Electrolyte

A chemical compound (salt, acid, or base) that dissociates into electrically charged ions when dissolved in a solvent. The resulting electrolyte (or electrolytic) solution is an ionic conductor of electricity. Very often, the so formed solution itself is simply called an “electrolyte.” Also, molten salts and molten salts solutions are often called “electrolytes” when used in electrochemical cells.

Electron

A stable elementary particle which is the negatively charged constituent of ordinary matter, having a mass of about 9.11×10^{-28}g (equivalent to 0.511 MeV), a charge of about -1.602×10^{-19} C, and a spin of $^1/_2$.

Electroplating

The process that produces a thin, metallic coating on the surface of another metal (or any other conductor, e.g. graphite). The metal substrate to be coated is made the cathode in an electrolytic cell where the cations of the electrolyte are the positive ions of the metal to be coated on the surface.

Electrosynthesis

A reaction in which synthesis occurs as the result of an electric current.

Energy

The energy of a system expresses the ability of that system to do some useful work or generate heat. Energy can take many forms; e.g., mechanical, chemical, heat, electrical, etc. The different forms of energy can be converted into each other.

Galvanic cell

An electrochemical cell that converts chemical energy into electrical energy. A cell in which chemical reactions occur spontaneously at the electrodes when they are connected through an external circuit, producing an electrical current.

High surface area materials

These are materials which have a large surface-to-volume ratio. For example, a chunk of material with the radius R has a surface-to-volume ratio of 3/R. Thus, for smaller pieces of material, the surface-to-volume ratio becomes larger. For pieces of matter on a nanometer scale (nanoparticles), the contribution of the surface to the overall properties of such matter therefore becomes important.

Hydrogen

A colourless, highly flammable gaseous element, the most abundant element on earth, is the cleanest and ideal fuel. It is increasingly considered as the fuel of the future.

Hydrogen Evolution Reaction (HER)

An electrode reaction in which hydrogen gas is produced at the cathode of an electrolytic cell by the reduction of hydrogen ions or the reduction of the water molecules of an aqueous solution.

Ion

An electrically charged chemical particle (atom, molecule, or molecule fragment).

Irradiation

The act of exposing or the condition of being exposed to radiation.

Membrane

A membrane is defined as a thin film separating two phases and acting as a selective barrier to the transport of matter. The membrane, through which mass transfer may occur under a variety of driving forces, has lateral dimensions much greater than its thickness.

Micron

A linear measure equal to one millionth of a meter. The symbol for the micron is the Greek letter "μ". The smallest particle visible to the human eye is 40 microns.

Metallizing

Is the general name for the technique of coating metal on the surface of non-metallic objects. Because a non-metallic object tends to be a poor electrical conductor, the object's surface must be made conductive before plating can be performed.

Microporous

Pore size in the micrometer range. Known also as macroporous according to prevailing materials science terminology.

Overpotential

The difference in the electrode potential of an electrode between its equilibrium potential and its operating potential when a current is flowing. The overpotential represents the extra energy needed to force the electrode reaction to proceed at a required rate. Consequently, the operating potential of an anode is always more positive than its equilibrium potential, while the operating potential of a cathode is always more negative than its equilibrium potential.

pH (potential of Hydrogen)

A measure of the degree of the acidity or the alkalinity of a solution as measured on a scale ("pH scale") of 0 to 14.

Pores

The complex network of channels in the interior of a particle of a sorbent.

Potentiostat

An electronic instrument that controls the electrical potential between the working and reference electrodes of a three electrode cell. It forces whatever current is necessary to flow between the working and counter electrodes to keep the desired potential, as long as the needed cell voltage and current do not exceed the compliance limits of the potentiostat.

Polarization

The change of potential of an electrode from its equilibrium potential upon the application of a current.

Porosity

The ratio of the volume of all the pores in a material to the volume of the whole.

Proton

An elementary particle that is the positively charged constituent of ordinary matter and, together with the neutron, is a building block of all atomic nuclei; its mass is approximately 938 MeV and spin $^{1}/_{2}$.

Saturated calomel electrode (SCE)

A commonly used reference electrode. It is very similar to the silver/silver-chloride electrode both in construction and in theory of operation. The silver metal is replaced by mercury (electrical connection is made by an inert metal wire), the salt is mercury chloride, and the solution is saturated potassium chloride.

Silver/silver-chloride electrode

A commonly used reference electrode. The electrode assembly consists of a silver metal electrode in contact with solid silver chloride (usually as a coating on the silver metal) immersed in an aqueous chloride salt solution saturated with silver chloride.

Sputtering

A popular method for adhering thin films onto a substrate. Sputtering is done by bombarding a target material with a charged gas (typically argon) which releases atoms in the target that coat the nearby substrate. It all takes place inside a magnetron vacuum chamber under low pressure.

Track-etch membrane formation

This is a process for forming porous membranes with well-defined pores by exposing a dense film to ion bombardment followed by etching of the damaged region. It usually produces pores with a narrow size distribution.

Ultra filtration

A membrane type system that removes small colloids and large molecules from solutions. Ultra filtration removes particles in size range between 0.002 to 0.1 micron range. The process falls between reverse osmosis and micro-filtration as far as the size of particles removed is concerned.

TABLE OF CONTENTS

LIST OF TABLES

LIST OF FIGURES

LIST OF ABBREVIATIONS

A	Amperes
AFM	Atomic Force Microscopy
CA	Chronoamperometry
CV	Cyclic Voltammetry
CVD	Chemical Vapour Deposition
D_2	Quantitative parameter of membrane defects
Δ	Dispersion coefficient
EDAX	Energy Dispersive Analysis of X-rays
EDS	Energy Dispersive Spectrometry
HER	Hydrogen Evolution Reaction
hν/electrons	Energy of electrons
I	Current (A)
i	Current density ($A.m^{-2}$)
J_0	Water flux
L_s	Thickness of selective layer
MeV	Mega electronvolts
M_L	Molecular Weight
MPM	Model Protein Mixture
nm	Nanometer
OER	Oxygen Evolution Reaction
PC	Polycarbonate

PET	Polyethylene terephthalate
pI	Protein isoionic point
PSD	Pore Size Distribution
r_s	Stockes radius
R_{UF}	Effective ultrafiltration
S	Selectivity
SECM	Scanning Electrochemical Microscopy
SEM	Scanning Electron Microscopy
T	Time (s)
TEM	Transmission Electron Microscopy
UF	Ultrafiltration
V_B	Bulk etch rate
V_T	Track etch rate
XRD	X-ray Diffraction
μm	Micrometer

Chapter 1: LITERATURE REVIEW

Introduction

Nanomaterials are expected to exhibit novel and significantly improved physical, chemical and other properties, as well as to offer opportunities for manifestation of new phenomena and processes which, owing to the nanoscale dimensions, are not observed at the macroscopic level [1]. The large interest in nano- and microstructures results from their numerous potential application in various areas such as materials and biomedical sciences, electronics, optics, field emitters, magnetism, energy storage and electrochemistry [2, 3]. Of the many possible geometrical shapes and growth patterns, the simplest structure is probably an ensemble of wires.

Materials with micro- or nanoscopic dimensions not only have potential technological applications in areas such as device technology and drug delivery, but are also of fundamental interest in that the properties of a material can change in this transitional regime between bulk and molecular scales [4]. Ultra small building blocks have been found to exhibit a broad range of enhanced mechanical, optical, magnetic, and electronic properties compared to the coarser-grained matter of the same composition. Synthesis, manipulation, modification, and control on the nanometre or even atomic scale, has made tremendous progress in the past couple of years [5-8].

Many production techniques employed in the fabrication of nanomaterials have been developed, ranging from optical or electron-beam lithography, metallization, implantation and etching [2, 9-11]. The main weakness of these methods is, however, attributed to the poor control of final morphology of the produced nanostructures although some specific properties are exhibited only with enhanced molecular and super-molecular order [12].

A method termed “template synthesis” involves the preparation of a variety of micro- and nanomaterials of a desired morphology and provides a route for enhancing nanostructure order [2]. A template may be defined as a central structure within which a network forms in such a way that removal of the template creates a filled cavity with morphological and/or stereo-chemical features related to those of the template. Compared to the broadly applied lithographic methods, the accelerated ion technique has the advantage that each projectile creates an individual damage trail of a few nanometres in diameter [9]. This technique is suitable for structuring materials with small lateral dimensions and high aspect ratios, and it involves the combination of heavy ion irradiation and chemical etching.

The energetic ion technique involves synthesizing a desired material within the pores of a nanoporous membrane [13]. If the templates that are used have cylindrical pores of uniform diameter, mono-disperse nanocylinders of the desired material are obtained within the voids of the template material [2]. Each of these pores is viewed as a beaker in which a particle of the desired material is synthesized. Depending on the properties of the material and the chemistry of the pore wall, this nanocylinder may be solid (a fibril) or hollow (a tubule) [13]. These tubular or fibrillar nanostructures can be assembled into a variety of architectures. The nanostructures can remain inside the pores of the templates or they can be freed and collected as an ensemble of free nanoparticles. If the nanostructure-containing membrane is attached to a surface and the membrane is removed, an ensemble of micro- or nanostructures that protrude from the surface like the bristles of a brush, can be obtained.

There are a variety of interesting and useful features associated with template synthesis. The most useful characteristic is that it is extremely flexible with regard to the types of materials that can be prepared. This method has been used to prepare both tubules and fibrils composed of electronically conductive polymers [14-20], metals [18, 21-30], semiconductors [30, 31], carbon [32, 33] and other materials. Furthermore, nanostructures with extraordinarily small diameters can be prepared. Conductive polymer nanowires with diameters as small as 3nm have been prepared using this method [34]. It would be difficult to make nanowires with diameters this small using lithographic methods. Mono-disperse nanocylinders of the desired

material, whose dimensions can be carefully controlled, were obtained because the membrane employed contains cylindrical pores of uniform diameter.

1.1 Template method for the synthesis of novel nanomaterials

Metal nanowires are one of the most attractive materials because of their unique properties that may lead to a variety of applications [33]. Metal nanowires are also attractive because they can be readily fabricated with various techniques. An important fabrication technique that will be discussed in this thesis is the electrochemical method. The diameters of metal nanowires range from a single atom to a few hundred nanometers, and the lengths vary over an even greater range: from a few atoms to several microns.

Because of the large variation in the aspect ratio (length-to-diameter ratio), different names have been used in literature to describe the wires in order to reflect the different shapes. For example, wires with large aspect ratios (e.g. >20) are called *nanowires*, while those with small aspect ratios are called *nanorods*. Nanotubes and nanorods of various materials can be synthesized using a template-based approach. Polymers, metals, semiconductors, carbons, and other materials have been deposited within pores of previously characterized templates [8, 32].

History of template synthesis

Template synthesis for fabrication of micro- and nanostructured materials has an interesting history. The creation of nanowires by using the template method in combination with electrochemical deposition was pioneered by Bean [35]. In 1969, he was the first to demonstrate the art of filling the pores of a membrane with silver. Possin [36] followed in 1970 employing electrochemical deposition in etched fission tracks in natural mica to manufacture 40nm diameter tin, indium and zinc wires. Later Spohr [37] patented a method for fabrication of planar field emission cathodes based on the same cladding process.

This method was thereafter refined by Williams and Giordano [38] in 1984, who reported a reduced growth of 8nm diameter thin gold wires. In this case, a mica sheet with a thickness of 5μm and an area less than $1cm^2$ was used as a matrix after bombardment with ^{252}Cf (californium) fission fragments and etching with 8% hydrofluoric acid (HF). In 1987, Penner and Martin [39] used electroplating for the preparation of electrodes consisting of ultra-microdisks on an area of approximately $0.12cm^2$, by applying 10μm thin polycarbonate host membranes.

The studies by Martin *et al.* [13-33] marked the beginning of a surge in the development and application of these methods in recent years. They demonstrated that various nanostructures, including metal and conducting polymer nanowires and nanotubes, can be fabricated using the negative templates, which lead to many novel applications [22-33]. In 1991, Chakarvarti and Vetter [40] also reported the fabrication of microstructures of metallic elements (solid cylinders and hollow micro-tubules) and metal semiconductor hetero-structures using the same technique.

Since then, experiments have been realized employing a large variety of materials and membranes. Metallic wires as well as tubes composed of copper [34, 41], silver [42], gold [38, 43, 44], platinum [39], nickel [45], cobalt [45], iron [46], bismuth and cadmium [47] have been created either by electrochemical or by electroless deposition in both polymeric and porous alumina membranes, and studies about their optical [27] and magnetic [45] properties have been reported. Non-metallic materials such as conductive polymers and ionic crystals [48] have also been synthesized in the pores of commercially available polycarbonate membranes.

Polymeric nanostructures: Electronically conductive polymers, polypyrrole [49, 50], poly (3-methylothiophene) [51], and polyaniline were template-synthesized by electrochemical or oxidative polymerization. By controlling the polymerization time, conductive polymer tubules with thin or thick walls can be obtained. For polypyrrole, the tubules ultimately form solid fibrils.

In contrast, the polyaniline tubules will never close up, even at long polymerization times [13]. Following the dissolution of the template, polypyrrole nanotubes are freed. The characterization techniques used showed that the tubules were all 10μm long, which was equivalent to the thickness of the template, with their diameter being larger than the nominal pore diameter. Using the same technique, one-dimensional Au-polypyrrole nanoparticle arrays were obtained. Conducting polyaniline filaments were stabilized in the ordered, 3nm-wide hexagonal channels of the mesoporous aluminosilicate [51].

The structural data showed that about 20 aligned polyaniline chains could fit in the template channels. The fibrils showed good mono-dispersity of both length and diameter. The short nanotubes thickly wrapped in the PPA chains, exhibit a strong photo-stabilization effect, protecting the PPA chains from photo-degradation. Such a stabilization effect may not only trigger basic research on the understanding of the electronic properties of the nanotubes but also help find technological applications for the nanotubes in electronic and optical systems.

Nanometals: Through confinement of metals to a nano-sized dimension, a variety of changes in their characteristics are induced [10, 13, 24, 52]. The gold nanoparticles were electrodeposited by first sputtering a thin silver (Ag) layer followed by "plugs" electrochemically grown into the pores. From those 'nanoposts' gold (Au) nanoparticles are grown and finally the Ag foundations are chemically removed resulting in an array of Au nanorods. Depending on the pore diameter of the template, Au nanoparticles with different diameters can be obtained.

TEM analysis made possible the determination of aspect ratios of the nanoparticles. The hollow Au tubules that run the complete thickness of the template can also be obtained if the deposition is stopped before the pores are completely filled. Brumlik *et al.* [24] also prepared Au and Ag microtubules using various procedures. With the evaporation/electroplating method the smallest diameter tubules found had outer diameters of 400nm with the maximum tubule length about 1μm. Using the pore-wall-modification electrochemical method, longer Au tubules (around 3μm) were grown. 400nm diameter silver microtubules as long as 10μm were

obtained via the electroless deposition method (see **Figure 1.1**). However, tubules with extremely small diameters (30nm) can be prepared [24].

The potentiostatic electrochemical template synthesis yielded different metal nanowires with nominal pore diameters between 10 and 200nm. The wires produced were true replicas of the pores. The arrays of nickel and cobalt nanowires were fabricated by electrochemical deposition of the metals into the track-etched template. The nanowires were narrow (30nm) and continuous, with length equal to that of the matrix thickness. Tomassi and Buczko [53] obtained nanorods of the following metals: Ni, Cu, Sn, Fe, Co, Zn, Cd, Au, and Pt using the electrodeposition template technique. The diameter of metal particles depended on pore diameter and was found to be between 5 and 30nm.

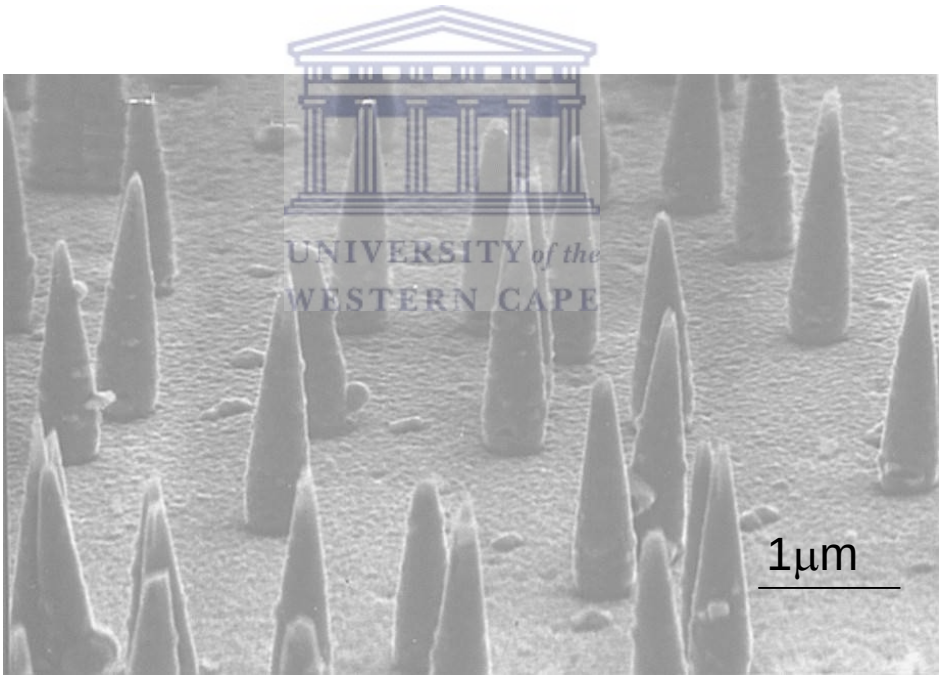

Figure 1.1: *Microwires, taken at 45°, produced by the deposition of metals into a track-etched template* [54].

Carbon Nanotubes: The general methods commonly used to produce carbon nanotubes – carbon arc and laser plasma techniques [55-57], catalytic pyrolysis of hydrocarbons [58], low pressure condensation of carbon vapours [59, 60], and condensed-phase electrolysis – suffer from the drawback that polyhedral carbon particles are also formed, the dimensions of the nanotubes are highly variable, and they have a disordered and bundle structure. Thus, growing "well ordered" carbon nanotubes on large-scale surfaces is important for their possible various applications. Templating methods have been successfully applied in producing ensembles of aligned and mono-disperse tubules of graphitic carbon with diameters as small as a few nanometers.

The chemical vapour deposition (CVD) technique has been commonly applied and hydrocarbons pyrolyzed in alumina templates yielded graphitic carbon nanofiber and nanotube ensembles with diameters as small as 20nm and lengths around 50μm [32, 61, 62]. Massive arrays of self-oriented mono-dispersed carbon tubes were also prepared by chemical vapour deposition of hydrocarbons on patterned porous silicon or within the pores of activated silica [63]. Both single- and multi-walled tubules were formed with diameters from 1-3nm and lengths up to tens of micrometers. An SEM micrograph of carbon nanotubes showing their diameters and distribution is shown in **Figure 1.2**.

Semiconductor nanotubes and fibres: In addition to conductive fibrils, metal and carbon nanorods and nanotubules, a variety of other nanostructures have been successfully synthesized by using a template technique. Hulteen and Martin [10] developed chemical strategies for preparing composite tubular nanostructures for which one can imagine a host of applications. Thus, a semiconductor-conductor tubular nanocomposite as well as conductor-insulator-conductor composite structures were fabricated with template synthesis. Also, 15nm diameter semiconductor nanotubules and nanofibres were deposited into the pores of a template membrane [10, 31].

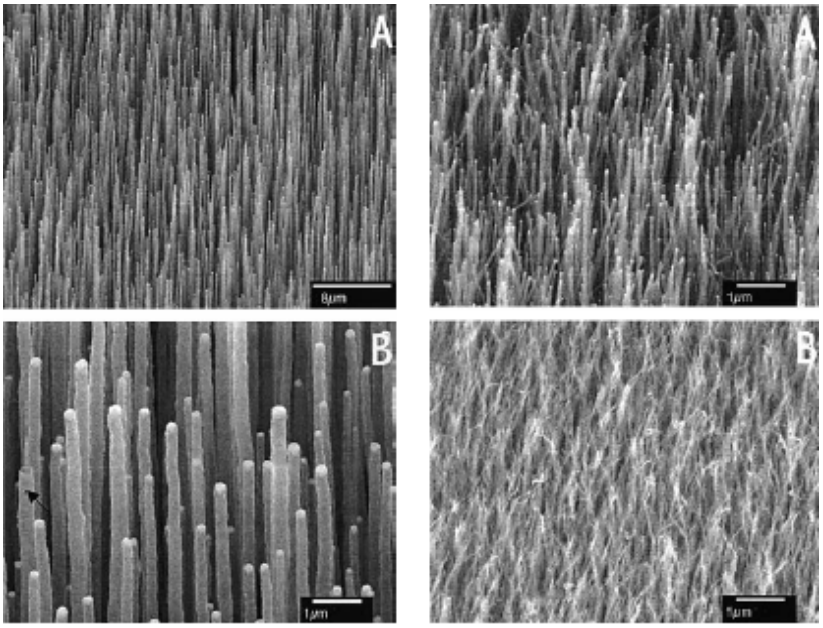

Figure 1.2: *SEM micrograph of carbon nanotubes showing their diameters and distributions. A site density of about 10^7 tubes/mm^2 was estimated* [64].

Dagani [65] reviewed a variety of applications for tailored composites in the range from 1 to 100nm, including structural materials, high-performance coatings, catalysts, electronics, photonics, and magnetic and biomedical materials. Near-mono-disperse hollow nanotubules of $MoSi_2$ were prepared by thermal decomposition of molecular precursors within the pores of an Al_2O_3 membrane template. Raman *et al.* [66] described the template-based approach to the preparation of amorphous, nanoporous silicas. Platinum or iron metal enclosed carbon tubes were obtained by using the electrochemical template technique. These composite nanotubes are uniform and their outer diameter and wall thickness could be estimated to be 30nm and about 5nm, respectively. Carbon nanotubes have been widely applied as removable templates for fabrication of oxide nanocomposites [51, 67].

Fundamental and applied studies of nanomaterials synthesized by the template method

One very exciting application of template synthesis is in the area of electrochemistry [10]. Nanoelectrodes offer opportunities to perform electrochemistry in highly resistive media and to investigate the kinetics of redox processes that are too fast to measure with conventional macroscopic electrodes [68]. The template method was used to prepare ensembles of gold (Au) nanodisk electrodes where the diameters of the Au disks are as small as 10nm. Using the electroless Au deposition procedure, Au nanowires were synthesized within the pores of a polycarbonate track-etch membrane. In addition, both faces of the membrane become coated with thin Au films. If one of these surfaces of Au films is removed, the disk-shaped ends of the Au nanowires traversing the membrane are exposed. The reason for research interest in nanowires and nanotubules of various materials is manifold. Thus, the conductivity of polymer fibrils, filaments, and tubules has been extensively investigated [20, 69].

The nanoscopic fibrils of heterocyclic polymers show electronic conductivities, along the fibril axis, that are substantially higher than conductivities of bulk films of the analogous polymer. Also the template-synthesized polyacetylene fibrils show enhanced super-molecular order and higher electronic conductivity [20]. Wu and Bein [69] demonstrated that the polyaniline filaments have significant conductivity while encapsulated in nanometre channels as measured by microwave absorption at 2.6GHz.

For polypyrrole fibrils the conductivity increases with decreasing diameter: values higher than one order of magnitude larger than the bulk value were deduced for nanostructures with diameters of around 30nm [69]. Nanometals have interesting optical, electronic, electrochemical, and magnetic properties [13]. The colloidal suspensions of Au differ in colour depending on the size of the spherical Au particles.

1.2 General principles of template synthesis

The limits to which materials can be used in template synthesis are defined by the chemistry required to synthesize the material. Almost any solid matter can in principle be synthesized within the nanoporous template, provided a suitable chemical pathway can be developed [2, 10]. There are, however, some concerns that need to be addressed when developing new template synthetic methods, for example: (1) will the precursor solutions used to prepare the material 'wet' the pores; (2) will the deposition reaction proceed too fast resulting in pore blockage at the membrane surface before tubule/fibre growth can occur within the pores; (3) will the host membrane be stable (i.e. thermally and chemically) with respect to the reaction conditions? The basic scheme of metal replication of etched ion-track polymer membrane is shown in **Figure 1.3** below.

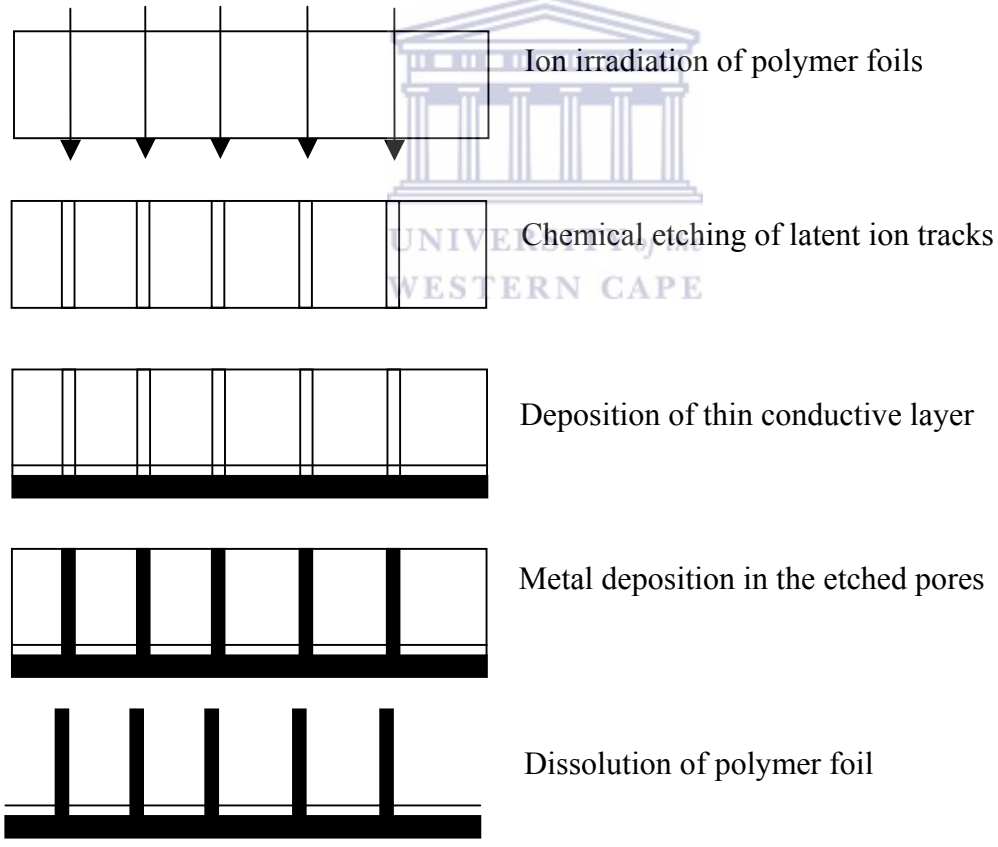

Figure 1.3: *The basic scheme of metal replication of etched ion-track polymer membrane.*

By depositing metals into the nanopores, nanowires with a diameter predetermined by the diameter of the nanopores are fabricated. There are essentially several representative chemical strategies to carry template synthesis within the alumina and polymeric template membranes [10, 12]. A schematic representation of the process flow for synthesizing regular arrays of oriented nanotubes on a substrate by catalyst patterning and CVD is shown in **Figure 1.4** below. The pattern was created on a hydrophilic substrate, such as glass, by the standard photolithography method, using a printed polymer foil as the photomask. To provide better electrical conduction, the hydrophilic substrates were metallized by thermal evaporation and photoresist lift-off.

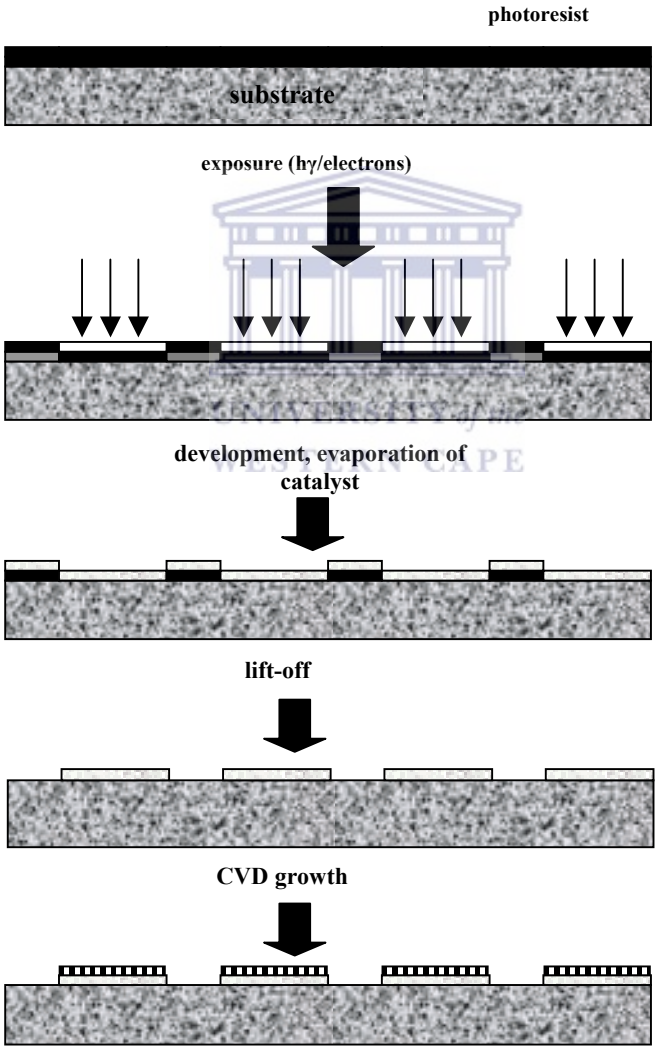

Figure 1.4: *Schematic process flow for the synthesis of regular arrays of oriented nanotubes on a substrate by catalyst patterning and CVD.*

1.2.1 Materials deposition techniques for template synthesis

Electrochemical deposition: There are several ways to fill the nanopores with metals or other materials to form micro- or nanowires, but the electrochemical method is a general and versatile method [32]. Electrodeposition is one of the most widely used methods to fill conducting materials into the nanopores to form continuous nanowires with large aspect ratios. One of the great advantages of the electrodeposition method is its ability to create highly conductive nanowires. This is because electrodeposition relies on electron transfer, which is the fastest along the conductive path.

Structural analysis showed that the electrodeposited nanowires tend to be dense, continuous, and highly crystalline in contrast to other deposition methods, such as chemical vapour deposition. The electrodeposition method is not limited to nanowires of pure elements. It can fabricate nanowires of metal alloys with good control over stoichiometry. Another important advantage of the electrodeposition method is the ability to control the aspect ratio of the metal nanowires by monitoring the total amount of passed charge. This is important for many applications. For example, the optical properties of nanowires are critically dependant on the aspect ratio [31].

Nanowires with multiple segments of different metals in a controlled sequence can also be fabricated by controlling the potential in a solution containing different metal ions. Electrochemical deposition of a material within the pores of the matrix is preceded by coating one face of the membrane with a metal film and using this metal film as a cathode for electroplating [10, 24-29, 34, 40, 42].

The lengths of these nanowires can be controlled by varying the amount of metal deposited. By depositing a small amount of metal, short wires can be obtained; alternatively, by depositing large quantities of metal, long needle-like wires can be prepared [25-27].

Hollow metal tubules can also be prepared via this method [29, 69]. To obtain tubules, one must chemically develop the pore wall so that the electrodeposited metal

preferentially deposits on the pore wall, that is, a molecular anchor must be applied. Gold tubules have been prepared by attaching a cyanosilane to the walls of the alumina template membrane prior to metal depositions [24, 29]. Owing to the large number of commercially available silanes, this method can provide a general route for tailoring the pore walls in the alumina membranes.

Electrochemical deposition can also be used to synthesize conductive polymers within the pores of these template membranes [19]. When these polymers are synthesized within the pores of track-etched template membranes, the polymer preferentially nucleates and grows on the pore walls, resulting in polymeric tubules at short polymerization times. By controlling the polymerization time, thin-walled tubules can be produced, also thick-walled tubules or solid fibrils.

The reason why the polymer preferentially nucleates and grows on the pore walls is straightforward [18]. Although the monomers are soluble, the polycationic forms of these polymers are completely insoluble. There is also an electrostatic component because the polymers are cationic and there are anionic sites on the pore walls [18]. Additional advantages of the electrochemical methods are the avoidance of vacuum systems, its flexibility and low costs, as well as its applicability to all substances suitable for deposition by electroplating.

Electroless deposition: In electrolytic metal deposition the electrons required for the reduction of the metal ions are supplied by an external current source. In electroless metal deposition, on the other hand, the electrons required for reduction are supplied by the catalytic or electrocatalytic oxidation of a reducing agent. Electroless metal deposition involves the use of a chemical reducing agent to plate a material from the solution phase onto a template surface [24, 50, 67, 68, 69, 70]. This method differs from electrochemical deposition in that the surface to be coated need not be electrochemically conductive.

This method involves applying a sensitizer (typically Sn^{2+}) to the membrane surfaces (pore walls and faces). The sensitizer binds to the surfaces via complexing with surface amine, carbonyl, and hydroxyl groups. This sensitized membrane is then

activated by exposure to Ag^+ resulting in the formation of discrete nanoscopic Ag particles on the membrane's surfaces.

The key feature of the electroless deposition process is that material deposition in the pores starts at the pore wall. Unlike the electrochemical deposition methods where the length of the metal nanowires can be controlled at will, electroless deposition yield structures that run the complete thickness of the template membrane [22]. These nanostructures generally have a length of the thickness of the template, so controlling their length at will is difficult.

For the nanotubes made with this method, the inside diameter may be decided by the deposition times, but their outside diameter is almost the same as that of the pores in the templates [22, 23]. The outside diameter of the nanotubes is determined by the diameter of the pores in the template membrane. It is interesting to note that carbon tubules can also be used as templates in the synthesis of nanorods and nanotubes in the chemical way. Different methods could be used to introduce various materials into the internal holes of the tubules.

Chemical polymerization: A variety of conductive polymers can be template synthesized by the polymerization of the corresponding monomer to yield tubular nanostructures [20, 32, 49, 66-68]. Chemical template synthesis of a polymer can be accomplished by simply immersing the membrane into a solution containing the desired monomer and a polymerization reagent. As with electrochemical polymerization, the polymer preferentially nucleates and grows on the pore walls, resulting in tubules at short deposition times and fibres at long times.

Conventional electronically insulating plastics, can also be chemically synthesized within the pores of these template membranes. For example, polyacrylonitrile (PAN) tubules can be prepared by immersing an alumina template membrane into a solution containing a polymerization initiator [32, 33]. The inside diameter of the resulting PAN tubules is varied by controlling the time the membrane remains in the polymerization bath. These PAN tubules have been further processed to create conducting graphitic carbon tubules and fibrils in alumina membranes, [32,

33]. This is accomplished by heating the PAN tubules alumina membrane composite to 700°C under an argon flow or under vacuum.

Sol-gel deposition: Sol-gel synthesis within the pores of templates can be conducted to create both tubules and fibrils of a variety of materials [51]. Sol-gel chemistry typically involves hydrolysis of a solution of a precursor molecule to obtain first a suspension of colloidal particles (the sol) and then a gel composed of aggregated sol particles. The gel is then thermally treated to yield the desired product. Various sol-gel syntheses have been conducted within the pores of the alumina membranes to create both tubules and fibres of a variety of inorganic semiconducting materials.

First, an alumina template membrane is immersed into a sol for a given period of time, where the sol deposits on the pore walls. After thermal treatment, either a tubule or fibril of the desired semiconductor is formed within the pores. As with the other template synthesis techniques, longer immersion times yield fibres with brief immersion times producing tubules.

The formation of tubules after short immersion times indicates that the sol particles adsorb on the alumina membrane's pore walls. This is expected because the pore walls are negatively charged while the sol particles used to date are positively charged. It has also been found that the rate of gelation is faster within the pore than in bulk solution. This is most likely due to the enhancement in the local concentration of the sol particles due to adsorption on the pore walls.

Chemical vapour deposition (CVD): CVD has long been applied in the commercial production of solid thin films [2]. The technique entails surface solidification of desired reactants resulting from their gas-phase chemical transformations. A major hurdle in applying CVD techniques to template synthesis has been that deposition rates are too fast. As a result, the surface of the pores becomes blocked before the chemical vapour can traverse the length of the pore.

Two template-based CVD syntheses have been developed. The first entails the CVD of carbon within porous alumina membranes. This involves placing an alumina membrane in a high-temperature furnace and passing a gas such as ethane or propane through the membrane. Thermal decomposition of the gas occurs throughout the pores, resulting in the deposition of carbon films along the length of the pore walls.

The second CVD technique utilizes a template-synthesized structure as a substrate for CVD deposition. The CVD method has been used to coat an ensemble of gold nanotubes with concentric TiS_2 outer nanotubules. The first step of this process requires the electroless plating or Au tubules of fibrils inside the pores of a template membrane. The Au surface layer is removed from one face of the plated membrane, and the membrane is dissolved away. The resulting structure remaining is a Au surface layer like the bristles of a brush.

1.2.2 Porous materials for template synthesis

Most of the studies in template synthesis, to date, have entailed the use of two types of nanoporous materials, 'track-etch' polymeric membranes and porous alumina or silica membranes. However, there are a variety of others, both natural and synthetic materials that could be utilized as templates. These materials contain a large number of straight cylindrical nanopores with a narrow distribution in the diameters of the nanopores. Previously synthesized nanostructures can also be used as templates.

Track-etched membranes: A number of companies sell microporous and nanoporous polymeric filtration membranes that have been prepared via the track-etched method [13]. The track-etch method entails bombarding a nonporous sheet of the desired material (standard thickness ranges from 6 to 20μm) with nuclear fission fragments to create damage tracks in the material via the so-called Coulomb explosion phenomena, and then chemically etching these tracks into pores [10]. The minimum width of the track before etching is only 2.5nm. The resulting porous materials contain randomly distributed cylindrical pores of uniform diameter.

The ion-track method has been applied to create nanopores in plastic membranes, such as polycarbonate and polyester [38]. Instead of using acid, alkaline solvent is used to "develop" the ion tracks in polycarbonate membranes [39]. The commercial membranes are available with pore diameters as small as 10nm (pore density ca. 10^9 pores cm^{-2}). These commercial membranes are prepared from polycarbonate or polyester [10, 13, 25]. The diameter of the pores can be controlled by controlling the etching time. An important advantage of these plastic templates over the mica films is that their surface wetting properties can be tailored, which is important for many applications. Another advantage is that they can be more easily dissolved without affecting the nanowires formed in the pores.

Owing to the random nature of the pore-production process, the angle of the pores with respect to the surface normal can be as large as 34° [10]. Therefore, depending on the specific diameter and pore density of the track-etched membrane, a number of pores may actually intersect within the membrane. Theory predicts a specific wavelength maximum in the absorption band of isolated metal nanoparticles [25-27]. However, physical contact between the metal nanoparticles synthesized within the pores can shift this absorption maximum by 200nm or more.

Porous alumina: Anodic porous alumina is another commonly used template. Porous alumina membranes are prepared via the anodization of aluminium metal in an acidic solution [10, 13]. The individual nanopores in the alumina can be ordered into a close-packed honeycomb structure. These membranes contain cylindrical pores of uniform diameter arranged in a hexagonal array. The diameter of each pore and the separation between two adjacent pores can be controlled by changing the anodization conditions. The fabrication method of anodic porous alumina can be traced back to the work done in the 1950's, which involves a one-step anodization process. This original one-step anodization method is still used to fabricate most commercial alumina membrane [42, 43]. However, unlike the track-etch membrane, the pores in these have little or no tilt with respect to the surface normal resulting in an isolating, non-connecting pore structure. Although such membranes are sold commercially, a very limited number of pore diameters are available.

Membranes of this type with a broad range of pore diameters have been prepared. Membranes with pore diameters as large as 200nm and as small as 5nm have been made. The anodic porous alumina has a much higher pore density (~10^{11} pores cm^{-2}), and with typical membrane thicknesses ranging from 10 to 100μm allows one to fabricate a large number of nanowires at one time [71]. The higher pore density would allow a greater number of nanostructures to be produced per unit area of template membrane. Another interesting feature of the porous alumina template is that the chemistry of the pore walls can be altered via reaction with silane compounds [44].

Other nanoporous materials: Thurn-Albrecht *et al.* [72] showed a simple and robust chemical route to fabricate ultra high-density arrays of nanopores with high aspect ratios using di-block copolymer. The method is based on self-assembly of incompatible block copolymers into well-ordered structures of molecular dimensions. Tonucci *et al.* [73] have recently described a nano-channel array glass with pore diameters as small as 33nm and pore densities as high as 3 x 10^{10} pores cm^{-2}. Beck *et al.* [74] have prepared a new class of mesoporous zeolites with large pore diameters. Douglas *et al.* [75] have shown that the nanoscopic pores in a protein derived from a bacterium can be used to transfer an image of these pores to an underlying substrate. Clark and Ghadiri have prepared arrays of polypeptide tubules [76]. Finally, both Ozin [11] and Schollhorn [77] have discussed a wide variety of nanoporous solids that could be used as template materials.

Nanostructures as templates: Using carbon nanotubes as templates, various ceramic oxides, nanotubes were prepared from silica, vanadium pentoxide, zirconia, molybdenum oxide and yttria-stabilized zirconia [2]. Multi-walled carbon nanotubes are usually obtained by the arc-discharge method [78] or from metal-catalyzed decomposition of ethylene in the presence of hydrogen [68, 70, 79]. The carbon template can be later removed by heating the coated or filled nanotubes in air at elevated temperature [2]. Thus, the nanoscale rods or tubules with typical diameters of between 2 and 30nm and lengths of up to 20μm are separated. The carbon nanotube acted as a removable template in the synthesis of silicon and boron nitride nanorods

[79]. The platinum nanorods and nanoparticles were also prepared using carbon nanotubes previously obtained by a template carbonization technique and an anodic aluminium oxide film.

1.3 Ion track etching technology for unique porous template production

Basic principles of track-etched membrane production

Track-etched membranes have been widely used recently as templates for the creation of nanowires and nanotubes. There are two steps followed in the production of etched ion track membranes. The first is the formation of latent tracks by heavy-ion irradiation which is followed by the subsequent enlargement of the tracks to pores by chemical etching. Variation of the irradiation and etching conditions enables the production of suitable membranes with pores of different geometries, sizes and aspect ratios.

There are two basic methods of producing latent tracks in the foils to be transformed into porous membranes [79]. The first method is based on the irradiation with fragments from the fission of heavy nuclei such as californium (Cf) or uranium (U). Exposing a uranium target to a neutron flux from a nuclear reactor initiates the fission of ^{235}U. Typical energy loss of the fission fragments is about 10 keV/nm.

The second method is based on the use of ion beams from accelerators [80]. The intensity of the ion beam should be at least 10^{11}ions/s to be competitive in the track membrane industry. Modern accelerators provide beams of higher intensities. The energies of the accelerated ions are a few MeV per nucleon. The beams can be pulsing or continuous. To irradiate large areas, a scanning beam is normally used.

Track-etched membranes have the advantage over conventional membranes because of their precisely determined structure. However, many large-scale applications are “insensitive” to such a brilliant property. Track membranes occupy a

niche in biological, medical, analytical and scientific applications. These membranes are indispensable for property manipulation with small particles of living tissue and any other matter.

The track membranes seem to be the best porous material for providing a controllable transport of solutes. Further progress in track-etch membrane technology can be linked to the creation of membranes having particular properties for a particular use. Membranes that do not adsorb proteins, membranes with various functional groups on the surface, amongst others, might be developed and introduced into industry.

Heavy-ion Irradiation: Track-etch membranes in the form of nuclear track filters have emerged as a spin-off from solid state nuclear track detectors. The size of the channels or the pores depend upon various factors, viz. the nature and energy of the incident particles, the target material, etching conditions, e.g. temperature, nature of etchant, pre-etch storage conditions, etc. The pore sizes, which are controllable, may range from a few nanometres to millimetres. Nuclear track filters have numerous other applications besides their use in the synthesis of nano and microstructures [34, 81].

The design of irradiation facilities has been described in the literature. The advantages of the accelerator tracking method are that there is no radioactive contamination of the material when the ion energy is below the Coulomb barrier; identity of the bombarding particles means all tracks showing the same etching properties; a higher energy of particles equals larger range equals thicker foils that can be perforated; better conditions for producing high-density ($>10^9$ cm^2) track arrays; particles heavier than fission fragments can be used; and it is easier to control the impact angle and produce arrays of parallel tracks or create some particular angular distributions for getting rid of merging pores. However, the stability of the particle flux from an accelerator is usually lower. Another disadvantage is a higher cost of irradiation.

Chemical etching: The technique of ion track etching has found diverse use in science and technology. Chemical etching is a process of pore formation [82]. The mechanisms of track evolution during chemical treatment have been the subject of intensive research aimed at the development of nano- and microstructures with precisely determined pore sizes and pore densities. During chemical etching the damaged zone of a latent track is removed and transformed into a hollow channel. It is the pore-size-determining and pore-shape-determining stage of the technology. Under suitable conditions, the chemically modified material along the ion track of the polymer is dissolved at a faster rate than the non-irradiated bulk material [9]. Consequently, two different etching rates are defined: a fast etch rate along the track, V_T, which depends on the damage density in the track, and the isotropic etch rate of the undamaged bulk material, V_B. This rates are applicable to larger (>1μm in diameter) pores. The conical pore shape is transformed into a cylindrical one at $V_T > V_B$. The geometry of smaller pores is also determined by the size and structure of the damaged zone around the particle path.

The sub-microscopic kinetics of pore formation can be described using the method proposed by Mazzei *et al*. [83]. Even more complex kinetics of pore growth takes place in an etchant containing a surfactant. The bulk etch rate depends on the material, on the etchant composition and on the temperature. The track etch rate depends on a much greater number of factors. They can be classified into a few categories: sensitivity of the material, irradiation conditions, post-irradiation conditions, and etching conditions. The ratio between both rates is called the selectivity S and depends on the irradiated material and on the etching condition, namely, concentration and temperature of the etching solution.

Pores of different geometries can be produced by varying the selectivity: an extremely high ratio of V_T/V_B leads to a cylindrical pore geometry, while $V_T/V_B \geq 2$ results in biconical-shaped pores. Conical pores have also been created by etching foils only from one single side [84]. By performing several successive etchings such as creating a cylindrical pore and then producing a conical shape or vice versa, funnel-shaped pores and other pore geometries can be produced [85].

The acceleration of this process with the help of exposure to ultraviolet light (UV) is used in a technological production process of PET track membranes [86, 87]. There are some other methods of track sensitization. Heavy ion tracks in PET can be effectively sensitized by the treatment with organic solvents. The storage at elevated temperature leads to fading of tracks in most polymers, however, there are some polymers showing opposite behaviour. An example is polypropylene in which a moderate heating enhances the particle tracks due to thermo-oxidation. In most cases the variations of the etchant composition, component concentrations and temperature give researchers a chance to vary the track to bulk etch rate ratio over a very wide range.

In polycarbonate (PC), the etch rate ratio of 10^5 can be achieved for UV-sensitized heavy ion tracks if etching is performed in aqueous alkali solutions. The same tracks show an etch rate ratio of 2–4 in etchants composed of alkali and alcohols such as methanol, ethanol or propanol. A typical SEM micrograph of a polymeric membrane surface after etching is shown **Figure 1.5** below.

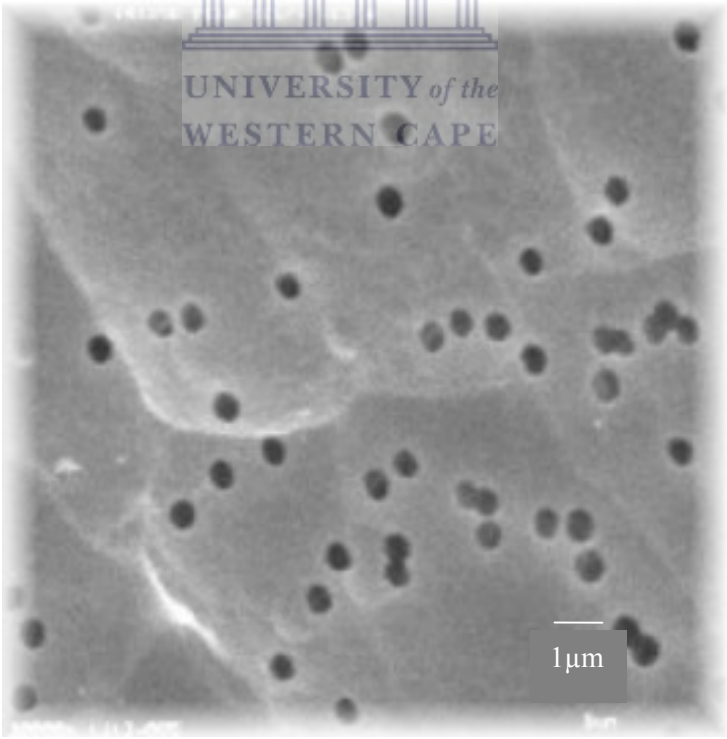

Figure 1.5: *SEM image of a polymeric membrane surface after etching* [54].

The activation energy of the track etching process often differs from that of the bulk etching. Thus, changing the temperature during etching can be used to increase or decrease the etch rate ratio. Another key parameter is the size of the damaged zone that dissolves at a different rate compared with that for the bulk material. Systematic measurements have been performed with PC and PET for the estimation of the etch rate parameter depending on the linear energy transfer (LET) of bombarding particles [79, 82].

The heaviest ions produce a larger damaged track core and a larger cross-linked halo. At the same time, the heaviest ions do not necessarily provide the highest etch rate ratio. From the comparison of the response function with the damaged zone diameter vs. LET function the conclusion was made that the ions with moderate masses (Kr or Xe) are favoured for tracking the polymer foils.

Polymers for track-etched membrane production

Polyethylene terephthalate (PET): The process of track formation and etching in PET membrane is well studied [79]. PET is rather stable in acids, organic solvents, biologically inert, and mechanically strong. A high etch ratio is achievable, when using UV sensitization, which makes it possible to produce a wide range of membranes with different pore diameters. The etching procedure is simple and fast. Alkali solutions, sometimes with additives, are used to develop tracks. The membranes are relatively hydrophilic without any additional modification. The registration properties of PET have been found to be quite good [88].

Polycarbonate (PC): PC has been used for track membrane production since the seventies [79]. The production technology is very close to that of PET. The sensitivity of PC is higher, compared to PET, which makes it possible to produce membranes with a pore diameter as small as ~10nm and to omit the UV sensitization stage. Polycarbonate track membranes differ from PET membranes by a lower resistance to organic solvents and a lower wettability.

Polypropylene (PP): PP was investigated as a raw material for membranes to be used for the filtration of some aggressive liquids such as strong alkali solutions of inorganic acids [79]. Chemical etching in strong oxidizers (chromium trioxide) is effective in developing the latent tracks in PP. The etching procedure is considerably more complex than the etching of PET or PC. Samples of PP track membranes with various pore diameters ranging between 0.1 and 3μm have been fabricated on a laboratory scale. The membranes are hydrophobic. Commercial production of PP membranes has not been launched because of the limited estimated market.

Polyvinylidene fluoride (PVDF): Much effort was expanded in developing track membranes from fluorinated polymers. The best results were obtained with PVDF that exhibits good chemical, mechanical and particle registration properties. PVDF also has some special properties (piezoelectricity) that attract the attention of researchers. Samples of PVDF track membranes were produced and tested in several laboratories [80, 89, 90].

Polyimides (PI): PI has an excellent stability at high temperatures, excellent mechanical strength, and extraordinary radiation resistance. Films of polypyrromelithimide with different thickness as have been available for the past 20 years. Research work on PI as a track-recording medium has been performed in several laboratories [80, 91]. The possibility of track membrane manufacturing has been demonstrated.

CR-39: It is highly sensitive to ionized particles and being a highly transparent material, can be used to fabricate track-etch membranes for special purposes. Some copolymers of CR-39 have been shown to have an even higher sensitivity than CR-39 itself [92]. The polymer is brittle which impedes the manufacturing and use of thin foils.

Polysulphide and Polyetherketones: Attempts have been made to produce track-etched pores in aromatic polysuphfide [79] and polyetherketones [92]. These highly aromatic materials showed a very low sensitivity to energetic heavy particles and, consequently, a very low etch ratio preventing the formation of a homogeneous porous structure.

Modification methods of track-etched membrane

The modification methods that change the surface and bulk properties of track membranes or impart new functions to them are sorption of some small or large molecules on the surface; surface treatment with plasma; immobilization of functional substances on the surface by covalent bonding using chemical reaction, and graft polymerization of various monomers.

Hydrophilization of PET and PC track membranes by adsorption of polyvinyl pyrrolidone is a widely used procedure in industry. Similarly, covering the surface with silicone oil or paraffin can make the membranes hydrophobic. Plasma treatment improves wettability of many polymers due to the formation of new polar groups on the surface. Stability of the modified surface depends significantly on the conditions during plasma treatment [93].

Electrochemical properties of track-etched pores can be modified by covalent bonding of charged groups or by adsorption of ionic polyelectrolytes [79]. The immobilization of amino acids on the PET track membranes based on the reactions of end carboxyl and hydroxyl groups was reported [94]. However, the surface density of the immobilized species by this route is rather low.

Properties and application of track-etched membrane

Track membranes are known as precise porous films with a very narrow pore size distribution [95]. A unique property of track-etched membrane is that the number of pores and the pore size are two almost independent parameters which can be varied over a very wide range. The pore density can vary from 1 to $10^{10}cm^{-2}$. In most cases, the pore geometry is very simple (cylinders, cones or combinations of these) which leads to simple relationships between the membrane structure parameters and its transport characteristics such as the gas or water flow rate.

In the production process the finished membrane is normally subjected to rigorous evaluation by SEM, gas and water flow rate methods, bubble point, and some other measurements [87]. Pore shape can be made cylindrical, conical, funnel-like, and cigar-like at will. Various asymmetric structures can also be produced. The separation properties of track-etched membranes depend, first of all, on the structural parameters. In the absence of adsorption, the track membrane acts as a "screen" membrane. The retention of particles is determined by the relationship between the pore diameter and the particle size. If the surface of the membrane adsorbs the particles, the retention characteristics change drastically. In this case the result depends on the nature of the membrane surface and the nature of the particles, and also depends on the pH, presence of surfactants, etc.

Adsorption of solutes leads to a decrease in the filtration rate or to the loss of a substance that is expected to pass through the membrane [96]. An example is sorption of proteins onto the PET membrane surface that is negatively charged at medium and high pH. To solve such problems, track membranes with various specific surface properties have to be manufactured.

Application for commercially produced track-etched membranes can be categorized into three groups, namely; process filtration, biological cell culture and laboratory filtration. Process filtration implies the use of membranes mostly in the form of cartridges with a membrane area of at least 1cm^2. Purification of deionised water in microelectronics, filtration of beverages, separation and concentration of various suspensions are typical examples.

There is strong competition with other types of membranes available on the market. Casting membranes often provide a higher dirt loading capacity and a higher throughput. In recent years, a series of products were developed for the use in the domain called biological cell and tissue culture. Adapted over the years to a variety of cell types, porous membrane filters are now recognized as providing significant advantages for cultivating biological cells.

The use of permeable support systems based on track-etched membranes has proven to be valuable too in cell biology. A traditional application of track membranes is laboratory filtration [79]. Track membrane is a very good device for collecting small particles on its surface for subsequent analysis. For such purposes, track membranes are delivered in the form of disks and filtration kits. The use of specially produced track-etched pores, to solve various scientific tasks, are mentioned separately.

One pore, oligo-pore and multi-pore samples can serve as unique models for studying the transport of liquids, gases, particles, solutes, electrolytes, and electromagnetic waves [97] through narrow channels. Many experiments of this kind are relevant to biological and medical topics [98]. Track membranes can also serve as templates for making various micro- and nanostructures. Magnetic, conducting and superconducting nanowires possessing special properties have been manufactured in this way [94].

1.4 Nickel deposition and impregnation into polymer templates

The Ni plating electrochemical technique

Nickel plating is similar to other electroplating processes that employ soluble metal anodes. It requires the passage of direct current between two electrodes that are immersed in a conductive, aqueous solution of nickel salts. It is the electrolytic deposition of a layer of nickel on a substrate. The process involves the dissolution of one electrode (the anode) and the deposition of metallic nickel on the other electrode (the cathode) [99]. Direct current is applied between the anode (positive) and cathode (negative). Conductivity between the electrodes is provided by an aqueous solution of nickel salts. When nickel salts are dissolved in water, the nickel is present in solution as divalent, positively charged ions (Ni^{2+}). When current flows, divalent nickel ions absorb with two electrons ($2e^-$) and are converted to metallic nickel (Ni^0) at the cathode.

The reverse occurs at the anode where metallic nickel dissolves to form divalent ions. The electrochemical reaction in its simplest form is: $Ni^{2+} + 2e^- = Ni^0$. Because the nickel ions discharged at the cathode are replenished by the nickel ions formed at the anode, the nickel plating process can be operated for long periods of time without interruption.

Estimating thickness: The amount of nickel that is deposited at the cathode is determined by the product of the current and the time. If the area being plated is known, the average thickness of the nickel coating can be estimated. Thickness equals the weight of nickel divided by the product of the area and the density of nickel. Because a small percentage of the current is consumed at the cathode in discharging hydrogen ions, the efficiency of nickel deposition is less than 100% [99]. This fact must be taken into account in estimating the weight and the thickness of nickel that will be deposited under practical plating conditions.

Anode efficiency is normally 100%. Because anode efficiency exceeds cathode efficiency by a small percentage, nickel-ion concentration and pH will rise as the bath is used. The pH of the solution is normally maintained by adding acid.

Metal distribution: It is desirable to apply uniform thicknesses of nickel to all significant surfaces to achieve predictable service life and to meet plating specifications that require minimum coating thickness values at specified points on the surface. The amount of the deposit on the surface of any object being plated is proportional to the current that reaches the surface [100]. Recessed areas on the surface receive less current, because the electric field is highest at points/surface with the smaller curvatures. The current density and, consequently, the rate of metal deposition in the recessed area is lower than points that project from the surface.

The weight of nickel deposited at the cathode is controlled by natural laws that make it possible to estimate the thickness of the nickel deposited. These estimates must be adjusted to account for variations in cathode efficiencies for specific processes. Normally, cathode efficiency values are between 93% and 97% for most nickel processes.

Process: The basic constituents – nickel sulphate, nickel chloride, and boric acid – serve the same purposes as they do in the *Watts* solution [99] (see **Table 1.1**). Nickel sulphate is the principal source of nickel ions; nickel chloride improves anode dissolution and increases solution conductivity, while boric acid helps to produce smoother, more ductile deposits. Anionic anti-pitting or wetting agents are required to reduce the pitting due to the clinging of hydrogen bubbles to the products being plated.

Table 1.1: *Nickel electroplating solutions and typical properties of the deposits* [99].

	***Watt* Nickel**	**Conventional Sulphamate**	**Concentrated Sulphamate**
	Electrolyte composition, g/L		
$NiSO_4.6H_2O$	225 to 300		
$Ni(SO_3NH_2)_2.4H_2O$		315 to 450	500 to 650
$NiCl_2.6H_2O$	37 to 53	0 to 22	5 to 15
H_3BO_3	30 to 45	30 to 45	30 to 45
	Operating conditions		
Temperature, °C	44 to 66	32 to 60	Normally 60 or 70
Agitation	Air or mechanical	Air or mechanical	Air or mechanical
Current density, A/dm^2	3 to 11	0.5 to 32	Up to 90
Anodes	Nickel	Nickel	Nickel
pH	3.0 to 4.2	3.5 to 4.5	3.5 to 4.5
	Mechanical properties		
Tensile strength, MPa	345 to 485	415 to 620	400 to 600
Elongation, %	15 to 25	10 to 25	10 to 25
Vickers hardness, 100g load	130 to 200	170 to 230	150 to 250
Internal stress, MPa	125 to 185 (tensile)	0 to 55 (tensile)	

Bright nickel plating solutions: Bright nickel solutions contain at least two types of organic addition agents, which complement each other and yield fully bright nickel deposits [99]. One type produces deposits that are mirror-bright initially, but are unable to maintain the mirror-like appearance of the deposit as its thickness is increased. This class includes compounds like benzene disulphonic acid, and benzene trisulphonic acid and benzene sulphonamide, and sulphonimides such as saccharin.

The organic compound is reduced electrochemically at the cathode, and this is accompanied by the reduction and incorporation of sulphur (as sulphide) in the deposit. Fully bright nickel deposits typically contain 0.06% to 0.12% sulphur. These reactions control the structure and growth of the nickel as it is deposited.

The second type may be termed levelling agents because they make the surface smoother as the thickness of the deposit is increased. They are sulphur-free, bath-soluble organic compounds containing unsaturated groups and generally introduce small amounts of carbonaceous material into the deposit. The combination of organic addition agents makes it possible to obtain smooth, brilliant, lustrous deposits over wide ranges of current density.

Industrial nickel plating: Engineering or industrial applications for electrodeposited nickel exist because of the useful properties of the metal [99]. Nickel coatings are used in these applications to modify or improve surface properties, such as corrosion resistance, hardness, wear, and magnetic characteristics. The operating conditions significantly influence the mechanical properties of electrodeposited nickel. The mechanical properties of electrodeposited nickel vary with the temperature to which the coatings are exposed. Nickel deposits from sulphamate solutions are stronger at cryogenic temperatures than deposits from the *Watts* bath.

Nickel also has the ability to protect itself against certain forms of attack by developing a passive oxide film. When an oxide film forms and is locally destroyed,

as in some hot chloride solutions, nickel may form pits. In general, nickel is resistant to neutral and alkaline solutions, but not to most of the mineral acids.

Nickel is generally electrodeposited from sulphate or sulphamate electrolyte with or without additives, and also from a *Watts*-type electrolyte containing nickel sulphate, nickel chloride and boric acid [98]. Additives have more of an influence on deposit properties than on any other plating variables. When used at controlled, limited concentrations, organic additives refine the grain structure, provide desired tensile and ductility properties, impart levelling characteristics to the plating solution, and act as brighteners [100].

The electroless Ni plating technique

Electroless plating is undoubtedly the most important catalytic plating process in use today. The principal reasons for its widespread commercial and industrial use are to be found in the unique properties of the electroless nickel deposits. The chemical and physical properties of an electroless nickel coating depend on its composition, which in turn depends on the formation and operating conditions of the electroless plating bath. Typically, the constituents of an electroless nickel solution are: a source of nickel ions, a reducing agent, suitable complexing agents, stabilizers/inhibitors and energy [101].

The nickel source: The preferred source of nickel cations is nickel sulphate [101]. Other nickel salts, such as nickel chloride and nickel acetate, are used for very limited applications. The chloride anion can act deleteriously when the electroless plating bath is used to plate aluminum, or when the electroless nickel deposit is used as a protective coating over ferrous alloys in corrosion applications. The use of nickel acetate does not yield any significant improvement in bath performance or deposit quality when compared to nickel sulphate. Any minor advantages gained by nickel acetate are offset by its higher cost vs. the cost of nickel sulphate. The ideal source of nickel ions is the nickel salt of hypophosphorus acid, $Ni(H_2PO_2)_2$. The use of nickel

hypophosphite would eliminate the addition of sulphate ions and keep to a minimum the build-up of alkali metal ions while replenishing the reactants consumed during metal deposition.

Reducing agents: Four reducing agents are used in the chemical reduction of nickel from aqueous solutions: sodium hypophosphite, sodium borohydride, dimethylamine borane and hydrazine [101]. Some of the characteristics of the process are:

- The reduction of nickel is always accompanied by the evolution of hydrogen gas.
- The deposit is not pure nickel but contains either phosphorus, boron or nitrogen, depending on the reducing medium used.
- The reduction reaction takes place only on the surface of certain metals, but must also take place on the depositing metal.
- Hydrogen ions are generated as a by-product of the reduction reaction.
- The utilization of the reducing agent for depositing metal is considerable less than 100 percent.
- The molar ratio of nickel deposited to reducing agent consumed is usually equal to or less than 1.

Hypophosphite

Nickel deposition by hypophosphite was represented in the literature by the following equation:

$$Ni^{2+} + 2H_2PO_2^- + 2H_2O \rightarrow Ni^0 + 2H_3PO_3^- + 2H^+$$

The Borohydride Ion

The borohydride reducing agent may consist of any water-soluble borohydride compound. Sodium borohydride is generally preferred because of its availability. The borohydride ion is a powerful reducing agent:

$$4Ni^{2+} + BH_4^- + 8OH^- \rightarrow B(OH)_4^- + 4Ni^0 + 4H_2O$$

Hydrazine

Hydrazine is a powerful reducing agent in aqueous alkaline solutions. The hydrolyzed nickel ion mechanism can be modified to represent the experimental observations made during nickel reduction with hydrazine:

$$Ni^{2+} + N_2H_4 + 2OH^- \rightarrow Ni^0 + N_2 + 2H_2O + H_2$$

Complexing agents in electroless nickel plating

The additives referred to as complexing agents in electroless nickel plating solutions are, with two exceptions, organic acids or their salts [101]. The two exceptions are the inorganic pyrophosphate anion, which is used exclusively in alkaline electroless nickel solutions, and the ammonium ion, which is usually added to the plating bath for pH control or maintenance. There are three principal functions that complexing agents perform in the electroless plating bath:

- They exert a buffering action that prevents the pH of the solution from decreasing too fast.
- They prevent the precipitation of nickel salts, e.g. basic salts or phosphates.
- They reduce the concentration of free nickel ions.

Stabilizers: An electroless nickel plating solution can be utilized under normal operating conditions over extended periods without adding stabilizers. However, it may decompose spontaneously at any time [101]: bath decomposition is usually preceded by an increase in the volume of hydrogen gas evolved and appearance of a finely-divided black precipitate throughout the bulk of the solution. This precipitate consists of nickel particles, and either nickel phosphide or nickel boride, depending on the reducing agent being used.

Energy: Catalytic reactions, such as electroless nickel plating, require energy in order to proceed. The energy is supplied in the form of heat. Temperature is a measure of the energy (heat) content of the plating solution. Energy which is added to the plating bath is considered a bath variable like other reactants. The quality of energy required by the system or added to it is one of the most important factors affecting the kinetics and rate of the deposition reaction [101].

Effect of variables on the process: The metal and the electron source (the reducing agent) are consumed in the electroless plating reaction and so their concentrations in the bath are continuously decreasing [101]. There are no anodes available to maintain a near-constant metal concentration, and no external electron source (rectifier) to keep a constant flow of electrons moving into the system, as in an electrolytic plating process. In order to have a continuous and consistent electroless plating process, the reactants must be replenished. The electroless plating reaction not only yields a nickel alloy; it also generates by-products, which accumulate in the solution. As the concentrations of the by-products increase, their influence on the plating reaction also increases. There are a few variables that influence the deposition reaction, namely, the effect of reactants and temperature on rate, pH etc. The rate of the deposition reaction is dependent on temperature in an exponential manner, and the relationship is independent of the acidity or alkalinity of the solution. As the plating reaction proceeds, the pH of an alkaline solution decreases.

1.5 Nickel and Ni-alloys as materials for application and development of hydrogen economy

Nickel and its composite platings are important in several industries, which include automotive, manufacturing, chemical processing, etc. [102]. This is because nickel and nickel-based deposits are normally employed for their hardness, wear resistance and as anti-corrosive coatings.

Nickel is stable at intermediate pH and in basic solutions, and the $NiOOH/Ni(OH)_2$ couple is an active redox pair for many anodic reactions [103, 104]. Nickel and nickel-based deposits are also attractive for electrocatalytic synthesis. In addition, nickel alloyed with other transition metals, for example Zn, Mo, Co, Cr, etc., is one of the electrocatalysts with the lowest overpotential for hydrogen evolution. Nickel and nickel-based deposits are also used as active coatings on some substrates such as glassy carbon, stainless steel, etc. [103, 104, 105] in development of electrocatalysts.

As a result of the great practical importance of nickel and nickel-based oxides in a wide range of technological applications, their electrochemical properties in the alkaline media have been widely studied [106]. In addition, a model representing the Ni(III)/Ni(II) transition has been established as follows:

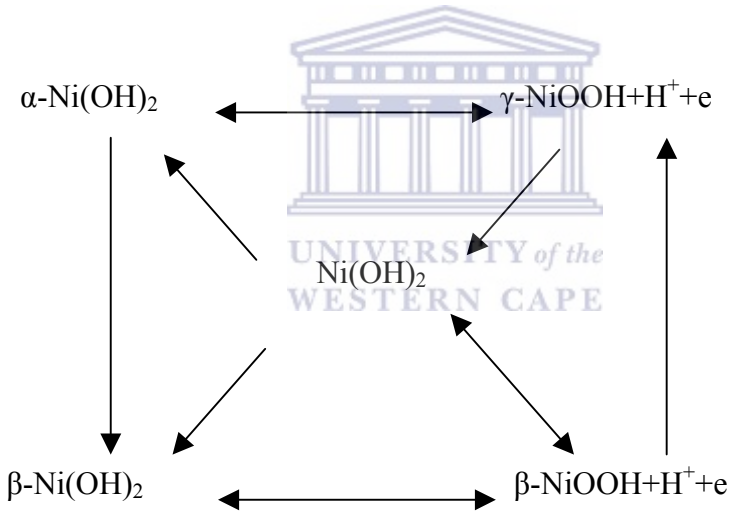

Several important steps are still unexplained because of the complicated redox properties of nickel oxides. However, the actual reasons responsible for the complicated nature of Ni-based oxides is still not clearly understood. It was found that doping the nickel oxide matrix with foreign cations for example, Co^{2+} and Zn^{2+}, improves the utilization of the electro-active material and depresses the capacity loss during long charge-discharge cycles [106].

Nickel and nickel-based oxides are also important electrode materials in nickel-based batteries. These batteries were usually prepared by a sol-gel process or a

cathodic precipitation using galvanostatic or potentiostatic methods [106]. Employing the cathodic precipitation is more desirable when preparing nickel oxides. On the other hand, it is very possible that the cathodically precipitated film is a mixture of metallic nickel and nickel hydroxide, especially in the solutions consisting of chloride precursors, since metallic Ni is very easily deposited from the cathodic electroplating of free nickel ions.

The incorporation of metals into/onto microporous matrices (pore size 0.1 to 100μm) or nanoporous matrices (several nm to 100nm) is relevant to a wide range of applications [107]. These include catalytic membrane reactors, high surface area electrocatalysts used in fuel cells and batteries [108] and modified electrodes. Furthermore, when the microporous material is used in separation/filtration processes, its partial metallization offers exciting opportunities for process improvement by electrochemical scrubbing or electro-filtration of the species to be separated [109]. If the matrix pores are completely filled with metal and the matrix is easy to etch off, as is the case for many polymeric matrices, then a reticulated metal structure can be obtained for use as a high surface area electrode, filtering medium or flame arrestor.

Anodic techniques developed for preparing nickel oxide in a wide range of technological applications in batteries, electro-chromic devices, water electrolysis, electrosynthesis and fuel cells, are considered to be more desirable. This anodic technique was not often employed for the electrode material preparation [102], especially in batteries application. Anodic deposition processes were developed to fabricate nickel oxides by means of a potentiostatic technique or cyclic voltammetry. These oxides are deposited from $NiCl_2$ to illustrate the powerful features of anodic deposition in preparing metal oxides since the electroplating of metal oxides from chloride precursors was recognized as a difficult issue. Nickel oxides anodically deposited by cyclic voltammetry and potentiostatic techniques from the chloride precursor solution, were demonstrated to be promising materials for nickel-based batteries. A typical cyclic voltammetry pattern of sintered nickel support, in 6M KOH is shown in **Figure 1.6**.

Raney-nickel and carbonyl nickel powder are employed as catalysts for the hydrogen electrode in an AFC because of their low corrosion rates in alkaline solution [110]. They can also be adapted in the field of chloralkine industries for use as an electrode active material in an electrolytic cell, where Raney-nickel survives as a coarse surface structure and contributes to the large surface area with the existence of micro/macropores. The total surface area of Raney-nickel catalyst is affected by the preparation method and the existence of promoters.

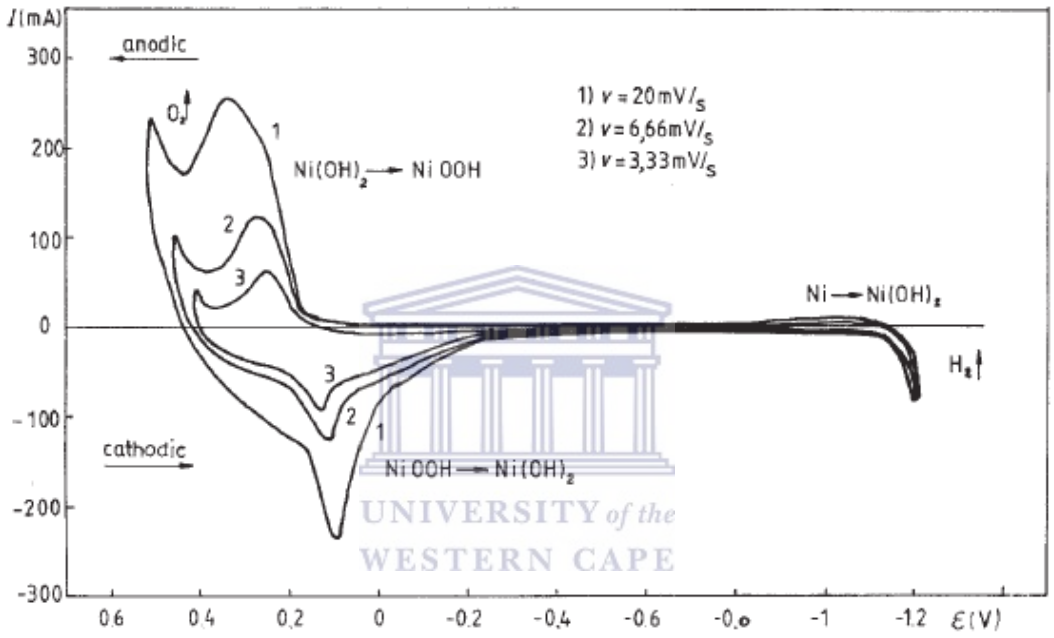

Figure 1.6: *A typical cyclic voltammetry pattern of sintered nickel support, in 6M KOH*. [111].

Raney-nickel is usually employed as the cathodic material for the hydrogen evolution reaction (HER), due to its capability to generate high currents per unit of external surface [112]. This property is based on both, its intrinsic electrocatalytic activity and its very high internal area originating from its nanoporous structure (pore diameter < 10nm). However, such small pore diameters cause a strong variation in the concentration of the dissolved molecular hydrogen inside the pore during the HER. The consequence of this concentration gradient is that only a small fraction of the

interfacial surface is efficiently used [113, 114]. In this context, macroporous nickel electrodes can be of great interest as an alternative to Raney-nickel since, although they have smaller roughness factors, their electrode surface is much more accessible.

It is well known that the surface morphology at both microscopic and nanoscopic levels exerts a marked influence on the electrocatalytic activity of an electrode [115]. At a microscopic level, the existence of pores, crevices, microcavities, etc. favours the increase of the electrode surface area, though mass transfer and ohmic bubble overvoltages prevent the rate of electrochemical reactions from increasing proportionally. An example is the Raney-nickel electrode used as cathodic material for the hydrogen evolution reaction, where it was found that only 1.5% of the available area was used in certain cases [116]. At nanoscopic levels, a change in the superficial ordering of the metal atoms can produce a significant effect in the kinetics of reactions involving adsorbed intermediates.

The most interesting features of Ni-based materials are that they have high specific energy and relatively low cost. However, an unstable maker capacity turnover has kept this interesting system from penetrating the market on a large scale. By end of the 1980s, the nickel–metal hydride system appeared in the market [117]. The main improvement compared to the other nickel-based rechargeable systems is the replacement of the anode by a material capable of reversibly storing hydrogen. This development was enabled by the availability of new hydrogen-storing alloys which are stable under exposure to strong caustic media and a high number of charge/discharge cycles [118]. Increased specific capacities and high capacity densities of the negative electrode, resulting from the employment of these hydride materials have been the reason for a considerable increase of energy storing capacity of cells manufactured therewith. Particularly, the increased energy density has been highly desired by the upcoming market for new portable applications in the last decade bringing about a variety of new electronic products such as notebook computers, mobile phones, consumer electronics, etc. NiMH batteries have subsequently taken over the biggest part of the NiCd market.

1.6 Nickel and Ni-oxides for alkaline water electrolysis

Hydrogen's energetic potential lies in its ability to serve as an energy source and medium, and its suitability for efficient energy storage, transport and manipulation with little or no pollution [119]. In addition, using different techniques, hydrogen can be directly converted into heat or electricity. The latter conversion principle offers much higher efficiencies of hydrogen utilization to produce electricity (up to 60%), than via its combustion in a thermal machine like thermo-electrical power plants.

Recent progress in technology makes hydrogen a realistic energy option thus hydrogen energy is becoming increasingly important. It is a long-term energy option, which means its one of "fuels of the future" for buildings, transportation, in portable application, vehicles and as a propellant for space mission, etc. It can be used as storage medium for intermittent and seasonal renewable technologies. It is also used for upgrading many metallurgical processes, as well as a chemical in different kind of industries. Hydrogen will join with "electricity" in the 21st century as a primary energy carrier in the sustainable energy future. Both electricity and hydrogen in the future will be mostly derived from either renewable or nuclear energy sources [119].

Hydrogen as an energy storage medium has attracted worldwide interest, as it is a clean and fully recyclable substance with a practically unlimited supply [120]. The hydrogen energy system consists mainly of three processes: its production, transport or storage, and utilization. Large-scale, cheap production of hydrogen is one of the key links in the course of developing the novel hydrogen energy system.

Water electrolysis is considered an attractive process for the production of hydrogen, in particular for the large-scale production of hydrogen gas today [121, 122, 123]. The main operating cost of the process is the cost of electrical power which is used to activate the charge transfer reactions at the electrode/electrolyte interface and to overcome the resistivity of the electrolyte [124]. However, a lowering of the electrolytic energy consumption is required in order to make water electrolysis more

competitive and more efficient. One of the ways of lowering the energy consumption is to reduce the hydrogen evolution overpotential of the cathode in the electrolysis process. Several materials [125] have been studied as electrocatalysts for the hydrogen evolution reaction.

The electrolyte used in the conventional alkaline water electrolysers has traditionally been aqueous potassium hydroxide (KOH), mostly with concentration of 20-40 wt.% operating at temperatures ranging from 20 to 90°C. A small amount (4%) of the world's hydrogen is produced by electrolysis of water. For users requiring small amounts of extremely pure hydrogen, electrolysis can be a cost-effective means of obtaining the required hydrogen. Water electrolysis is a very important technology for the large scale production of hydrogen [123].

1.7 Conclusions and scope of investigation

Preparation of finely dispersed powders, metals, compounds and superfine-grained materials, intended for various areas of science and engineering, is one of the challenges faced in modern nanotechnology. The consolidated nano- and microcrystal materials have attracted fundamental and applied interest. The template synthesis method, based on the use of ultraporous polymeric and inorganic templates, is currently actively used for synthesizing consolidated materials. This method allows for the fabrication ensembles of nano- and microstructured tubes and wires consisting of conducting polymers, metals and semiconductors. The structure of these materials is an exact replica of the template matrix.

The electrochemistry of micro- and nanoelectrodes is one of the fast developing application areas of structures obtained by the template synthesis method. Here we investigate an alternative approach to preparation and research on the properties of a new category of materials, namely the nano- and microstructured nickel, as medium in hydrogen electrochemical systems. From a fundamental research perspective, synthesis of this class of materials permits solutions to problems influenced by dimensional effects caused by changes to physical and chemical

properties of substances at the transition from bulk materials to nanostructures. From the applied research point of view the developed materials open up new prospects for the creation of microelectrodes for hydrogen generation, electrochemical power sources, and electrochemical mini-analyzers.

The fundamental purpose of this research is to create consolidated nanomaterials using scientifically proven technology. Nickel was selected as one of the ideal materials. Firstly, a wide range of physical and chemical properties of nickel in macro or bulk form, especially the electrochemical properties, have been well investigated. Secondly, nickel is one of the metals considered for hydrogen evolution which was roughly developed in the last decade and where template synthesis opens up new prospects. It allows synthesis of nanomaterials on a substrate with various aspect ratios which are easy to investigate.

The objectives of these study were as follows:

1. To determine the optimal conditions for a homogeneous growth and, in addition, to find the deposition parameters, namely overvoltage, temperature and electrolyte solution, required for the growth of crystalline nickel micro- and nanowires. Track-etched membranes, which allow varying size of nickel materials between 30nm and 10μm, will be used as template. As a fundamental method of template pore filling, an electrochemical deposition method for nickel will be used.

2. To investigate the influence of electrolyte composition on the electrochemical deposition of nickel in pores of the template on structural parameters of attained materials (*Mirror*, *Hard* and *Watt* bath solutions). As a fundamental method of analysis, SEM will be used. No study was found in the literature which directly used *Hard* and *Mirror* nickel electrolyte solutions to prepare the micro- and nanostructures.

3. To synthesize a unique porous track, templates with pore diameter about 10nm were identified as a significant size for nanomaterials and to use them as base

for nickel nanostructures. Structural properties analysis would be undertaken by SEM, TEM and AFM.

4. To investigate hydrogen and oxygen reactions of nickel wires with diameter between 0.01 and 1μm diameter and length 10μm. The investigation will be more focused on the hydrogen evolution reaction. The electrochemical methods used for analysis will be Cyclic Voltammetry (CV) and Chronoamperometry (CA) where a three electrode system will be used.

5. To investigate the catalytic properties of material using different electrochemical deposition conditions during nickel structure preparation. Track membranes with 0.4μm pore diameter were used as the template. *Mirror*, *Hard* and *Watt* nickel plating baths were used as electrolytes for electrodeposition of nickel.

6. To develop an electroless method for nickel pore filling of templates and to investigate a use of this method for the fabrication of nanomaterials. To carry out a comparative analysis of the catalytic properties of materials obtained by electrochemical and chemical deposition methods.

7. To study the role played by thermal annealing on microstuctured nickel in the area of the recrystallization temperature ($T = 0.35T_{Melting}$) and to study its catalytic properties.

8. To investigate the crystallinity of prepared nickel materials by the XRD technique and to determine the influence of the template parameters on crystallinity of obtained nickel.

Different materials can be deposited into the pores electrochemically to replicate ion tracks in membranes. This is the basic idea of the so-called template method [2]. This technique is applied to fabricate large-area arrays of identical micro- and nanowires. Template synthesis is the deposition of solids into matrices. The incorporation of metallic particles into polymer matrices has gained wide interest for

electrolytic purposes. In the preceding paragraphs an overview of the different types of template matrices was provided. The basic principles of template synthesis, pore filling and conductive layer deposition were investigated. This was followed by an overview and development of different metal structured electrodes for hydrogen production. In the experimental section a short summary of the nickel deposition techniques (**Chapter 2**) and characterization tools will be given. Afterwards the most important electrochemical techniques and measurements set-up applied throughout this study are introduced. This thesis deals with two different aspects, "*fabrication of novel nickel wires using the template synthesis technique*" and "*characterization of modified electrodes for hydrogen evolution reaction*". Experimental details of electrode treatment and characterization as well as of the specific measurement set-up are shortly described. The results section provides a description of measurements performed on different electrodes. A comparative discussion of these results contains analysis of the hydrogen evolution reaction on different electrodes. **Chapter 3** also deals with the investigation of modified nickel electrodes. The experimental details of the applied measurement set-up and the electrode pre-treatment will be described. This is followed by the presentation of the morphological and electrochemical results obtained from measurements.

1.8 References

[1] G.B. Khomutov, V.V. Kislov, M.N. Antipina, R.V. Gainutdinov, S.P. Gubin, A.Yu. Obydenov, S.A. Pavlov, A.A. Rakhnyanskaya, A.N. Sergeev-Cherenkov, E.S. Soldatov, D.B. Suyatin, A.L. Tolstikhina, A.S. Trifonov and T.V. Yurova, *Microelectronic Engineering* 69, (**2003**) 373.

[2] A. Huczko, *Applied Physics* A70, (**2000**) 365.

[3] Sanjeev Kumar, Rajesh Kumar, Shyam Kumar and S.K. Chakarvarti, *Current Science* 87, (**2004**) 642.

[4] R.T. Bate, *Nanotechnology* 1, (**1990**) 1.

[5] R. Garcia, *Applied Physics Letter* 60, (**1992**) 1960.

[6] I.-W. Lyo and P. Avouris, *Science* 253, (**1991**) 173.

[7] M. Crommie, C.P. Lutz and D.M. Eigler, *Science* 262, (**1993**) 218.

[8] C.J.A. Monty, *High Temperature Chemistry Processes* 3, (**1994**) 467.

[9] Maria Eugenia Toimil Molares, *Fabrication and characterization of copper nanowires electrochemically deposited in etched ion-track membranes,* Ph. D Dissertation, Ruperto-Carola University of Heidelberg, Germany, **2001**.

[10] J.C. Hulteen and C.R. Martin, *Journal of Material Chemistry* 7, (**1997**) 1075.

[11] G.A. Ozin, *Advanced Materials* 4, (**1992**) 612.

[12] G. Hodes, I.D.J. Howell and L.M. Peter, *Journal of the Electrochemical Society* 139, (**1992**) 3136.

[13] C.R. Martin, *Chemical Materials* 8, (**1996**) 1739.

[14] R.V. Parthasarathy and C.R. Martin, *Journal of Polymer Science* 62, (**1996**) 875.

[15] C.R. Martin and R.V. Parthasarathy, *Advanced Materials* 7, (**1995**) 487.

[16] R. Parthasarathy and C.R. Martin, *Nature (London)* 369, (**1994**) 298.

[17] C.R. Martin, R.V. Parthasarathy and V. Menon, *Synthetic Metals* 55-57, (**1993**) 1165.

[18] C.R. Martin, *Advanced Materials* 3, (**1991**) 457.

[19] Z. Cai, J. Lei, W. Liang, V. Menon and C.R. Martin, *Chemistry of Materials* 3, (**1991**) 960.

[20] W. Liang and C.R. Martin, *Journal of the American Chemical Society* 112, (**1990**) 9666.

[21] J.C. Hulteen, V.P. Menon and C.R. Martin, *Journal of the Chemical Society, Faraday Transactions* 92, (**1996**) 4029.

[22] V.P. Menon and C.R. Martin, *Analytical Chemistry* 67, (**1995**) 1920.

[23] M. Nishizawa, V.P. Menon and C.R. Martin, *Science* 268, (**1995**) 700.

[24] C.J. Brumlik, V.P. Menon and C.R. Martin, *Journal of Materials Research* 9, (**1994**) 1174.

[25] C.A.J. Foss, G.L. Hornyak, J.A. Stockert and C.R. Martin, *Journal of Physical Chemistry* 98, (**1994**) 2963.

[26] C.A.J. Foss, G.L. Hornyak, J.A. Stockert and C.R. Martin, *Advanced Materials* 5, (**1993**) 135.

[27] C.A.J. Foss, G.L. Hornyak, J.A. Stockert and C.R. Martin, *Journal of Physical Chemistry* 96, (**1992**) 7497.

[28] C.J. Brumlik, C.R. Martin and K. Tokuda, *Analytical Chemistry* 64, (**1992**) 1201.

[29] C.J. Brumlik and C.R. Martin, *Journal of the American Chemical Society* 113, (**1991**) 3174.

[30] G.L. Hornyak and C.R. Martin, *Journal of Physical Chemistry* 101, (**1997**) 1548.

[31] J.D Klein, R.D.I. Herrick, D. Palmer, M.J. Sailor, C.J. Brumlik and C.R. Martin, *Chemistry of Materials* 5, (**1993**) 902.

[32] R.V. Parthasarathy, K.L.N. Phani and C.R. Martin, *Advanced Materials* 7, (**1995**) 896.

[33] J.C. Hulteen, X.C. Chen, C.K. Chambliss and C.R. Martin, *Nanostructured Materials* 9, (**1997**) 133.

[34] S.K. Chakarvarti and J. Vetter, *Nuclear Instruments and Methods in Physics Research* B62, (**1991**) 109.

[35] C.P. Bean, U.S. Patent No. 34,83,095, **1969**.

[36] G.E. Possin, *Review of Scientific Instruments* 41, (**1970**) 772.

[37] R. Spohr, US Paten 4338164, **1982**.

[38] W.D. Williams and N. Giordano, *Review Science and Instruments* 55, (**1984**) 410.

[39] R.M. Penner and C.R. Martin, *Analytical Chemistry* 59, (**1987**) 2625.

[40] S.K. Chakarvarti and J. Vetter, *Nuclear Instruments and Methods in Physics Research* B62, (**1991**) 109.

[41] D. Dobrev, J. Vetter, N. Angert and R. Neumann, *Applied Physics* A69, (**1999**) 233.

[42] M. J. Tierney and C. R. Martin. *Journal of Physical Chemistry* 93, (**1989**) 2878.

[43] W. Kautek, S. Reetz and S. Pentzien, *Electrochimica Acta* 40, (**1995**) 1461.

[44] D. Dobrev, J. Vetter, N. Angert and R. Neumann, *Electrochimica Acta* 45, (**2000**) 3117.

[45] T.M. Whitney, J.S. Jiang, P.C. Searson and C.L. Chien, *Science* 216, (**1993**) 1316.

[46] D. Dobrev, J. Vetter, N. Angert and R. Neumann, *Applied Physics* A72, (**2001**) 729.

[47] D. Al-Mawlawi, C. Z. Liu and M. Moskovits, *Journal of Materials Research* 9, (**1994**) 1014.

[48] D. Dobrev, J. Vetter and R. Neumann, *Nuclear Instruments and Methods in Physics Research* B146, (**1998**) 513.

[49] S. De Vito and C.R. Martin, *Chemistry of Materials* 10, (**1998**) 1738.

[50] M. Nishizawa, K. Mukai, S. Kuwabata, C.R. Martin and H. Yoneyama, *Journal of the Electrochemical Society* 144, (**1997**) 1923.

[51] B.B. Lakshmi, C.J. Patrissi and C.R. Martin, *Chemistry of Materials* 9, (**1997**) 2544.

[52] B.Z. Tang and H. Xu, *Micromolecules* 32, (**1999**) 2569.

[53] P. Tomassi and Z. Buczko: *XIth Seminar Tempus JEP 09032-95*, Athens, 7-9.05.**1998**.

[54] Joint Institute for Nuclear Research website. Available online in http://flerovlab.jinr.ru/flnr/index.htm.

[55] S. Iijima, *Nature* 354, (**1991**) 56.

[56] T.W. Ebbesen and P.M. Ajayan, *Nature* 358, (**1992**) 220.

[57] H. Lange, A. Huczko, P. Byszewski, E. Mizera and H. Shinohara, *Chemical Physics Letters* 289, (**1998**) 174.

[58] V. Ivanov, J.B. Nagy, Ph. Lambin, A. Lucas, X.B. Zhang, X.F. Zhang, D. Bernaerts, G. Van Tendeloo, S. Amelinckx and J. Van Landuyt, *Chemical Physics Letters* 223, (**1994**) 329.

[59] L.A. Chernozatonskii, Z.Y. Kosakovskaya, E.A. Fedorov and V.I. Panov, *Physics Letters* A197, (**1995**) 40.

[60] M. Ge, K. Sattler, *Applied Physics Letters* 64, (**1994**) 710.

[61] G. Che, B.B. Lakshmi, E.R. Fisher and C.R. Martin, *Nature* 393, (**1998**) 346.

[62] T. Kyotani, L.-F. Tsai and A. Tomita, *Chemistry of Materials* 8, (**1996**) 2109.

[63] X.-Y. Song, W. Cao, M.R. Ayers and A.J. Hunt, *Journal of Materials Research* 10, (**1995**) 251.

[64] Z.F. Ren, Z.P. Huang, J.W. Xu, J.H. Wang, P. Bush, M.P. Siegal and P.N. Provencio, *Science* 282, (**1998**) 1105.

[65] R. Dagani, *Chemical and Engineering News* **79**, (204) 14.

[66] N.K. Raman, M.T. Andreson and C.J. Brinker, *Chemistry of Materials* 8, (**1996**) 1682.

[67] P.M. Ajayan, O. Stephen and Ph. Redlich, *Nature* 375, (**1995**) 564.

[68] W. Han, S. Fan, Q. Li and Y. Hu, *Science* 277, (**1997**) 1287.

[69] C.-G. Wu and T. Bein, *Science* 264, (**1994**) 1757.

[70] E.W. Wong, B.W. Maynor, L.D. Burns and C.M. Lieber, *Chemistry of Materials* 8, (**1996**) 2041.

[71] D. Al-Mawlawi, N. Coombs and M. Moskovits, *Journal of Applied Physics* 70, (**1991**) 4421.

[72] T. Thurn-Albrecht, J. Schotter, G.A Kaestle, N. Emley, T. Shibauchi, L. Krusin-Elbaum, K. Guarini, C.T. Black, M.T. Tuominen and T.P. Russell, *Science* 290, (**2000**) 2126.

[73] R.J. Tonucci, B.L. Justus, A.J. Campillo and C.E. Ford, *Science* 258, (**1992**) 783.

[74] J.S. Beck, J.C. Vartuli, W.J. Roth, M.E. Leonowicz, C.T. Kresge, K.D. Schmitt, C.T.-W. Chu, D.H. Olson, E.W. Sheppard, S.B. McCullen, J.B. Higgins and J.L. Schlenker, *Journal of the American Chemical Society* 114, (**1992**) 10834.

[75] K. Douglas, G. Devaud and N.A. Clark, *Science* 257, (**1992**) 642.

[76] T.D. Clark and M.R. Ghadiri, *Journal of American Society* 117, (**1995**) 12364.

[77] R. Schollhorn, *Chemical Materials* 8, (**1996**) 1747.

[78] P.Yu. Apel, *Radiation Measurements* 34 (1-6), (**2001**) 559.

[79] P. Vater, *Nuclear Tracks and Radiation Measurement* 15, (**1988**) 743.

[80] W. Han, S. Fan, Q. Li, B. Gu, X. Zhang and D. Yu, *Applied Physics Letters* 71, (**1997**) 2271.

[81] C.R. Martin, *Science* 266, (**1994**) 1961.

[82] P.Yu. Apel, A.Yu. Didyk, B.I. Fursov, L.I. Kravets, V.G. Nesterov, L.I. Samoilova and G.S. Zhdanov, *Radiation Measurements* 28, (**1997**) 19.

[83] R. Mazzei, O.A. Bernaola, G. Saint Martin, B. Molinary de Ray, *Nuclear Instruments and Methods in Physics Research* B9, (**1985**) 163.

[84] D. Dobrev, J. Vetter, R. Neumann and N. Angert, *Journal of Vacuum Science and Technology* B19, (**2001**) 1385.

[85] C. Trautmann, W. Brueckle, R. Spohr, J. Vetter and N. Angert, *Nuclear. Instruments and Methods in Physics Research* B111, (**1996**) 70.

[86] V.I. Kuznetsov, A.Yu Didyk and P.Yu Apel, *Nuclear Tracks and Radiation Measurements* 19, (**1991**) 919.

[87] P.Yu. Apel, *Radiation Measurements* 25, (**1995**) 667.

[88] W. Starosta, B. Wawszczak, B. Sartowska, and M. Buczkowski, *Radiation Measurements* 31, (**1999**) 149.

[89] Y. Komaki, N. Ishikawa, T. Sakurai, N. Morishita and M. Iwasaki, *Nuclear Instruments and Methods in Physics Research* B34, (**1988**) 332.

[90] V.V. Shirkova and S.P. Tretyakova, *Radiation Measurements* 28, (**1997**) 791.

[91] K. Ogura, T. Hattori, M. Hirata, M. Asano, M. Yoshida, M. Tamada, H. Omichi, N. Nagaoka, H. Kubota and R. Katakai, *Nuclear Tracks and Radiation Measurements* 25, (**1995**) 159.

[92] C. Daubresse, E. Ferain and R. Legras, *Nuclear Instruments and Methods in Physics Research* B122, (**1997**) 89.

[93] S.N. Dmitriev, L.I. Kravets and V.V. Sleptsov, *Nuclear Instruments and Methods in Physics Research* B142, (**1998**) 43.

[94] J. Marchand-Brynaert, M. Deldime, I. Dupont, J.-L. Dewez, and Y.-J. Schneider, *Journal of Colloidal Interface Science* 173, (**1995**) 236.

[95] J.I. Calvo, A. Hernandez, G. Martinez and L. Martinez, *Journal of Colloid and Interface Science* 175, (**1995**) 138.

[96] E.M. Tracey and R.H. Davis, *Journal of Colloid Interface Science* 167, (**1994**) 104.

[97] A.V. Mitrofanov, F.A. Pudonin, P.Yu. Apel and T.I. Gromova, *Nuclear Instruments and Methods in Physics Research* A282, (**1991**) 347.

[98] C.A. Pasternak, G.M. Alder, P.Yu. Apel, C.L. Bashford, D.T. Edmonds, Y.E. Korchev, A.A. Lev, G. Lowe, M. Milovanovich, C.W. Pitt, T.K. Rostovtseva and N.I. Zhitariuk, *Radiation Measurements* 25, (**1995**), 675.

[99] George A. DiBari, Nickel Plating, *International Nickel Inc.*, Saddle Brook, N.J, **1989**.

[100] Aleksander Ciszewski, Szymon Posluszny, Grzegarz Milczarek and Marek Baraniak, *Surface and Coatings Technology* 183, (**2004**) 127.

[101] G.O. Mallory and J.B. Hajd (editors), *Electroless Plating: Fundamentals and Applications*, American Electroplaters and Surface Finishers Society, Orlando, FL, **1990**.

[102] Chi-Chang Hu, Chiou-Yi Lin and Ten-Chin Wen, *Materials Chemistry and Physics* 44, (**1996**) 233.

[103] T.-C. Wen, C.-C. Hu and Y.-J. Li, *Journal of the Electrochemical Society* 140, (**1993**) 2554.

[104] T.-C. Wen, S.-M. Lin and J.-M. Tsai, *Journal of the Electrochemical Society* 24, (**1994**) 449.

[105] C. Fan, D.L. Piron, A. Sleb and P. Paradis, *Journal of the Electrochemical Society* 141, (**1994**) 382.

[106] Chi-Chang Hu and Chen-Yi Cheng, *Journal of Power Sources* 111, (**2002**) 137.

[107] S. Sotiropoulos, I.J. Brown, G. Akay and E. Lester, *Materials Letters* 35, (**1998**) 383.

[108] S. Ye, A.K. Vijh and L.H. Dao, *Journal of the Electrochemical Society* 144, (**1997**) 90.

[109] Hong-Ki Lee, Eun-Ey Jung and Ju-Seong Lee, *Materials Chemistry and Physics* 55, (**1998**) 89.

[110] T. Tomida and I. Nakabayashi, *Journal of the Electrochemical Society* 136, (**1989**) 3296.

[111] Eleonora Maria Rus, Delia Maria Constantin, Liviu Oniciu and Lucretia Ghergari, *Croatica Chemica Acta* 72 (1), (**1999**) 25.

[112] C.A. Marozzi and A.C. Chialvo, *Electrochimica Acta* 46, (**2001**) 861.

[113] S. Rausch and H. Wendt, *Journal of Applied Electrochemistry* 22, (**1992**) 1025.

[114] S. Rausch and H. Wendt, *Journal of the Electrochemical Society* 143, (**1996**) 2852.

[115] C.A. Marozzi and A C. Chialvo, *Electrochimica Acta* 45, (**2000**) 2111.

[116] H. Ogawa, M. Koma, H. Kawano and J. Matrumoto, *Journal of Power Sources* 12, (**1988**) 339.

[117] Uwe Kohler, Christina Antonius and Peter Bauerlein, *Journal of Power Sources* 127, (**2004**) 42.

[118] Dragica Lj. Stojic, Milica P. Marceta, Sofija P. Sovilj and Scepan S. Miljanic, *Journal of Power Sources* 118, (**2003**) 315.

[119] C.-C. Hu and T.-C. Wen, *Electrochimica Acta* 43, (**1998**) 1747.

[120] H. Cheng, K. Scott and C. Ramshaw, *Journal of the Electrochemical Society* 149(11), (**2002**) D172.

[121] Weikang Hu and Jai-Young Lee, *International Journal of Hydrogen Energy* 23(4), (**1998**) 253.

[122] N. Nagai, M. Takeuchi, T. Kimura and T. Oka, *International Journal of Hydrogen Energy,* 28 (**2003**) 35.

[123] M.S. El-Deab, M.E. El-Shakre, B.E. El-Anadouli and B.G. Ateya, *International Journal of Hydrogen Energy* 21(4), (**1996**) 273.

[124] M.J. Giz, S.C. Bento and E.R. Gonzalez, *International Journal of Hydrogen Energy* 25, (**2000**) 621.

[125] C.E. Gregoire Padro and V. Putsche, *Survey of the Economics of Hydrogen Technologies*, *National Renewable Energy Laboratory*, (**1999)** 8.

Chapter 2: Materials and Methods

This section provides a thorough description of the methodology and materials used in this study. Production of stable nickel structures in polyethylene terephthalate (PET) membrane by electrodeposition using etched ion tracks as template is illustrated in **Figure 2.1**. In the first step, the PET membrane was created by heavy-ion irradiation and chemical etching (**2.1(a)**) as described in detail in sections 2.1.2 & 2.1.3, respectively. Then, a conductive layer was evaporated on one side of the membrane and reinforced by galvanostatic electroplating with nickel (**2.1(b)**) (see section 2.2).

This conductive layer provides a stable substrate for the growth of the wires and serves as a cathode during pore filling. The deposition process can be stopped during the growth of nickel in the pores forming wires (**2.1(c)**), or it can be continued over a longer time forming in addition, caps on top of the wires (**2.1(d)**). For characterization of the resulting structures by scanning electron microscopy (SEM), the PET membrane is dissolved in an appropriate solvent, e.g., potassium hydroxide (KOH) or sodium hydroxide (NaOH) (**2.1(e&f)**).

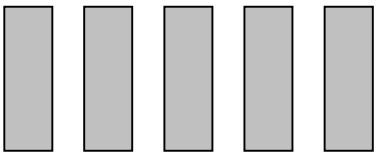

(a) *Etching of the latent ion track by an appropriate etchant to required diameters of the pores (see* ***section 2.1****).*

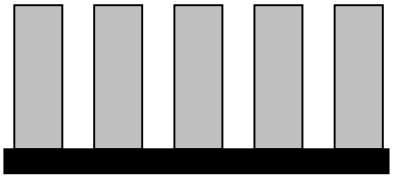

(b) *Sputtering or evaporation and electrochemical deposition of nickel conductive film onto one side of the obtained membrane (see* ***section 2.2****).*

(c) *Electrofilling of the PET pores through their open side (see* ***section 2.3****).*

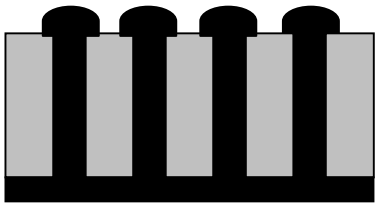

(d) *Caps overgrowth on the PET template surface (as shown in* ***section 2.3****.).*

(e) *Removal of the template by dissolution (see* ***section 2.3****).*

(f) *Removal of the template by dissolution (see* ***section 2.3****).*

Figure 2.1: *Principal diagram of the method for fabrication of stable standing microstructures using etched ion track templates.*

2.1 Preparation of track-etched templates

Material Used*: Polyethylene terephthalate (PET) membrane*

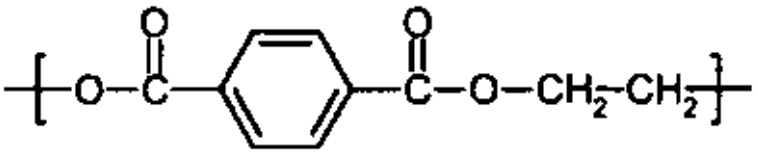

Figure 2.2: *Structural formulae of polyethylene terephthalate membrane (PET).*

In this investigation PET membrane foils (trade names Hostaphan and Lavsan) were employed. PET foils possess high heat resistance and chemical stability. Due to the production process it is not transparent. PET membranes are resistant to acids, bases, some solvents, and oils and fats. PET was chosen because homogeneous cylindrical pores can be created. PET is used for high-impact resistant containers under suitable conditions. It is used for packaging of soda, mouthwash, pourable dressings, edible oils, and peanut butter. Lavsan fabric is used in the dairy industry for filtering and in medicine for plastic vessels and implantation.

Track membranes made of PET have high mechanical strength at low thickness, narrow pore size distribution, and low content of extractables [1]. The mechanical strength and chemical compatibility of the PET films are satisfactory for many applications [[87]:**Chapter 1**]. The quality of the PET films is highly reproducible which is of key importance for membrane production. Some properties of the PET polymeric membrane are given in **Table 2.1**. The physical and chemical properties of track-etched membranes are determined by their matrix material i.e. by the type of the polymer.

Table 2.1: *Polyethylene terephthalate membrane properties* [[88]:**Chapter 1**].

Parameters	*Property*
Gas transition temperature	78°C
Continuous use temperature	130°C
Shrinkage (190°C, 5min, MD)	>2%
Hydrolysis resistance (retention of tensile strength, 90°C, 1689 hrs)	30%
Water vapour transmission	20g/m^2/day
Weather resistance (time to 50% reduction in tensile strength)	500hrs
Young's Modulus	4000Mpa

Irradiation of PET membranes

In this investigation stacks of PET foils, of thickness 10 - 30μm, were irradiated with 11MeV/u high charged xenon (Xe) ions at normal incidence. The fluences used for irradiation are in the range 10^6 to 10^9 ions/cm^2. During irradiation by swift ions, latent ion tracks were formed along the path of the ions. Under these conditions, the penetration range of the ions in the PET was larger than the total thickness of the stack, and the linear energy loss of the ions in the polymer was well above the threshold required for homogeneous etching. Next, the samples were exposed to ultra-violet (UV) radiation. This sensitization treatment improves the track etch selectivity, i.e. higher aspect ratios, smaller statistical distribution of etching rate and thus of final dimensions of etched pores.

After the sensitization of tracks with UV radiation and chemical etching, pores with defined shapes were obtained. In this way, pores of various shapes can be fabricated, e.g., cylindrical, conical, bi-conical and funnel-shaped [[85]:**Chapter 1**] as shown in **Figure 2.3**. Besides, depending on the material, the chemistry of the pore wall, and the techniques employed, the resulting cylinders may be solid or hollow, forming wires or tubes, respectively [2, [24]:**Chapter 1**]. In most cases, the material adopts the shape and the size of the hosting hole.

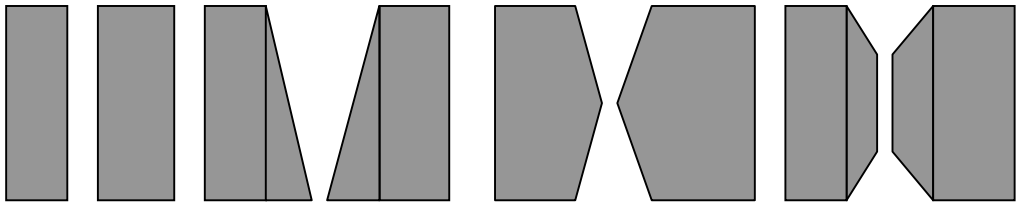

Figure 2.3: *Schematic representation of various geometries that can be created by etching heavy ion tracks in PET polymer membranes: (a) cylindrical, (b) conical, (c) bi-conical and (d) funnel-shaped.*

PET polymer films are most frequently used for track membrane production [3]. All the polymer foils employed in this work were irradiated using the cyclic accelerator V-400 at the Joint Institute for Nuclear Research (JINR) in Dubna (Russia).

Etching: After irradiation, the latent tracks created by ions on their way through the foils were enlarged to cylindrical pores with diameters between 100 and 400nm by exposure to a suitable etchant. For PET exposed to Xe ions, a change in the concentration of aqueous alkali solutions enabled a gradual change in the etch rate ratio from units to thousands. In the present work, the method of layer by layer etching as described by Vilensky *et al.* [3] was used as chemical treatment. The radiolysis products from the core and from the linear track area were extracted by water to the full elimination from tracks [4, 5]. After that the radiolysis products from the other track areas were extracted by a combination of etching processes at different temperatures.

The etching was performed in aqueous NaOH solution with addition of methanol, either by completely dipping the irradiated foils into an etching pot in the case of cylindrical pores, or by exposing only one side of the membrane to the etching solution after inserting the foil in an electrolytic cell consisting of two chambers. The solution was prepared with de-ionised water. The two parameters which are important for the shape of the resulting pore are the bulk etch rate, the etch rate of the non-irradiated material, and the etch track rate, i.e. the etch rate along the ion track. Cylindrical pores were obtained for high track etch rate/bulk etch rate ratios. The diameter of the resulting pores increased linearly with etching time.

After etching, the samples were carefully rinsed with de-ionised water. Pieces of samples were then placed in a sample holder and a thin nickel layer was vacuum evaporated on the surface. The etched samples were then characterized by SEM. Pore diameter and density were carefully determined for each sample piece. The author would like to acknowledge the JINR institute in Dubna for the extensive help with sample etching.

Preparation of asymmetrical nanoporous track-etched membranes

Presented next is a description of a unique technique used to fabricate and characterize asymmetric track-etched membranes which were prepared in close collaboration with the JINR research group in Dubna under the supervision of Prof. Y. Apel and the State Institute of Highly Pure Biopreparations (SIHPB) in St. Petersburg.

Irradiation: Single foils or foil stacks of PET (23μm thick) membranes were irradiated perpendicular to the surface in the heavy ion accelerator (U-100) at JINR. During the irradiation, the film was kept in the ion beam, and the final irradiation fluence was calculated from measured ion beam fluence and irradiation time. Various ions such as ^{132}Xe and ^{84}Kr were used at fluences of 4.9×10^9 ions/cm^2.

Conditions of etching: Chemical etching of the tracks in PET foils was performed in 5M KOH aqueous solution at 70°C. To etch the track from one side, the irradiated foil was placed between the two chambers of a cell. One chamber of the cell was filled the etchant (i.e. 5M KOH at 70°C) while the other side of the membrane was protected by a stopping medium (1% of Triton x100). Immediately, when the etchant reaches the opposite surface of the sample, a stopping solution neutralizes the KOH etchant. Longer etching leads to a gradual increase of the pore opening. The duration of the etching process was 15, 17 and 20 minutes, respectively. Due to the etching velocity of the treated layer being lower than that of the bulk material, this led to the formation of track-etched membranes with asymmetric structure. A Schematic diagram of the cell used during the etching of asymmetrical membranes is shown in **Figure 2.4**.

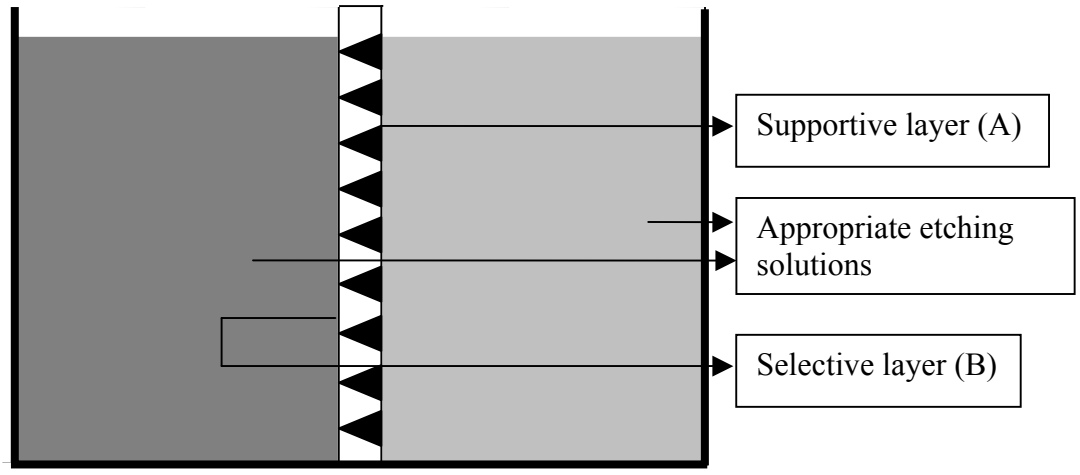

Figure 2.4: *Schematic diagram of the cell used during the etching of asymmetrical membranes.*

Pore structure analysis: The asymmetrical membrane structures were investigated by a calibration method developed by Prof. A.N. Cherkasov [6, 7]. To study the structure of ultrafiltration (UF) membranes, a number of physical and chemical methods are typically used. Among these methods are different kinds of microscopy, namely, transmission, scanning, atomic force, etc. Besides the highly informativeness of these methods, their use is limited by the high cost of instrumentation and difficulty in handling the delicate membrane. Therefore, to characterize selective and structural properties of asymmetrical track-etched membranes, the calibration method was used.

Using the data acquired from the membrane calibration method provides the possibility not only to assume membrane retention curve but also to determine an average pore size and pore size distribution (PSD). It can also be used to detect the defects of ultrafiltration (UF) membranes and to assess the thickness of selective layers. Membrane calibration is distinct from most structure analysis methods. No expensive equipment is needed because membrane characteristics can be determined from data of simple UF equipment. It must also be emphasized that this type of structure analysis is highly time-efficient. The summary of experimental procedure is presented in **Table 2.2**.

Table 2.2: *Summary of experimental parameters used during the preparation of asymmetrical membranes.*

Sample Name	Membrane thickness (L), μm	Pore density x 10^9 cm^{-2}	Etching time min
ATM1	23	4.9	15
ATM2	23	4.9	17
ATM3	23	4.9	20

The calibration procedure is carried out by either passing solutions of different water soluble polymers, like dextranes, polyethylene glycols, proteins etc., through the membrane while checking the concentration in the permeate and bulk, or by passing the mixtures of these polymers in Gel Chromatographic Concentration Analysis. The membrane calibration method which uses protein mixtures, appeared to be more reliable and less difficult compared to the well established methods. For characterization of asymmetrical track-etched membrane, the protein mixtures with different molecular weights were used (as shown in **Table 2.3**).

Table 2.3: *Summary of model protein mixtures (MPM) used for PET calibration.*

	N	M 10^3, g/mol	r_S, Å	pI	*	**	***
1	Tryptophan	0.204	3.7	-	+	+	
2	Bacitracin	1.45	8.3	7.1-7.2	+		
3	Vitamin B_{12}	1.36	7.8	-		+	
4	Cytochrome C	12.4	17.6	10.6	+	+	+
5	Chymotrypsinogen	24.0	22.7	9.5		+	+
6	Ovalbumin	44.0	28.6	4.6		+	+
7	Bovin serum albumin	67.0	34.0	4.7		+	
8	Γ-globulin	160.0	46.5	7.1		+	+
9	Catalase	232.0	53.5	5.4-5.7			+
10	Ferritin	440.0	68.0	-			+
11	Thyroglobulin	690.0	83.0	4.5			+

* Low molecular MPM (MWCO ÷ (100-20 000) g/mol), ($C_\Sigma \approx 0.12\%$)

** Middle molecular MPM (MWCO ÷ (100-200 000) g/mol), ($C_\Sigma \approx 0.6\%$)

***High molecular MPM (MWCO ÷ (5000-1 000 000) g/mol), ($C_\Sigma \approx 0.6\%$)

Where M is the molecular weight, r_S is Stockes radius of protein and pI is protein isoionic point.

Since the results of the calibration method are largely determined by the concentration polarization level, to determine the characteristics of the membrane structure one must use data obtained under more or less "standard" calibration conditions i.e. cells with laminar stirring, 200 – 600 min^{-1}, calibration with globular proteins at a total concentration of ~10^{-1}% and pressure ≈ 1bar. The results of the analysis of track-etched membranes are presented in **Table 2.4**.

Table 2.4: *Permeability, selectivity and structure of asymmetrical track-etched membranes.*

Sample Name	J_0 10^6 m/s (1bar)	M_L 10^{-3} g/mol	R_{UF} nm	L_S μm	Δ	D_2
ATM1	70	50	9.0	0.12	1.0	0
ATM2	50	40	8.4	0.12	1.0	0
ATM3	40	30	7.5	0.2	1.1	0

Where J_0 is water flux at 1bar, M_L is the molecular weight, R_{UF} is the effective ultrafiltration pore sizes, L_S is the thickness of PET selective layer, Δ is dispersion coefficient and D_2 is the quantitative parameter of membrane defects. The surface morphology and porous parameters of this template have been investigated by SEM (presented in **Chapter 3**) and Atomic Force Microscopy (AFM) (as shown in **Figure 2.5**).

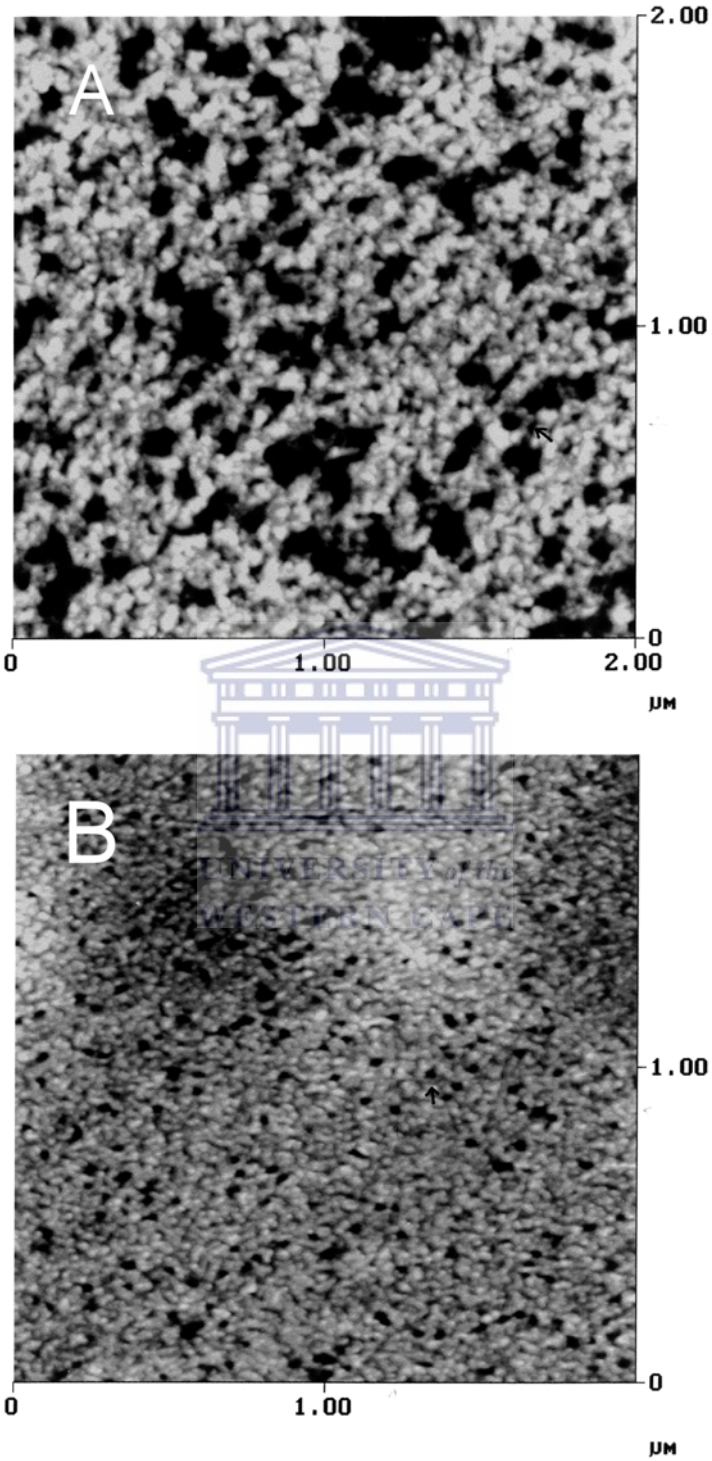

Figure 2.5: *The AFM micrographs of PET surfaces before (A) and after (B) preliminary treatment.*

2.2 Ni conductive layer deposition techniques

2.2.1 Vacuum deposition

Polymer cleaning process: The cleanliness of the PET polymer membrane surface is of outmost importance for the subsequent deposition process. Any residue left on the membrane surface may result in peeling and delamination of the film from the template substrate. The polymer membranes needed to be sonically cleaned in acetone for 5 minutes. After acetone, the membranes were rinsed with de-ionized (20μΩ-cm) water.

Deposition: After the nickel material to be evaporated was adequately pre-heated, to reduce sputtering and gaseous outbursts, the actual evaporation was carried out using an e-beam evaporator at the Materials Research Group of iThemba Laboratory for Accelerator Based Sciences (iThemba LABS). The system was fitted with a shutter that could be opened or closed, without breaking the vacuum, by means of a magnet. The pressure during deposition was between 10^{-6} and 10^{-7} mbar. In our investigation nickel films were deposited onto the PET polymer membranes without breaking the vacuum, using an electron gun. The electron gun consists of a tungsten filament which produces electrons that are focussed on the crucible by a magnetic field. By increasing the electron-beam current from 0 to 200mA the output power of the electron gun could be changed while maintaining the output voltage at 4 kV. **Figure 2.6** shows a schematic representation of the ultra high vacuum deposition chamber used to evaporate nickel conductive layer on the PET polymer membrane.

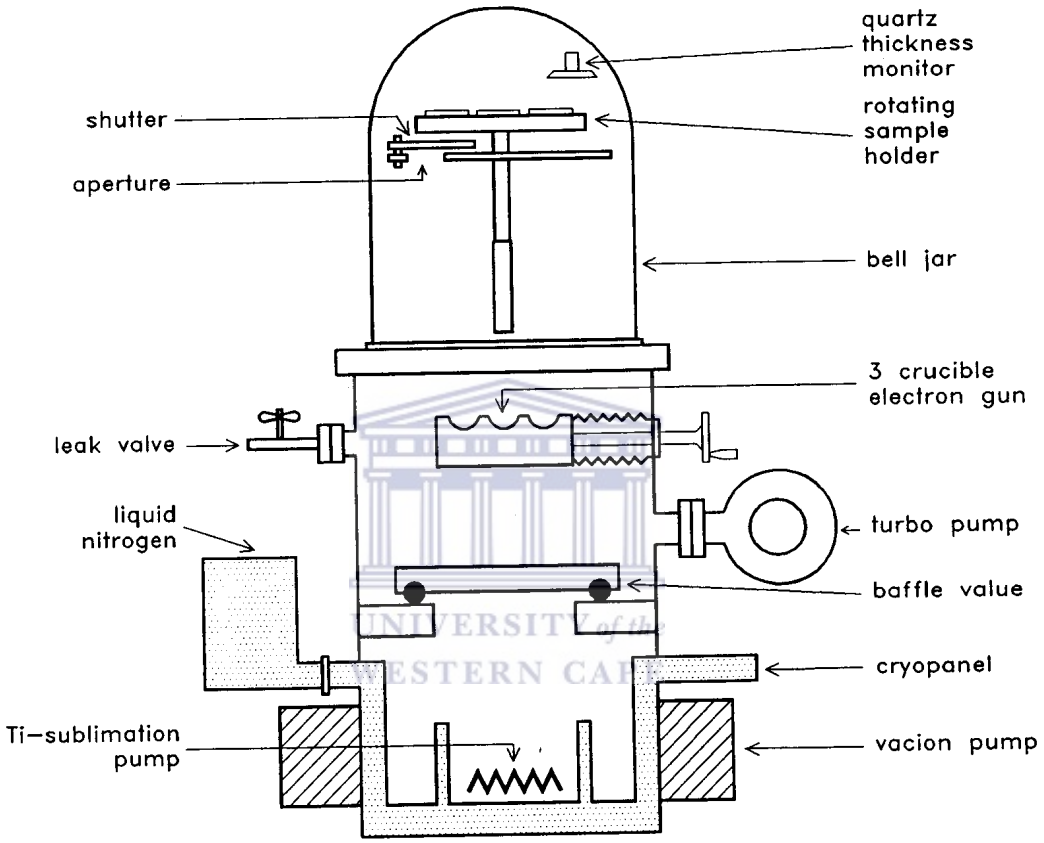

Figure 2.6: *Schematic representation of the ultra high vacuum (UHV) deposition chamber used to prepare the nickel conductive layer on the polyethylene terephthalate (PET) polymer membranes.*

Thickness measurement: A quartz crystal thickness monitor was used to control the deposition rate and thickness of the films. The thickness monitor was at a higher position than that of the PET polymeric membrane holder. Thus correlation coefficients (calibration) between the thickness on the monitor and that on the substrate for the nickel source material to be evaporated, was obtained. During evaporation, the accumulation of material on the vibrating quartz crystal causes a change in the frequency of the crystal. This information was then fed into a microprocessor which calculated the rate of evaporation as well as the evaporation thickness. During the preparation of the samples the rate of deposition was maintained between 0.18 and 0.36 nm/s. The total thickness of the deposited nickel layer was between 60 and 200nm for all samples.

2.2.2 Electroless deposition

The electroless deposition of metal onto a polymer surface is a simple and convenient method to metallize the polymer surface [8]. Electroless deposition involves the use of a chemical agent to plate a material from the surrounding phase onto a template surface [[2]:**Chapter 1**]. The polymer can be activated by either the "two-step" sensitization-activation method or the "one-step" activation approach [8, 9]. **Figure 2.7** shows a schematic representation of the main stages in the electroless plating process using the "two-steps" sensitization-activation approach. Both methods involve the introduction of catalytic nuclei onto non-catalytic surfaces. Redox reactions are initiated by these nuclei specifically at the activated surface. In the case of the "two-step" method, the polymer is immersed successively in $SnCl_2$ and then $PdCl_2$ solution [10]. The "one-step" process uses a mixture of $SnCl_2/PdCl_2$ solution. Both of these methods involve the use of $SnCl_2$. Accordingly, it is important to develop a tin-free activation process [11].

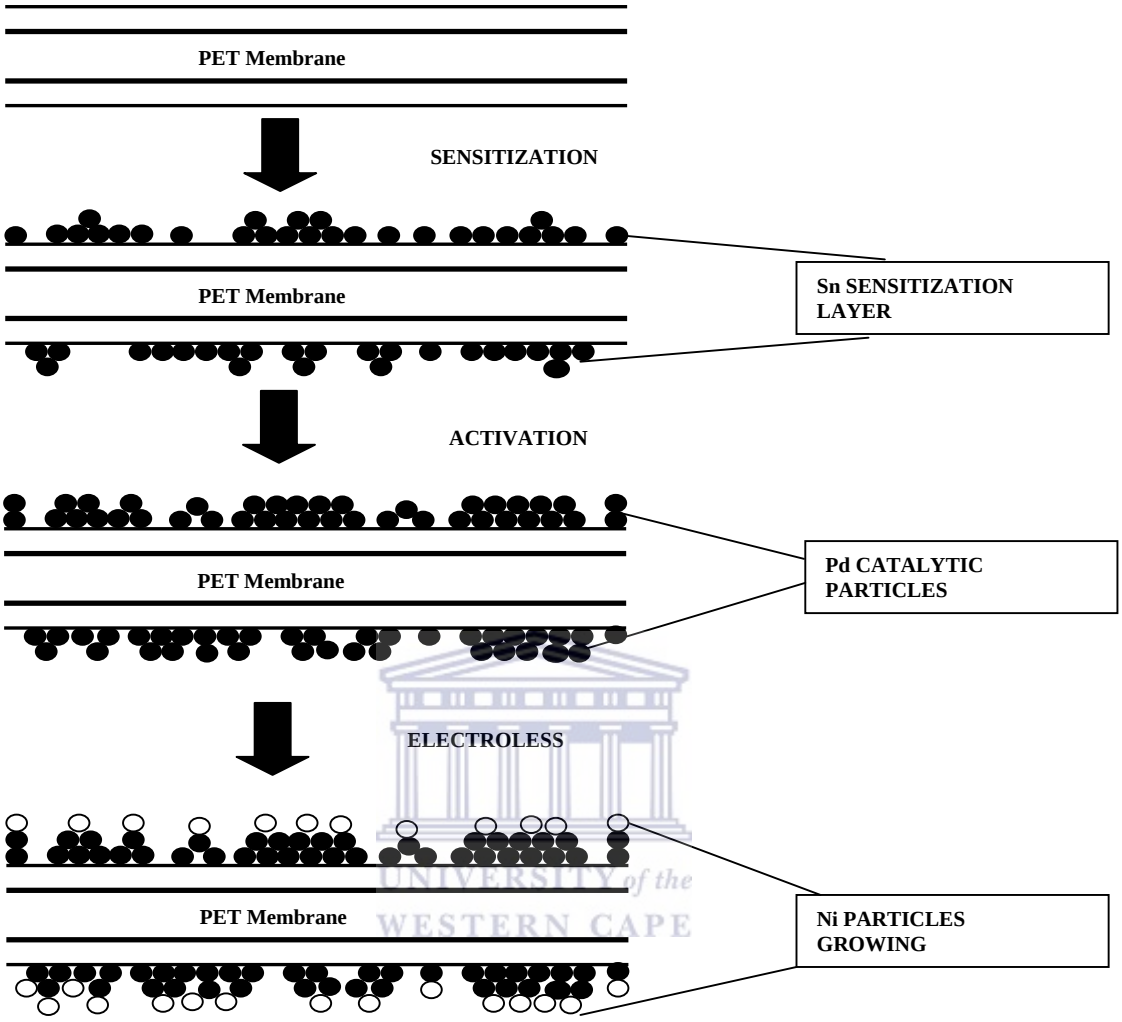

Figure 2.7*: Schematic representation of the main stages in the electroless plating process using the "two-step" sensitization –activation approach.*

In our investigation, PET membranes of varying pore diameters were activated through the direct immobilization of the palladium catalyst for the subsequent electroless nickel plating. The sensitization of the PET membrane was carried out by directly immersing the polymer in an aqueous solution prepared by dissolving 1g/L $PdCl_2$, 50g/L $SnCl_2.2H_2O$, 170g/L of KCl and 150ml/L of HCl(ρ = 1.19g/ml) in de-ionized water (as shown in **Table 2.5**) and then washed with copious amounts of di-ionized water. The temperature of the solution was kept between 18 and 25°C. The sensitization reduces the induction period of the Ni deposition reaction and promotes complete coverage of the surface and improves the plating quality [10, 11]. The Sn sensitizing layer enhances Pd adsorption as well as the binding strength of Pd to the surface. Thus,

$$Sn^{2+} + Pd^{2+} \rightarrow Sn^{4+} + Pd^{0}$$

Table 2.5: *Compositions and characteristics of sensitization and activation bath components.*

Component	**Amount (mg/L)**
$PdCl_2$	1
$SnCl_2.2H_2O$	50
KCl	170
HCl	150 ml/L
Na_2SO_4	60
Temperature (°C)	25
pH	2

The nickel metallization was carried out via electroless plating. The surface-activated membranes were immersed in a Ni electroless plating bath at a temperature of between 20 – 30°C for 5 – 30min. The basic bath composition and the plating conditions are listed in **Table 2.6**.

Table 2.6: *Composition of nickel electroless bath and plating conditions.*

Component	Amount
$NiCl_2 – 6H_2O$	25 g/L
NH_4Cl	27 g/L
$NaH_2PO_2 – H_2O$	37 g/L
NH_4OH	35 ml/L
$NaNO_2$	0.05 g/L
pH	10
Bath temperature	20 – 30°C
Time	5 – 30 min

2.3 Electrochemical deposition of Ni into pores of template membranes

The basic concept necessary to understand the electrochemical deposition in membranes is discussed in this chapter. The aim of this investigation was to determine the optimal conditions for the homogeneous growth of large arrays of nickel micro- and nanowires. In our study, electrodeposition of nickel material within the pores of the template matrix was accomplished by initially vacuum or electroless depositing one side of the template membrane with a nickel film layer and using this nickel film

as a cathode for electroplating (see **Figure 2.1(b)**)[[2]:**Chapter 1**]. The additional thickness of nickel layer was cladded on top of it.

The foil was mounted in the electroplating cell so that the deposited surface faces the anode. The additional 10 – 20µm nickel layer was deposited by electroplating. Thus, the pore orifices were completely closed from this side. In order to avoid an undesirable filling of the pores during electrodeposition of the supporting layer, the opposite side of the membrane was insulated. The thick nickel layer deposited in this way provides a stable substrate for the homogeneous growth of nickel wires after removing the matrix foil by dissolution. Under these conditions the resulting nickel layer was found to homogeneously cover the pore entrances. However, a good attachment of the wires to the supporting layer can only be reached if the displacement deposition of the metal is prevented. Hence, the deposited and the supporting layer should be from the same metal as that used for pore filling or from a more electro-positive metal. Moreover, the fact that the substrate and wires consist of the same metal (nickel), avoids possible stress and misfitting due to different lattice constants.

Good adhesion between the polymer foil and the metal layer was found to be essential to avoid the electrolyte from slipping between the conductive layer and the polymer surface during the electrodeposition of the wires. A suitable thickness of the nickel layer had to be chosen. If it is too thin, the layer will not conduct, and it will not be possible to clad it with additional nickel. If it is too thick, stress is induced and both surfaces, polymer and the nickel will separate. Arrays of Ni micro- and nanowires were electrodeposited from sulphate solution as shown in **Table 2.7**. The results of a systematic study of the potentiostatic and galvanostatic deposition of nickel in pores with large (several hundred nm) and small (several tens nm) diameters are explained in **Chapters 3**.

Table 2.7: *Compositions and characteristics of the different Ni plating baths used in this investigation.*

Component	*Ni-Watt*	*Ni-Hard*	*Ni-Mirror*
$NiSO_4 – 7H_2O$	**140 – 200 g/L**	**180 g/L**	**405 g/L**
$NiCl_2 – 6H_2O$	**30 – 40 g/L**		**2.5 g/L**
NH_4Cl		**25 g/L**	
H_3BO_3	**25 – 40 g/L**	**30 g/L**	
Na_2SO_4	**60 – 80 g/L**		
Malonic Acid			**10 g/L**
Saccharin			**1 g/L**
Butynediol			**0.2 g/L**
pH	**5.2**	**5.6 – 5.9**	**3**
Bath temperature	**20 – 55°C**	**40 – 55°C**	**40 – 50°C**
Current density	**0.5 – 2.0 A/cm^2**	**2 – 10 A/cm^2**	**2 – 5 A/cm^2**
Anode	**Nickel**	**Nickel**	**Nickel**

The electroplating set-up during nickel plating employed in this investigation is shown in **Figure 2.8.** It consisted of two electrodes, namely, a working electrode or cathode and a counter electrode or anode. The schematic view of the experimental set-up used to carry out the electrochemical deposition of nickel in ion track membranes is shown in **Figure 2.9.**

Figure 2.8: *The electroplating setup during nickel electroplating employed in this work.*

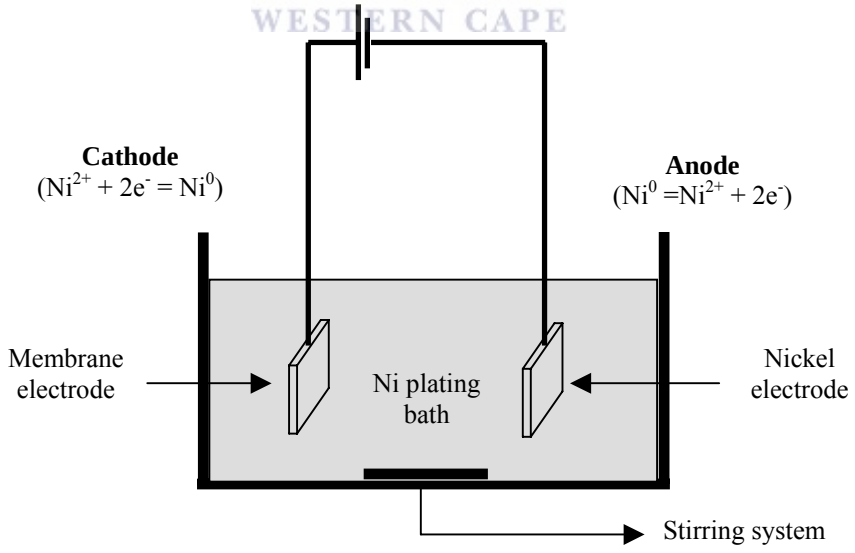

Figure 2.9: *Schematic view of the experimental set-up used to carry out electrochemical deposition of nickel in ion track membranes.*

Conditions for electrodeposition

The electrolyte is the medium between the electrodes in the electrochemical cell. It consists of the solvent and a high concentration of an ionized salt as well as the electro-active species. It may also contain other materials, complexing agents, buffers, etc. Electrode reactions can be extremely sensitive to impurities in the solution; for example, organic species are often strongly adsorbed even at 1 x 10^{-4} mol/L bulk concentration from aqueous solutions. Hence, salts should be of the highest available purity and/or recrystallised, the solvent should be carefully purified, and the solutions must be carefully de-oxygenated.

The selection of the electroplating baths and the related deposition conditions are of primary importance. Numerous studies have shown that the physico-mechanical properties of the nickel coatings depend strongly on the deposition parameters and the bath conditions [12]. Details on chemical baths and concentrations of electrolytes are explained below. All electroplating solutions used in this investigation were prepared using de-ionised water (Millipore, 18.2 MΩ-cm). The measurements were performed in a 500cm^3 cell with the anode and cathode electrodes 5cm apart. The anode was a plate of technical nickel with the geometrical area of 3x10cm^2.

Potentiostatic or voltage-controlled modes of operation are generally not encouraged. Maintaining a constant potential difference allows the current to fluctuate which has a negative effect on the uniformity of the plating, especially in the case of high aspect ratio microstructures. Instead, galvanostatic or current-controlled practices are recommended in order to meet minimum coating thickness requirements and to produce deposits with consistent and predictable properties.

Electrochemical deposition baths used

The nickel electrodeposition was carried out by the steady-state galvanostatic technique from nickel plating baths. The nickel plating solutions used were *Mirror*, *Hard* and *Watt* baths. The composition of the plating bath solutions for nickel electrodeposition are given in **Table 2.7**.

Mirror Bath: This bath consisted of $NiSO_4.6H_2O$, $NiCl_2.6H_2O$, Malonic acid, Saccharin and Butynediol [12]. The malonic acid was chosen because it is highly soluble in the nickel-plating bath; it is available and does not pollute the environment [12]. Saccharin is used to lower the stress of the electrodeposit. The pH was adjusted to 3.0 and the temperature was maintained between 40 and 50°C. The current densities ranged from 1 to $10Adm^{-2}$. The amount of time required to produce a certain nickel film thickness depends on the current density and the surface area to be covered. An estimate of the surface area to be plated is made prior to initiating the electrodeposition to facilitate the monitoring process.

Hard Bath: It was made of Nickel Chloride ($NiSO_4.7H_2O$), Ammonium Chloride (NH_4Cl) and Boric acid (H_3BO_3). The depositions were carried out galvanostatically, at a temperature of 45 – 50ºC, in an open cell, with a stirred electrolyte, on the template. The deposition current density was $60mAcm^{-2}$. The operating temperature of the bath was controlled to +/-2°C of the suggested value because temperature changes can have a significant impact on the properties of the nickel deposits. The anode was technical nickel. The thicknesses of the nickel coatings were 20µm.

Watt Bath: The solution used for nickel plating was composed of $NiSO_4.6H_2O$, $NiCl_2.6H_2O$ and H_3BO_3. The volume of the pores was continuously filled up beginning from the pore bottom. Thus, the length of a nanostructure can be controlled by varying the amount of material deposited. Both metal and conductive polymer nanorods and nanotubules can be synthesized using this bath. The process was carried out at constant current so that the deposition could be monitored from the potential response. The basic components of the nickel electroplating solution that must be controlled are the nickel metal content, the chloride concentration, boric acid level and the concentrations of the additional agents. Nickel metal concentration in the more common solutions can range between 22 and 46%.

Conditions affecting the structure and properties of Ni plating

The characteristics of electrodeposited metals and metal alloys are mainly influenced by the environment in the immediate vicinity of the cathode. Electrodeposits are undoubtedly crystalline in nature, and the form of the deposit depends largely on two factors: first, the rate of formation of the crystal nuclei by the discharge of the ions at the cathode, and, second, the rate at which these nuclei grow into large crystals. If the conditions are such as to favour the rapid formation of fresh nuclei on the cathode, the deposit will tend to consist of small, fine-grained crystals. The metal being deposited will then be smooth and relatively hard. On the other hand, if the circumstances are such that the nuclei increase in size rapidly, the deposit will consist of relatively large crystals and will be rough in appearance. There are many parameters that influence the above-mentioned factors, namely, current density, concentration of electrolyte, temperature, impurities and pH.

Current density: At low current densities the discharge of ions happens at a slow rate, which allows ample crystal-nuclei growth time, but the formation of fresh nuclei is necessary. The deposit obtained under these conditions exhibits a coarse crystalline structure. As the current density increases, the rate of discharge of the ions also increases, and fresh nuclei will tend to form. The resulting deposit will consist of smaller crystals. Thus, the increase in current, within certain limits, yields deposits that are more fine-grained. But there is a definite limit to this improvement, because at very high current densities the crystals tend to grow out from the cathode towards regions where the solution is more concentrated hence creating trees or nodules in the film.

Concentration of electrolyte: Increasing the concentration of the solution can largely offset the bad effects caused by electroplating at high current densities. Likewise the use of agitation in the electrolyte will also postpone these harmful consequences, such as nodule formation until much higher current densities are introduced.

Temperature: Increasing the temperature seems to have two effects which counter one another. First of all, it promotes the diffusion of ions to the cathode, thereby preventing impoverishment, which leads to roughness of the deposit. On the other hand, it also increases the rate of growth of the crystal nuclei, so the deposit will have a tendency to be coarse. When operating at moderate temperatures, such as those generally applied to electroplated nickel, the first of the above mentioned effects predominates, thus the deposits are improved. But at high temperatures the quality of the deposit deteriorates.

Impurities: Electroplated films normally contain various types of inclusions or impurities. The source of these impurities may be from one or more of the following: added chemical, added particles, cathodic products, hydroxides and bubbles. While the effect of a particular additive is frequently specific for a given metal, a general statement can be made relating to the purpose of additives and the formation of fine-grained coatings. The additional agents are generally substances that have a high surface activity, i.e. they tend to be adhered to or be adsorbed by the surface. An excessive amount of additive in the electrolyte can cause the deposit to become brittle and break apart at the crystal interface, where there is a relatively thick layer of the added substance. Hydrogen, oxygen, carbon, sulphur and chloride are the most common impurities present in nickel deposits that adversely influence the physical properties (density, resistivity).

pH: The pH of the solution influences the discharge of hydrogen ions, thus causing the solution in the cathode layer to become alkaline and precipitate hydroxides or basic salts. The presence of a significant amount of these compounds will make the resulting deposit exhibit a fine grain structure, but it will be dark in colour (burnt), or spongy/powdery in character. Additionally, the evolution of hydrogen gas is often accompanied by the formation of spots and streaks in the film. As the pH of nickel plating increases during normal electroplating operations, small quantities of acid were added to keep it within range.

2.4 Morphological and structural analysis techniques

Many efforts are made to measure physical properties of nanostructures and, in particular, also of electrodeposited micro- and nanowires [[9]:**Chapter 1**]. A detailed study of the dependency of the morphology and crystallinity of nickel micro- and nanowires on the electrodeposition parameters was performed. Characterization methods are restricted to surface techniques. The morphology of the resulting micro and nanowires was systematically investigated by SEM. The texture of the wires was analyzed by X-ray diffraction (XRD). The information obtainable from these surface techniques is discussed in **Chapter 3**.

2.4.1 Scanning Electron Microscopy (SEM)

Topographic details of a surface can be revealed with great clarity and detail by utilizing the SEM. The SEM is one of the most frequently used instruments in materials research today because of the combination of higher magnification, larger depth of focus, greater resolution and ease of sample observation. Morphology details of less than 50nm can be resolved by SEM and it possesses a depth of focus more than 500 times higher than that of the optical microscope at equivalent magnification. Typical resolution for SEM is around 10nm. **Figure 2.10** shows a schematic depiction of the operation of SEM.

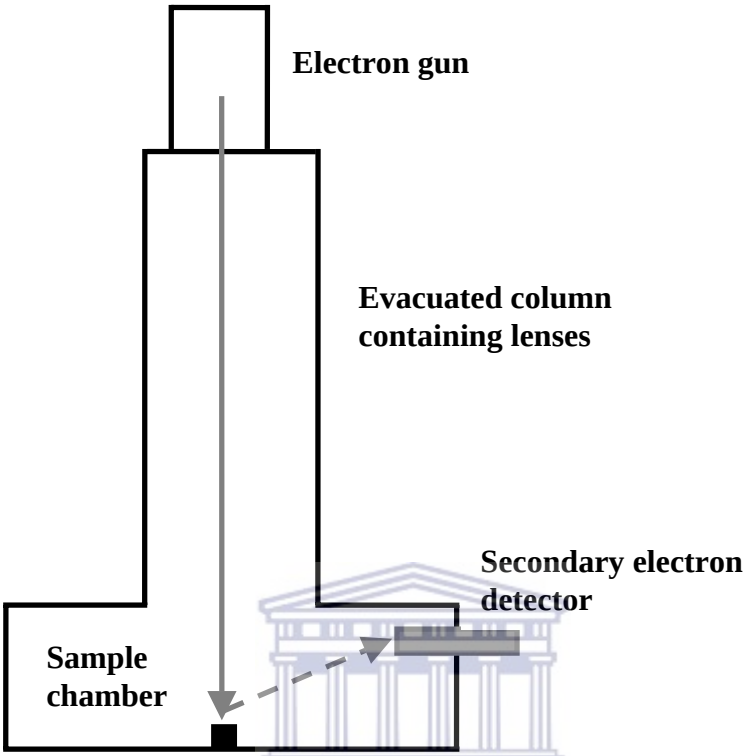

Figure 2.10: *Schematic diagram of scanning electron microscopy showing the electron beam path to the specimen.*

For SEM/EDS (Energy Dispersive Spectroscopy) measurements, a Hitachi X-650 microscope and a NORAN VOYAGER 3000 EDAX (Energy Dispersive Analysis of X-rays) at The University of the Western Cape in the Department of Physics was employed. The microscope beam energy can be varied over the range of 5-40 keV, with a maximum resolution of 10nm. The EDAX analyzer is equipped with an ultra-thin window, allowing light element analysis from carbon upwards. The electrode samples were dried in air after being washed in di-ionized water before starting the SEM and EDAX analyses.

A prerequisite for effective viewing is that the surface of the samples should be electrically conductive. During operation electrons are deposited onto the sample. These electrons must be conducted away to earth. Metallic samples can be placed directly into the SEM; non-metallic samples, for example the PET foils, were previously coated with a gold metal layer. In order to observe the formation of wires, electrodeposition was stopped at stages during the growth of the wires.

2.4.2 X-Ray Diffraction (XRD)

Another structural tool used in this thesis is XRD. X-rays are high energy/short wavelength forms of electromagnetic radiation [13]. The wavelengths are of the order of atomic spacings allowing them to be used to probe crystal structures. Thus, to observe a particular diffraction maximum, the appropriate sets of planes must be oriented in space such that the angle between the incident beam and the set of planes in the crystal is made equal to the angle θ. A plot of X-ray counts versus θ gives a series of peaks. The position of each peak defines the spacing between a set of planes. The intensity of the peak is determined by the interference of the X-rays reflecting off the other sets of planes in the crystal.

In this study, the XRD measurements were carried out using a Brucker D8 Advanced Powder Diffractometer using Cu (K_α) radiation having a wavelength of 1.54056Å in $\theta/2\theta$ mode. The X-ray tube source was operated at 40kV and 30mA. The diffraction system contained 0.05° and 1° slits mounted before a scintillation detector. Data was collected using MDI Datascan 3.2 software with a DACO interface. The experimental peak locations and their relative intensities were compared with powder diffraction files (PDF) contained in JADE^{TM} XRD Processing and Identification software. Several batches of nickel structures were analyzed to confirm the reproducibility of Ni morphologies, crystalline phases, and electrochemical behavior.

The sample was positioned horizontally while both the detector and X-ray tube moved symmetrically through an angle θ. The X-ray yield is plotted as a function of 2θ. The movement was computer controlled allowing variable scanning speed and digital data acquisition. The standard set up was 0.2° per step and 10 seconds per step.

2.5 Electrochemical characterization methods of Ni structures

Electrochemical methods cover a wide range of analytical techniques. The fundamental signal measured is electrical in nature, either current (Faradaic) or voltage (Potentiometric), resulting from redox reactions. Like other analytical techniques, electrochemical methods yield both quantitative and qualitative information. In addition, some electrochemical methods will give information about non-redox chemical processes occurring before or after redox reaction.

Charge transfer can occur homogeneously in solutions or heterogeneously on electrode surfaces. For a heterogeneous reaction, the electrode acts as either a source (for reduction) or a sink (for oxidation) of electrons transferred to or from species in solution. Because this is a surface phenomenon, the electroactive species in the solution needs to get to the electrode surface. Therefore, in a still solution, the concentration of species at the electrode surface depends on the mass transport of these species from bulk solution. If the kinetics of the electrode reaction is much faster than this transport, the reaction is reversible.

Standard electrode potentials, E^0, are measured relative to hydrogen. The standard potential is defined for a cell in which all activities are unity. The formal potential is the reduction potential that applies under specific conditions. Cyclic voltammetry, chronoamperometry are Faradaic techniques used in this investigation. The electrochemical methods are extremely useful for the characterisation of nickel structures, as well as being an attractive technique for their electrosynthesis.

2.5.1 Cyclic Voltammetry (CV)

In conventional cyclic voltammetry a triangular potential waveform is applied to the electrode and the corresponding current is recorded. This technique has been widely applied in the studies of the electrochemistry of solution species and in the study of electrochemical reactions with subsequent chemical reaction steps. Cyclic

voltammetry is the most common and perhaps most straightforward electrochemical technique used [14]. This technique finds a particular use in preliminary studies of new systems. It also shows the potential range over which the solvent is stable and the degree of reversibility of the electrode reaction. It is also useful for studying electrochemical cell characteristics [15, 16]. It enables independent estimation of oxidation as well as reduction reaction potentials and throws light on their mechanism. Furthermore, within certain limitations, it enables estimations to be made of various parameters such as charge capacity, coulombic efficiency, and reversible potential [15, 16].

This involves applying an external triangular voltage to the electrochemical cell, sweeping through a potential range and reversing the direction of the sweep in a cyclic fashion (as shown in **Figure 2.11**). The real power of this technique lies in its ability to investigate mechanisms and potentials of electrode reactions. The potential is increased linearly with time to some specified potential value and then decreased over the same period of time back to the initial potential.

The resulting current (I) is monitored as a function of applied potential (E) to give the I-E curve which in this kind of experiment is called a cyclic voltammogram. Typically, a three electrode potentiostated system is used: a working electrode, reference electrode and a counter electrode. The current flows between the working electrode and the counter electrode. The potential is controlled relative to the reference electrode which is placed as close to the working electrode as possible to reduce ohmic (IR) potential drop.

However, if the potential is scanned too far in an anodic direction, poorly defined irreversible peaks develop, corresponding to a loss in redox reversibility of the film. Cyclic voltammetry may also be used to show the ability of the film to store charge and to respond to the applied potential. The areas underneath the oxidation and reduction peaks show that approximately equal amounts of charge accompany each process demonstrating the electrochemical reversibility and efficiency of the redox process.

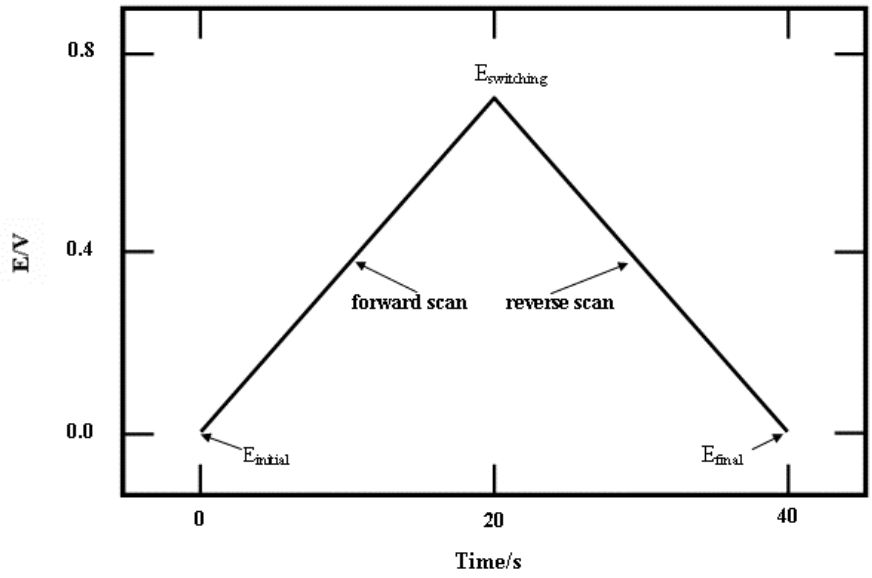

Figure 2.11: *Waveform excitation signal for cyclic voltammetry*.

2.5.2 Three-electrodes system

Working electrode: Designs of working electrodes (WE) are diverse. Most commonly in experiments to study mechanism and kinetics in the laboratory, the working electrode is a small sphere, disc, or a short wire, but it could also be metal foil, a single crystal of metal, an evaporated thin film, or a powder in the form of pressed disc or pellets. An essential feature is that the electrode should not react chemically with the solvent or solution components. The useful working range is difficult to define as it may be limited by a number of different processes such as oxide formation, hydrogen or oxygen evolution, or solvent decomposition, as well as depending on the reactants and products of the system under study. It is desirable to have an even current and potential distribution and, hence, for the cell to be designed so that all points on the working electrode surface are geometrically equivalent with respect to the secondary electrode (see **Figure 2.12**).

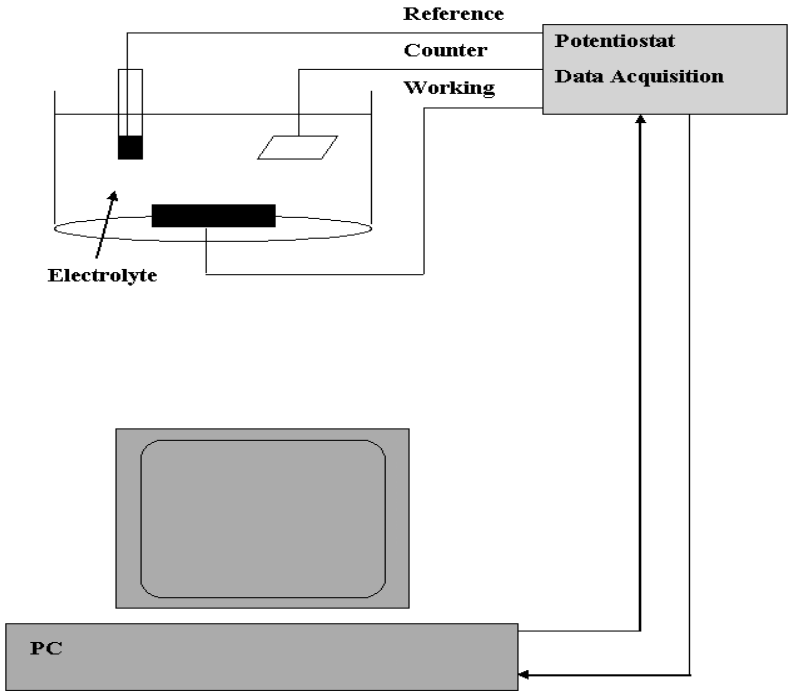

Figure 2.12: *A schematic diagram of a scanning electrochemical microscopy cell and sample holder.*

Counter electrode: The purpose of the counter electrode (CE) is to supply the current required by the working electrode without limiting the measured response of the cell. It is essential that the electrode process be a decomposition of the electrolyte medium or the oxidation/reduction of a component of the electrolyte, so that the current flows readily without the need for a large overpotential. In some cases, it can be arranged that the counter electrode reaction is a gas evolution or the reverse of the working electrode reaction, so that the composition of the electrolyte is unaltered. The products of the counter electrode reaction should always be considered since they must not interfere with the reaction being studied on the working electrode.

Reference electrode: The role of the reference electrode (RE) is to provide a fixed potential which does not vary during the experiments. It should be independent of current density. In most cases, it will be necessary to relate the potential of RE to other scales, for example, to the normal hydrogen electrode the agreed standard for

thermodynamic calculations. In potentiostatic experiments the potential between RE and WE is controlled by a potentiostat, and as the reference half cell is maintained at a fixed potential, any change in applied potential to the cell appears directly across the interface between WE and solution.

The RE serves dual purpose of providing a thermodynamic reference and also isolating the WE from the system. Thus, a good RE should be able to maintain a constant potential even if a few microamperes are passed through its surface (see **Figure 2.12**). Experiments were performed on Scanning Electrochemical Microscope (**SECM 270**) and an Autolab PG30 (Ecochemie, the Netherlands) electrochemical system with dedicated software (GPES).

2.5.3 Chronoamperometry (CA)

Chronoamperometry is a potential step method that has a square wave form. A potential is stepped from an initial value that causes no current to flow to a potential that causes current to flow. Because the experiment is diffusion controlled after a certain time almost all molecules that are able to reach the electrode are reduced (oxidised).

For many applications it is necessary to know the active area *A* of an electrode surface that differs from the macroscopic one. Also very often one has to determine a diffusion coefficient. This can be done by chronoamperometry if one of both parameters in known. A constant potential is applied and the resulting current *i* is measured. By plotting the current vs. 1/sqrt(*t*), the slope of the resulting straight line contains the desired information.

2.6 Conclusions

Polyethylene terephthalate (PET) foil was used as template membrane in this investigation. Tracks were created by heavy-ion irradiation and chemical etching in alkaline solution. Conductive layer was deposited using either vacuum or electroless deposition methods and the thickness was reinforced by galvanostatic electrodeposition. Asymmetric nanoporous track-etch membranes were prepared by etching PET membrane on one side. During pore filling three different nickel plating baths were used, namely, *Watt*, *Hard* and *Mirror* plating baths. The characterization of the structures was restricted to surface techniques. SEM and XRD were used to investigate the morphology and crystallinity of obtained structures, respectively. To study the electrochemical properties of the materials chronoamperometry and cyclic voltammetry were utilized in a three electrode system.

2.7 References

[1] N.I. Shtanko, V.Ya. Kabanov, P.Yu. Apel and M. Yoshida, *Nuclear Instruments and Methods in Physics Research* B151, (**1999**) 416.

[2] K.B. Jirage, J.C. Hulteen and C.R. Martin, *Science* 278, (**1997**) 655.

[3] A.I. Vilensky, O.G. Larionov, R.V. Gainutdinov, A.L. Tolstikhina, V.Ya Kabanov, D.L. Zagorski, E.V. Khataibe, A.N. Netchaev and B.V. Mchedlishvili, *Radiation Measurements* 34, (**2001**) 75.

[4] Z. Siwy, P. Apel, D. Dobrev, R. Neumann, R. Spohr, C. Trautmann and K. Voss, *Nuclear Instruments and Methods in Physics Research* B208, (**2003**) 143.

[5] P.Yu. Apel, *Nuclear Instruments and Methods in Physics Research* B208, (**2003**) 11.

[6] A.N. Cherkasov, *Journal of Membrane Science*, 50 (**1990**) 103.

[7] A.N. Cherkasov and A.E. Polotsky, *Journal of Membrane Science*, 106 (**1995**) 161.

[8] G.H. Yang, C. Lim, Y.P. Tan, Yan Zhang, E.T. Kang and K.G. Neoh, *European Polymer Journal* 38, (**2002**) 2153.

[9] L.M. Ang, T.S.A. Hor, G.Q. Xu, C.H. Tung, S.P. Zhao and J.L.S. Wang, *Carbon* 38, (**2000**) 363.

[10] T.N. Khoperia, *Microelectronic Engineering* 69, (**2003**) 391.

[11] G.H. Yang, E.T. Kang, K.G. Neoh, Y. Zhang and K.L. Tan, *Langmuir* 17(1), (**2001**) 211.

[12] Yu.D. Gamburg , M.Yu. Grosheva, S. Biallozor and M. Hass, *Surface and Coatings Technology* 150, (**2002**) 95.

[13] C. Kittel, *Introduction to Solid State Physics*, John Willey and Sons, Canada, **1976**.

[14] P.T. Kissinger, W.R. Heineman, *Journal of Chemical Education* 60(9), (**1983**) 702.

[15] Xianyou Wang, Jie Yan, Huatang Yuan, Zhen Zhou, Deying Song, Yunshi Zhang and Ligu Zhu, *Journal of Power Sources* 72, (**1998**) 221.

[16] P.V. Kamath and M.F. Ahmed, *Journal of Applied Electrochemistry* 23, (**1993**) 225.

Chapter 3: Results and Discussion

3.1 Consolidated Ni micromaterials: Template synthesis, morphology and electrochemical behaviour

3.1.1 Electrochemical investigation of Ni microwires grown within pores of track-etched membrane

All measurements presented in this section were performed with membranes possessing similar characteristics. They were irradiated with xenon (^{136}Xe) ions. The samples were simultaneously etched in a solution of NaOH at 40°C for a certain period of time until the visible diameter of the holes reached the desired dimensions. Under these conditions, the nominal pore diameter was about 0.4μm. Nickel microwires were fabricated through the pores of micropores of polyethylene terephthalate (PET) membrane using the galvanostatic electrodeposition technique and applying a constant current density of 25mA/cm^2.

The initiation and growth rate (current density) of the wires is important, it could determine if the wires become solid or tubular [1]. It can also influence the electrical contact resistance. The electrolyte used for this investigation was composed of $NiSO_4.7H_2O$ 180g/L, NH_4Cl 25g/L and H_3BO_3 30g/L. Two deposition temperatures were used namely 25 and 50°C and were maintained within the range of ±0.9°C. During pore filling, the electrolyte entered through the pore openings and propagated down the pore, facilitated by capillary forces [1]. Pre-treatment in ethanol improves the wetting properties of the PET membrane pores, which sometimes is a prerequisite for allowing electrolyte into the pores. After deposition, the samples were thoroughly washed with de-ionized water.

When a piece of metal is immersed into a solution containing its ions, the potential difference between both phases gives rise to an arrangement of the charges at the interface, that is known as the electrochemical double layer. Nickel deposition started from the bottom of the PET membrane. In order to understand this growth behaviour two hypotheses can be considered [2]. First during Ni vacuum deposition on the PET template to plug the pores and to provide a conductive surface for subsequent electrodeposition, Ni could have been deposited through the pores thereby providing a conductive path for the nickel during electrodeposition. Second, some trapped air pockets were created inside the pores when the template membrane was put into the electrolyte, which prevented the electrolyte from penetrating inside the pores [2].

In order to analyze the nickel electrodeposition process, current as a function of time curves were recorded for different applied potential. A typical current-time dependence at constant potential maintained on the cell is shown in **Figure 3.1**. Four different zones can be distinguished. The initial current increase of the process (**I**) is due to the electrical charge of the double layer and the diffusion layer [3, [2]:**Chapter 1**]. Later the current decreases as a result of metal ion depletion in the pores or the formation of the diffusion layer. The current remains nearly constant during the growth of the nickel wires in the pores at **II**. The current shows a steep increase as soon as the wires reach the upper surface (**III**). The process continues with the macroscopic growth of nickel on the whole surface (**IV**). The process can be stopped during zone **II** or **III**, to obtain only wires or wires with caps, respectively. The shape of the pores is actually reflected in the deposition current, a constant current is produced in the cylindrical sections of the pores and a fading/growing current if the cross section changes.

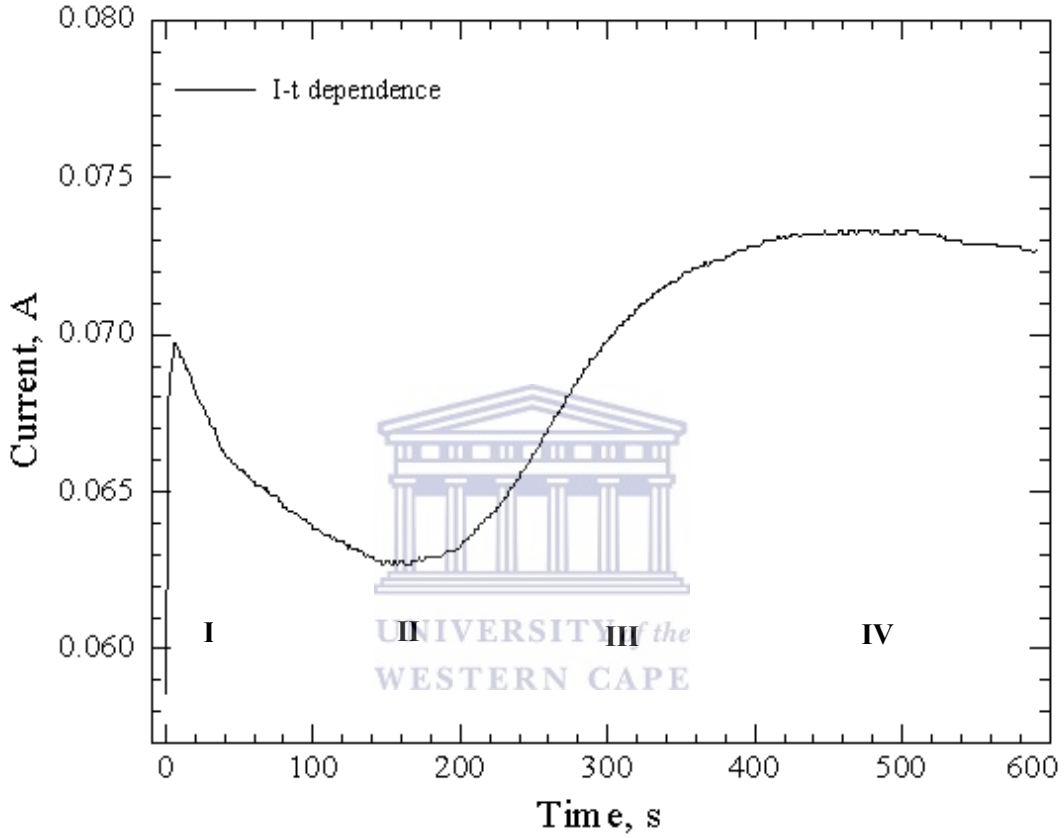

Figure 3.1: *A typical current-vs.-time curve for electrodeposition of nickel wires in polyethylene terephthalate (PET) templates. The applied potential was 0.7V and the current increases when the wires reach the surface.*

3.1.2 The effect of electrolyte composition on Ni microwires morphology

Scanning Electron Microscope (SEM) overviews of 0.4μm diameter microwires after dissolution of the polymer membrane are shown in **Figure 3.2**. *Mirror* and *Hard* bath solutions were used during deposition (as described in **section 2.3.2**). All micrographs have the same magnification and the scale bars in the micrographs correspond to 5μm. The smoothness of the contour and the uniformity along their length can be clearly seen for all the wires.

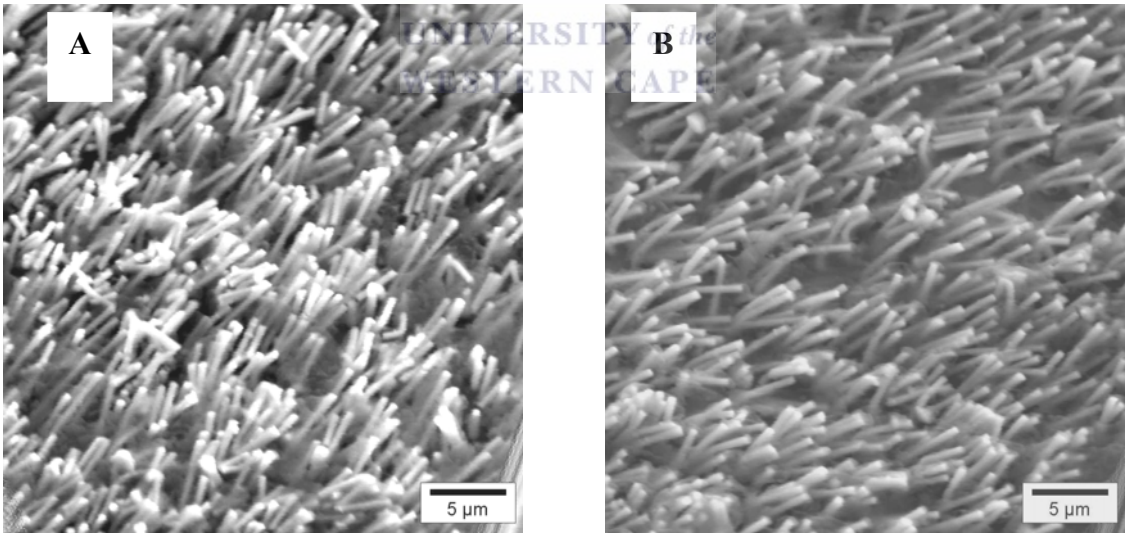

Figure 3.2: *SEM micrographs of 0.4μm diameter wires after dissolution of the polymer membrane, (***A)** – Hard *bath solution used, (***B)** – Mirror *bath solution used.*

The geometry of the wires depends on the irradiation and etching conditions. The surface smoothness of the wires depends on several factors such as the quality of the polymer and the etching process. It was observed that there was a strong indication that the conditions during electrodeposition play an important role. As the shape of the wires directly reflects the geometry of the pores in the PET, there is clear evidence that under the irradiation and etching conditions employed, the pores are well aligned and have cylindrical geometry [[3]:**Chapter 1**] (as shown in **Figure 3.2**). By replicating the pores it was also observed that their inner surface was very smooth and homogeneous. It should be emphasized that wires with cigar shapes, as discussed by several authors [4], were never observed. It is assumed that such an effect is linked either to special properties of the polymer or caused by additives to the etchant solution (e.g. surfactants) [5]. The influence of the surfactant is eliminated by etching at high temperatures.

The presence of bubbles in the pores i.e. from hydrogen evolution during depositions at very high overvoltages, or inferior quality of deposited metal at very high current densities, results in a rather large roughness of the wire surface [[25]:**Chapter 1**]. The properties of the templates employed in this work can therefore be of great importance if homogeneous wire growth is required. Problems due to large angular distributions, with tilt angles of more than 30°, in commercially available membranes have been reported [[25]:**Chapter 1**]. PET membranes, as presented here, provide suitable templates for basic research and for applications where a high degree of parallelism is of importance.

Hard Nickel Bath

Arrays of stable, standing nickel microsturctures are shown in **Figure 3.3** after removal of the PET template. It shows wires of 0.4μm in diameter and 23μm length grown on a surface area of 4.9cm^2. The overgrowth of hemispheres on the template surface becoming visible after dissolving the organic foil is shown in **Figures 3.3 C&D**. In spite of good quality, the microwires shown in **Figure 3.3** are slightly deformed. SEM analysis revealed that the pores of templates with thickness 10μm took between 10 and 15 minutes to be completely filled with Ni when the *Hard* bath was used.

As the wires approach the surface a new deposition regime was entered, since the wire growth is no longer confined to the cylindrical geometry of the pores. The wires started to grow in the radial direction, forming hemispherical "caps" (as clearly shown in **Figure 3.3C**) eventually covering the entire surface (**Figure 3.3D**). When the porosity of the template membrane is low, the diffusion zone, i.e. the electrochemical double layer, will have a hemispherical shape located around the pore opening, **Figure 3.4A** [1]. For a high porosity membranes the electrochemical double layer will have a flat appearance, **Figure 3.4B**.

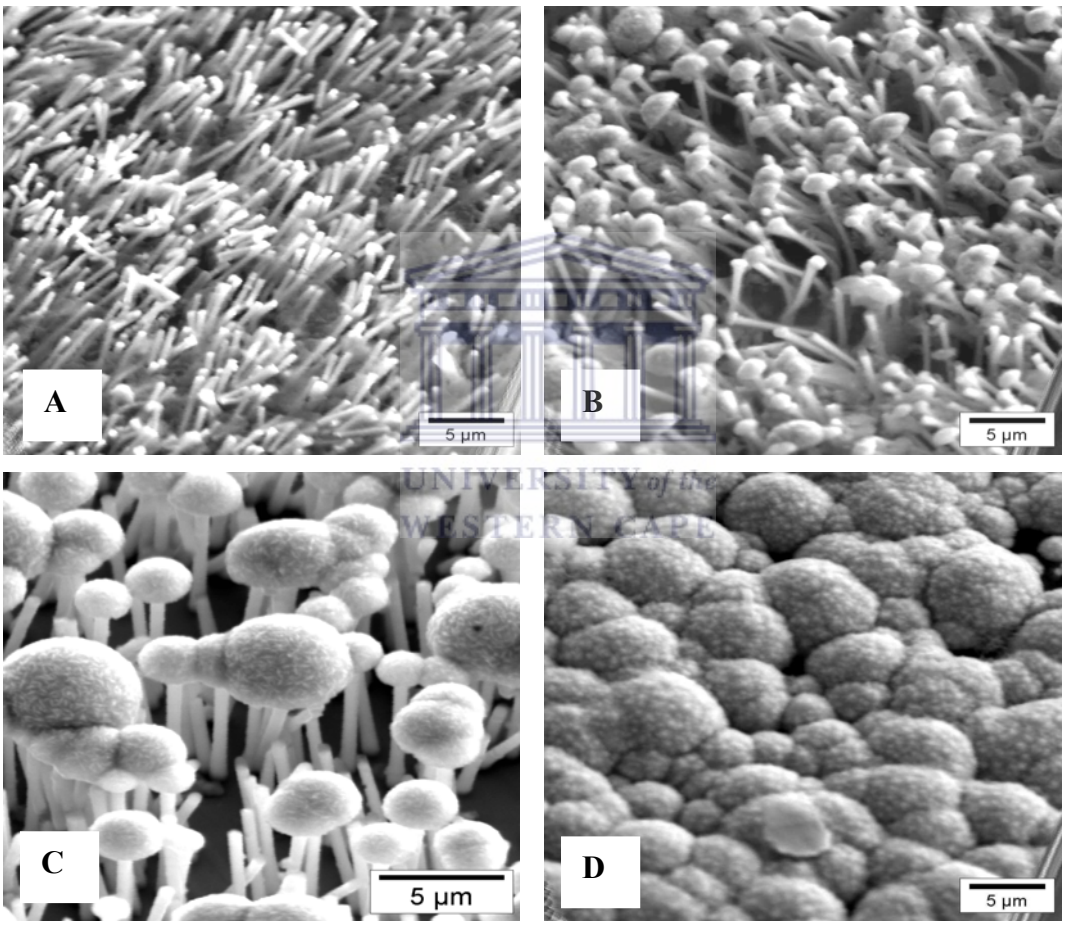

Figure 3.3: *SEM micrographs overviews of 0.4µm diameter wires electrodeposited with a* Hard *bath solution after the dissolution of the polymer membrane. (**A**) After pore filling for 10 minutes at 75mA/cm^2, (**B**) after 15 minutes, (**C**) after 20 minutes and (**D**) after 25 minutes. Hemispherical "caps" start to grow on the front surface at the end of the deposition.*

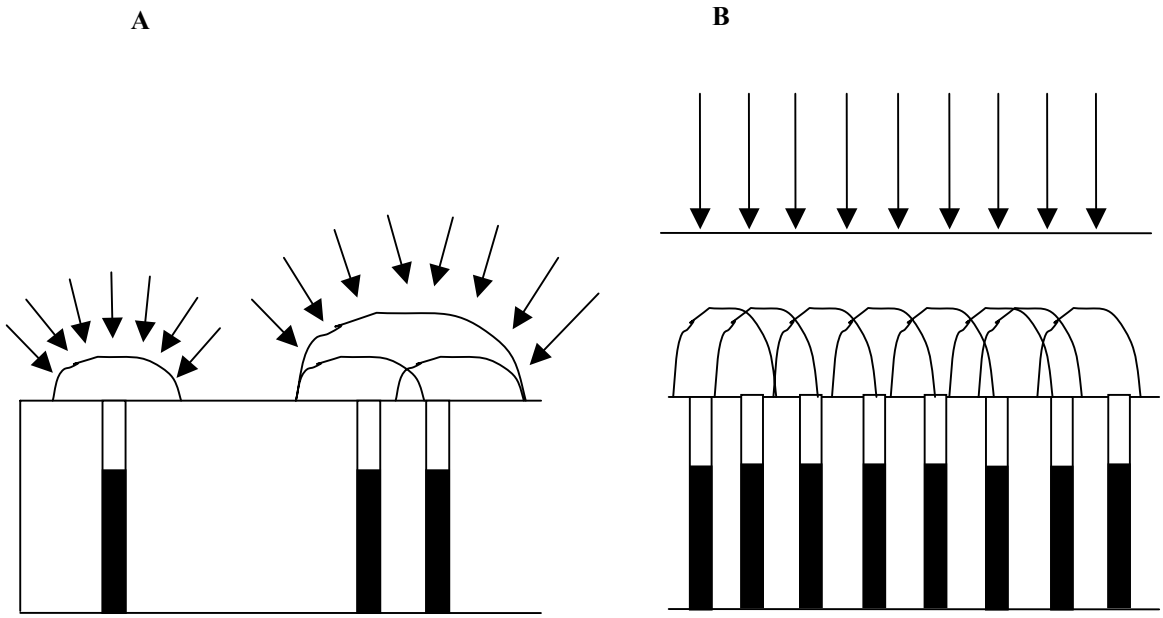

Figure 3.4: *Electrochemical diffusion around pore openings. (***A***) Low ion track density, diffusion is radial around the pores except for those pores that neighbour each other. (***B***) High ion track density, diffusion is linear with a thicker diffusion layer.*

Inside the pores the diffusion is limited to a one-dimensional 'random walk' process and the current is almost constant or increases slowly as the wire grows. The depletion is profound and the deposition is normally diffusion limited [1]. If there is a fluctuation in the arrival time of the wires to the surface, the wires that first reach the surface may grow at a greater rate on behalf of a reduced growth for the neighbouring wires (still inside the pores) as illustrated in **Figure 3.5**. The hemispherical diffusion zone around the caps can propagate and extend over nearby pores and inhibit their growth.

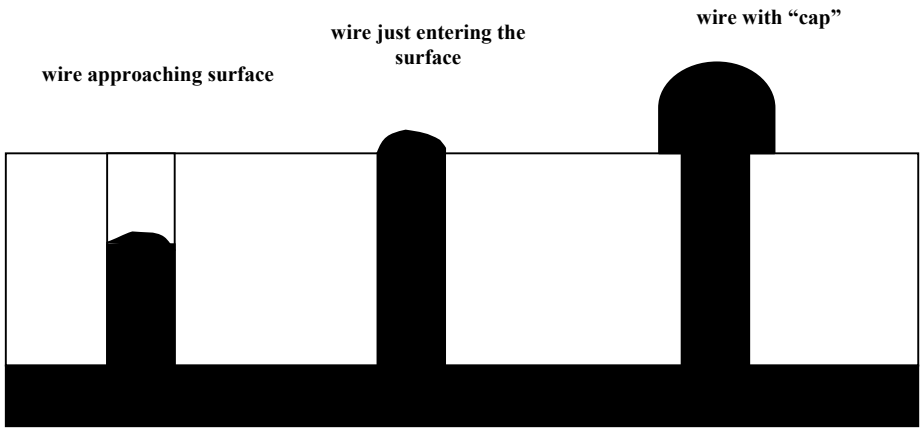

Figure 3.5: *Wires approaching the surface (left) and growing "caps" (right).*

Surface diffusion cannot be disconnected. It could contribute to faster electrochemical transportation along the surface and therefore a more flat appearance of the diffusion zone. A small fluctuation in growth is commonly found and could depend on an uneven thickness of the membrane, surface roughness or because the initiation time of wire growth is not perfectly uniform. Lindeberg [1] observed some rare artifacts in the electrodeposited structures, e.g. spherical formation (1-10µm in diameter), originating from gas bubbles that can be found in polyimide plastics. It's known that gas can be trapped in the liquid, viscous precursor during the manufacturing process.

Mirror Nickel Bath

Pore filling using the *Mirror* bath took a considerably longer time compared to the *Hard* bath solution (see **Figure 3.6**). PET templates with thickness of 23µm took between 20 and 25 minutes to be filled completely. The nickel wires have displayed some plastic properties. The wires can be mechanically bent after the dissolution of the organic matrix as demonstrated in the **Figure 3.6**.

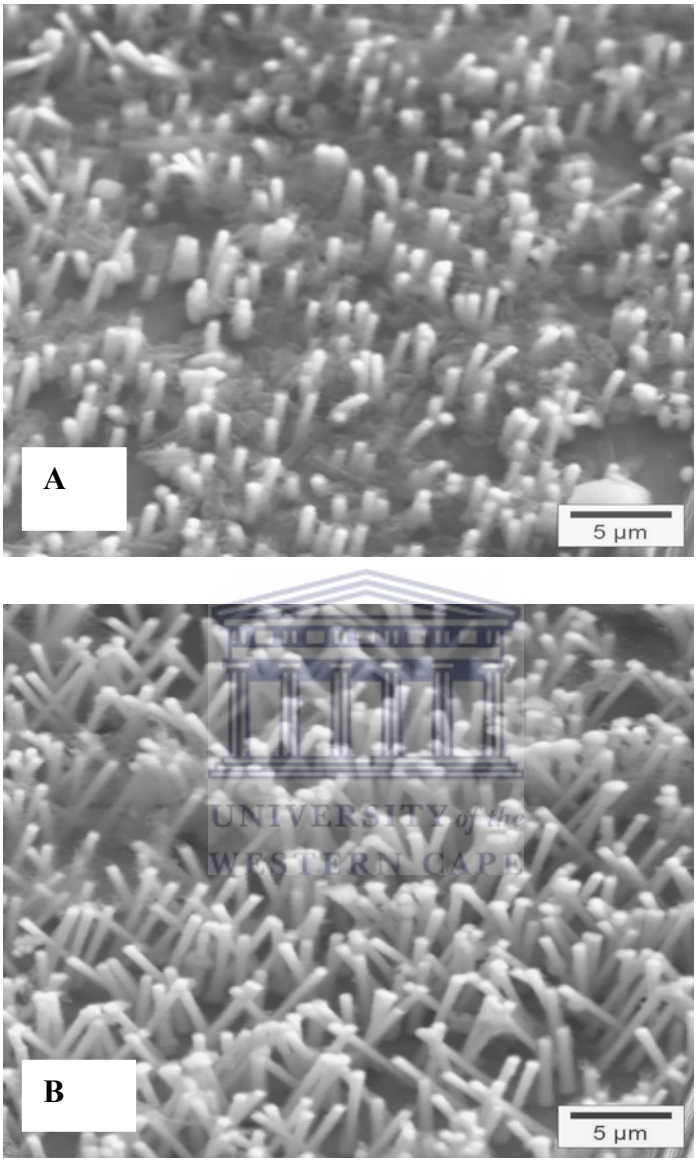

Figure 3.6: *Micrographs showing nickel wires microstructure grown through etched pores of PET polymer membrane at different times. (***A***) After 10 minutes of pore filling at 75mA/cm*^{2}*, and (***B***) after 20 minutes in* Mirror *bath.*

3.1.3 The effect of the electrodeposition method on the electrochemical behaviour of Ni microwires

A principal focus of modern research in electrocatalysis is to discover electrode materials that exhibit excellent electrochemical stability and show interesting activity towards typical electrochemical reactions [6]. It is also desirable that these materials be inexpensive, abundantly available, etc. Electrocatalytic hydrogen and oxygen evolution on various electrode materials and from various electrolyte solutions, are two of the most frequently studied electrode reactions. The reasons for this are both theoretical and practical, since the two gases represent major products or by-products of several industrial electrolytic processes. The present study is devoted to the hydrogen evolution reaction on nickel electrodes in alkaline electrolyte i.e. 0.1M KOH at room temperature.

The hydrogen electrode reaction, $2H^+ + 2e^- = H_2$, is a heterogeneous catalysis where an electrode material acts as the catalyst [7]. Its activity is closely related to the electronic configuration of these materials. A three-electrode, cylindrical electrochemical cell was used with nickel microwires as a working electrode, platinum as a counter electrode and Ag/AgCl as reference electrode. The geometric surface areas of the working electrode and counter electrode were 0.126 and 3.35 cm^2, respectively. The electrochemical behaviour was studied by applying a potential sweep rate of 50mV/s at room temperature. The electrochemical activities of nickel microstructured electrodes produced from the *Hard* and *Mirror* bath are shown in **Figure 3.7**. The start of hydrogen evolution on the *Hard* bath nickel structures occurs at -1.0V while the oxygen evolution takes place at +0.6V. The start of hydrogen evolution on the bulk nickel material occurs at about -1.3V, a shift of 0.3V when compared with hydrogen evolution on *Hard* bath nickel structures. The *i-E* relationship clearly indicates that the microstructured electrode prepared with the *Hard* bath solution was the most electrocatalytically active for hydrogen production. The difference in activity between *Hard* and *Mirror* bath is attributed to the wires, growth which is greater in the former than the latter.

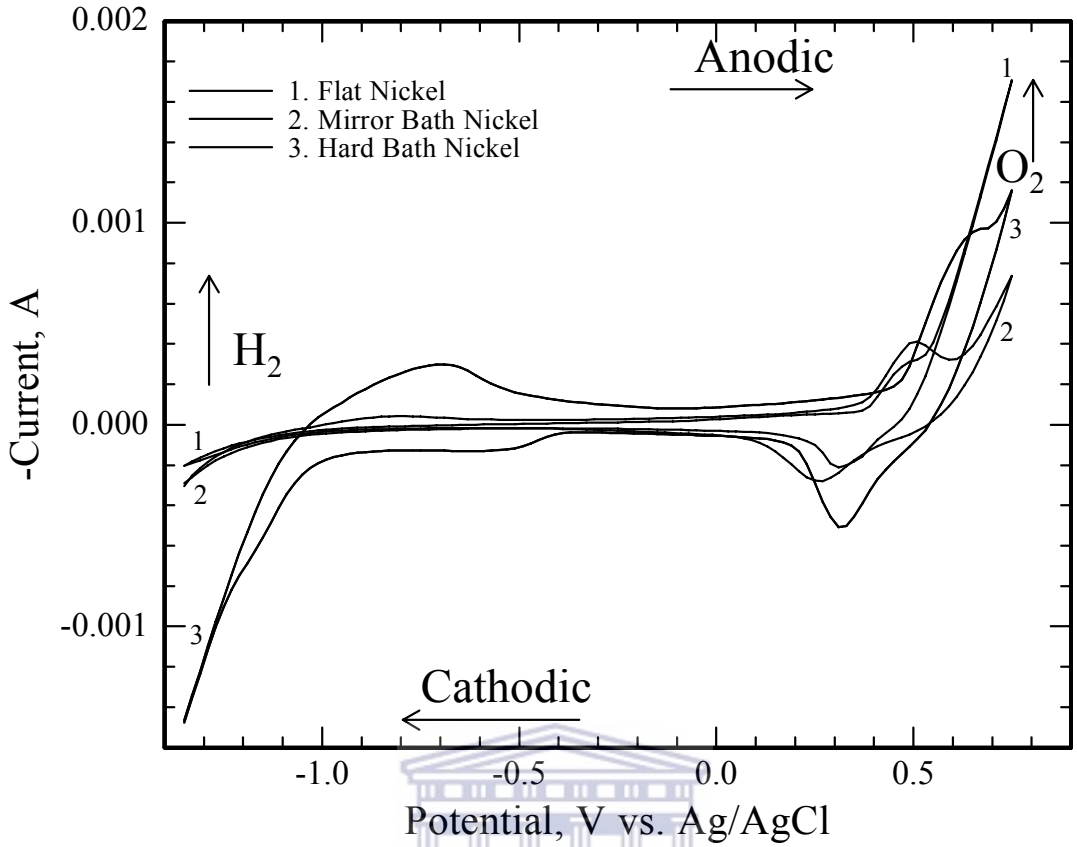

Figure 3.7: *Cyclic voltammograms of nickel microstructured electrodes prepared using different plating bath solutions for 10 minutes. Electrochemical testing was done in a 0.1M KOH electrolyte at 50mV/s sweep rate.*

All cyclic voltammograms show only one anodic peak and similarly only one reduction peak in the range of potential from -1.4 to 0.9V vs. Ag/AgCl. This anodic peak appears for the electrochemical transformation of Ni(II) oxide to Ni(III) oxide. Similar voltammograms have been reported for the nickel electrode in various alkaline solutions [8, 9, 10, 11]. The anodic peak appears at 0.480V and the reduction peak appears at 0.310V. This behaviour indicates that for both *Hard* and *Mirror* samples the oxidation and reduction peak potentials shift towards the positive and negative direction, respectively, compared to bulk nickel materials. A steady-state voltammogram was observed at this sweep rate after cycling continuously for 30 minutes.

The voltammetric behaviour of this bulk nickel deposit (**curve 1**) is fairly different from that of bulk Ni material reported in the literature [12]. This difference is attributed to the fact that the electrochemical properties of Ni are strongly dependent upon the preparation methods and conditions employed [13, 14, 15, 119:**Chapter 1**]. From a comparison of **curves 2 & 3**, although the main redox peaks are clearly found on both curves, a positive shift in peak potential of curve 3 is clearly seen. This result indicates that the electrochemical properties of nickel hydroxide have been modified by changing the plating bath solution (as shown in **Figure 3.7**). The positive shift in redox potential results in the fact that oxygen evolution commences immediately the electrode potentials just reach the redox potential of this redox couple, probably indicating a better catalytic activity for the oxygen evolution reaction (OER).

Figure 3.8 shows the comparison of the electrochemical behaviour of bulk nickel material and Ni microstructures fabricated in *Mirror* nickel bath solution for 10 and 20 minutes. On all curves shown in the figure, a pair of sharp anodic and cathodic peaks with their E_p at approximately 0.5 and 0.3V, respectively, were observed, and oxygen evolution commenced beyond 0.6V. These two asymmetric peaks are due to the redox transition of Ni^{3+}/Ni^{2+}. Peaks in the hydrogen production region were also observed. In the anodic sweep, the region between -0.8V and -1.0V, the formation of $Ni(OH_2)$ took place, corresponding to oxidation of part of nickel microwires. The oxidation of $Ni(OH)_2$ to NiOOH takes place at a different potential. In the cathodic sweep, the reduction of NiOOH to $Ni(OH)_2$ occurs at a potential between 0.2 and 0.4V, while reduction from $Ni(OH)_2$ to Ni is not observable because of the hydrogen evolution reaction (HER). It is therefore difficult to distinguish the voltammetric currents and charges between hydrogen desorption and nickel oxidation. It was found that hydrogen evolution commenced beyond -1.0V and the electrocatalytic activity of nickel microstructure prepared using *Mirror* plating bath were 20 times more than the bulk nickel material.

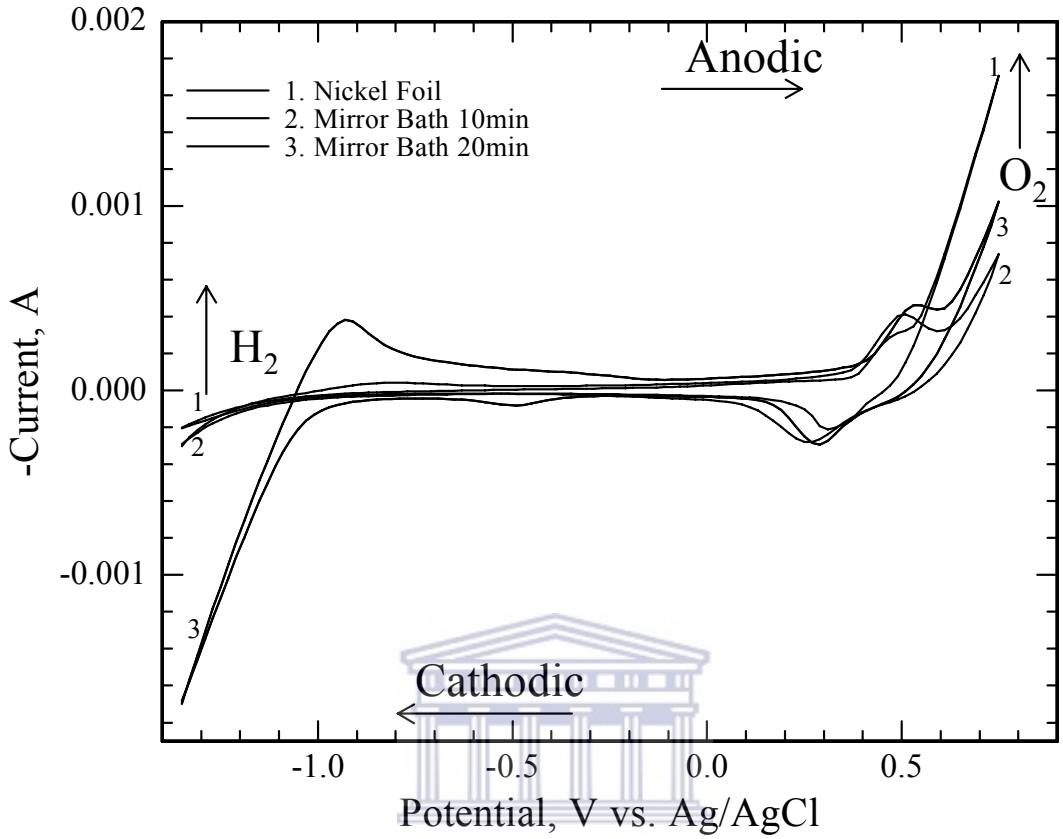

Figure 3.8: *Comparison of the electrochemical behaviour of nickel foil, and Ni structures prepared for 10 and 20 minutes in* Mirror *bath nickel plating solution. 0.1M KOH solution was used as electrolyte and a sweep rate of 50mV/s.*

3.1.4 Evaluation of consolidated Ni mirowires as hydrogen production electrodes

In this investigation water electrolysis of 40 wt.% KOH aqueous solution was conducted under atmospheric pressure using nickel microwires as working electrodes. The electrodes were completely immersed and fixed in parallel within a certain space. The height of the electrodes was chosen to be 8mm while the width of electrodes was fixed also at 8mm. The temperature of the KOH aqueous solution was controlled at

20°C, 40°C, or 60°C by heaters. The electrolyte solutions were, if necessary, de-aerated by bubbling nitrogen gas through them for at least 10 minutes prior to electrochemical measurements. The inclination angle of the electrodes was vertical. The efficiency of hydrogen production to water electrolysis was qualitatively evaluated and compared by the current density value at certain potentials. Since the amount of hydrogen gas is proportional to the electric current, current density becomes good index to represent the electric power necessary to produce a certain mass flux of hydrogen when compared to data of the same voltage value. Lower applied voltage means higher efficiency of water electrolysis.

In practice, a constant electrode potential is applied to the working electrode and the current density monitored until it remains constant for a specific time (5 to 10 minutes) and then the resulting current density is recorded. The applied electrode potentials were chosen according to the electrode material, temperature and electrolyte concentration used. All measurements were repeated with fresh solution at least twice under the same conditions to ensure reproducibility. Activity was performed on several electrode materials to evaluate the effectiveness of the materials for hydrogen evolution. From the viewpoint of electrochemical engineering, increased electrocatalytic activity can be achieved through increased intrinsic activity and/or increased real catalytic surface area [16]. The latter is the main contributor to the total increase in catalytic activity.

In **Figure 3.9**, the effect of temperature on the current-potential relationship for HER on nickel microwire electrodes is shown. It can be seen from the figure that there is an increase in current density by more than double due to a high hydrogen evolution reaction on the nickel wires compared to bulk nickel material. The high efficiency of the nickel wires is a result of its high surface area per unit volume, in addition to its intrinsic activity for hydrogen evolution reaction. Cathode materials affect the onset potential for the hydrogen evolution reaction. The nickel wires tested at 60°C showed the best propensity for hydrogen evolution under the quoted experimental conditions. For example, at 2V, current densities were 168, 198, 239, and 62, 85 and 118mA for Ni microwires at 25, 40, 60°C and Ni foil at 25, 40 and 60°C, respectively.

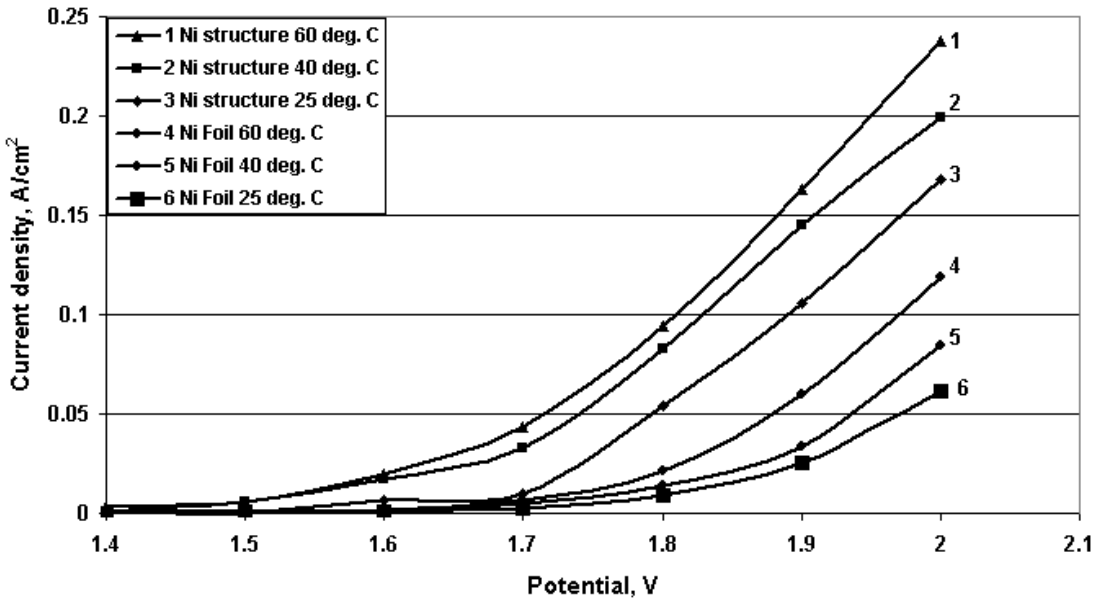

Figure 3.9: *Activity for hydrogen production of microstructured nickel electrodes (deposition in* Hard *bath solution) and nickel foil at different temperatures.*

As the temperature increases, the exchange current density increases. The measured effect is the sum of two effects i.e. the effect of temperature on the conductivity of the electrolyte and on the kinetics of the charge transfer step at the electrode/electrolyte interface. The increase in temperature leads to a decrease in the applied potential of the reaction and a decrease in the electrolyte resistivity. These results exhibit the expected behaviour: a lower voltage at higher temperatures because of the higher reaction rates. Thus, operating the electrolysis process at elevated temperatures decreases the activation and ohmic polarizations associated with HER. This means that energy consumption decreases with the rise in temperature.

Nickel microwire electrodes exhibit a reduction in potential compared to Ni bulk material. However, the Ni microwires tested in 60°C solution gave the maximum reduction in electrode potential when used in alkaline solutions, particularly at high potentials. The morphology of all nickel microwires were unchanged with hydrogen evolution because their structure is not significantly affected by this cathodic reaction unless the deposition of cations dissolves in the electrolyte.

3.2 Effect of thermal annealing on the morphology and electrochemical properties of Ni microwires

In the present work, the thermal annealing effect on the electrochemical activation of nickel microstructures galvanostatically electrodeposited from *Hard* bath solution was evaluated. The aim, therefore, is to compare the electrocatalytic properties of electrodeposited wires subjected to different post-annealing conditions. SEM and cyclic voltammetry were employed for characterizations of the microstructures.

The nickel structures were annealed at 300°C in air for 1 hour. Two samples were annealed in the furnace: one before etching the sacrificial membrane and the other after etching in NaOH solution. The effects of annealing treatment on electrochemical properties are reported. The microstructural aspects of annealed wires were shown to critically affect their electrochemical properties. Cyclic voltammograms recorded at a scan speed of $30mVs^{-1}$ for all wires under investigation is displayed in **Figure 3.10**. The position of the ill-defined anodic peak current shifts to more positive potentials when the sample was annealed prior to etching.

Irrespective of the annealing temperature, the values for the maximum current attained in the cathodic cycle were observed to be always equal to their anode analogues. As the crystal structure changes in heat treatment, the annealed structures may display significant changes in electrochemical properties when compared with the unannealed structure. The kinetics of the electrochemical hydrogen reaction were generally characterized by current density to evaluate the electrocatalytic activities of the structures and annealed states.

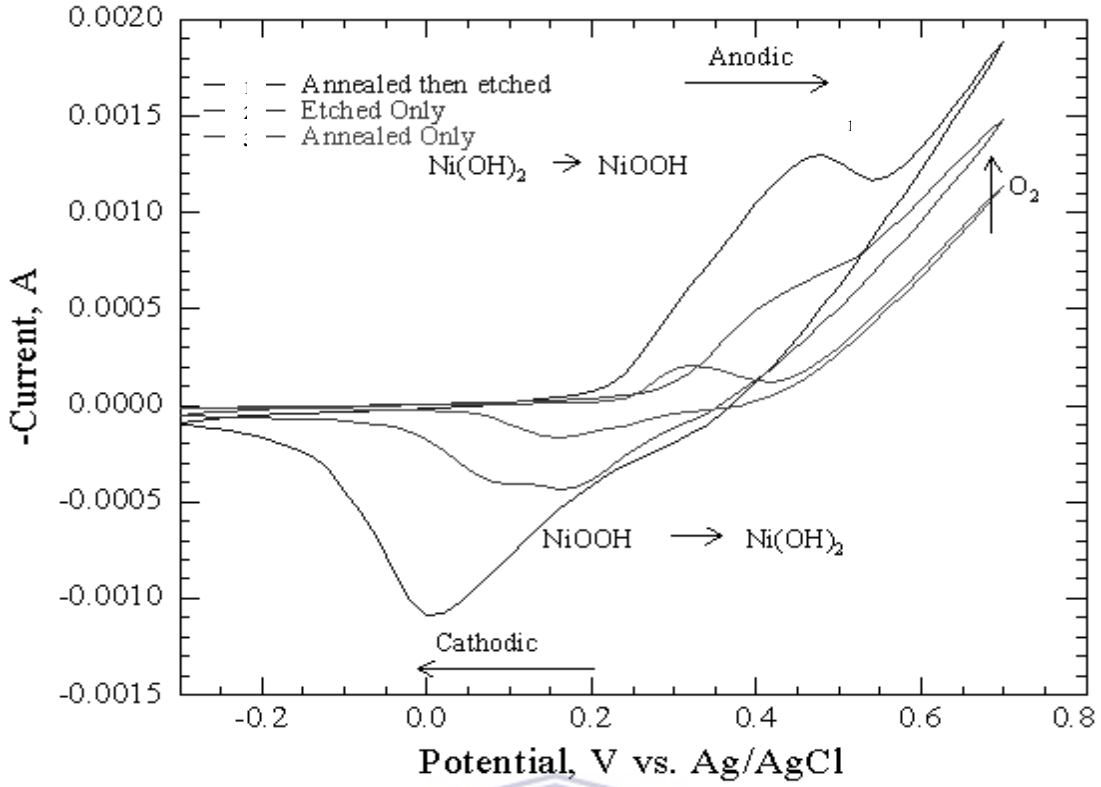

Figure 3.10: *Comparison of electrocatalytic activity of nickel structures annealed at 300°C in 0.1M KOH electrolyte. Sweep rate at 30mV/s.*

SEM micrographs allow one to identify the changes in the morphological characteristics of nickel structures caused by thermal treatment. **Figure 3.11** illustrates the difference in morphology of the nickel structures 'before' and 'after' thermal annealing at 300°C for 1 hour and 'before' and 'after' etching in alkaline solution. From the SEM micrographs it can be seen that the template membrane was not removed on the sample that was only annealed (as can be seen in **Figure 3.11C**). This indicates that the activation property of the annealed structures deteriorates (as shown **Figure 3.10**). The segregation of Ni is inevitable in the unannealed structures. The segregation of Ni is favourable for activation because Ni has good electrolytic activity. This favourable factor will be lost on structures that are only annealed due to homogenization during the annealing process. It is obvious that annealing prior to the etching treatment increase the activity of the nickel structures. This approach mainly studied the effects of annealing temperature on the catalytic properties and morphology of the microstructures.

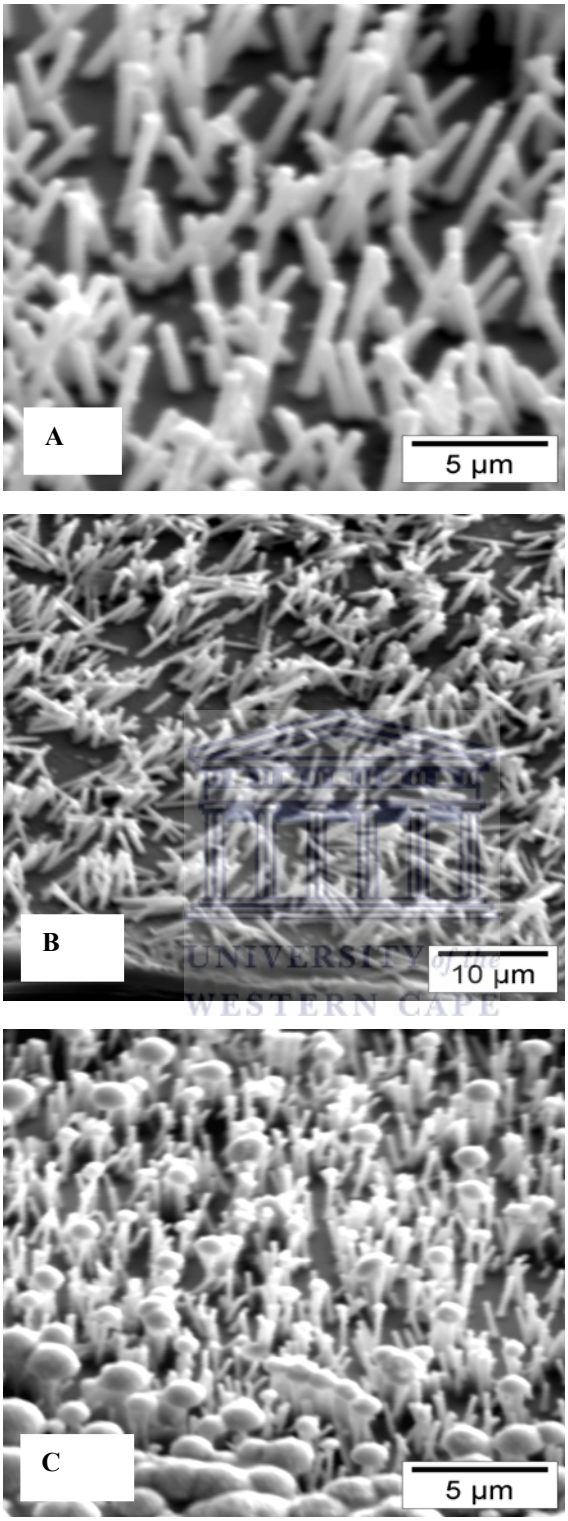

Figure 3.11: *Nickel microwires of 0.4µm in diameter electrodeposited in the PET template membrane. (***A***) Sample etched in NaOH electrolyte, (***B***) sample annealed before etching, (***C***) sample annealed and not etched.*

3.3 Influence of the template pore diameter on electrochemical behaviour of Ni materials

Membranes prepared by xenon bombardment of PET or polycarbonate (PC) were used. These membranes were cut into approximately 1cm^2 sized electrodes. A cycle of electrochemical analyses was performed on each sample.

Each high surface area nickel bulk sample was subjected to 1.4V over 600s in order to determine the coulombic response of the electrodes over time before making a comparison of these electrodes. Each sample was also subjected to cyclic voltammetry in normal mode in which the potential was increased in preset steps at the end of each time interval, and at which point the current was sampled. Cycling was performed between 0 and –1.5V for 5 cycles. The electrolyte used was 40 wt.% KOH solution.

Since nickel in its metallic form was the electrode of choice in the production of hydrogen gas, Petrik *et al.* [17] performed cyclic voltammetry and chrono-coulometric experiments over nickel electrodes that had not been exposed to an oxidizing cycle. The oxidation and reduction wave, onset of hydrogen evolution and increasing overpotentials over a number of cycles, were evaluated for some samples. Furthermore, some samples were exposed to high voltages of up to 2.5V during cyclic voltammetry. High surface area nanostructured nickel electrodes had configurations shown in **Table 3.1** and selected SEM micrographs of the most active and stable nickel electrodes are presented in **Figure 3.12**.

Table 3.1: *Configuration of high surface area nanostructured nickel electrodes [17].*

Sample number	Pore size (μm)	Diameter of structures (μm)	Length of structures (μm)	Thickness of support (μm)
Ni blank				
Ni 1	0.2	0.2	10	10
Ni 2	0.1			
Ni 3	0.2	0.2	6.5	14
Ni 4	0.05	0.05		
Ni 5	2.5			
Ni 6	1.5			

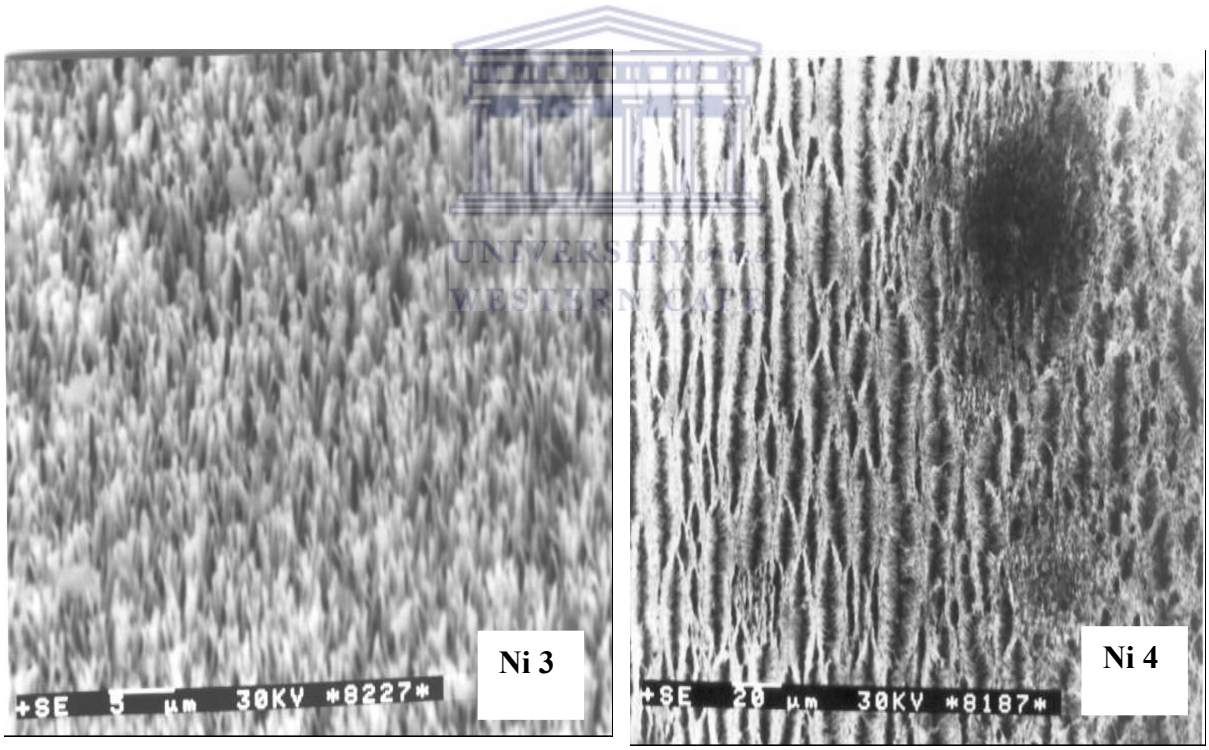

Figure 3.12: *SEM micrographs of selected nanostructured nickel electrodes [17].*

In order to differentiate the improvement gained in electrochemical activity by use of enhanced surface areas it was necessary to compare the response of the high surface area nickel electrodes with that of a smooth nickel electrode. The current densities obtained during water electrolysis at 1.4V for 600s using differently prepared secondary structured electrodes under identical conditions are presented in **Table 3.2**.

Table 3.2: *Current densities obtained using nanostructured nickel electrodes for water electrolysis [17].*

Sample No.	Current density (mA) at-1.4V
Ni 1	5.4
Ni 2	16.8
Ni 3	18.3
Ni 4	26.6
Ni 5	9.5
Ni 6	10.8
Flat Ni foil	3.4

The current densities achieved over secondary structured Ni electrodes 2-4 were significantly higher than nickel electrodes in flat foil configuration. The clustering of very finely divided secondary structures observable on Ni 4 gave rise to the greatest activity and durability.

Petrik *et al.* [17] also observed that the size of the evolving hydrogen gas bubbles was significantly different between the different samples, with the finest bubbles being observed on the finest secondary structures. The effective discharge of such minute gas bubbles from electrode surfaces probably resulted from lower surface adhesion between electrode surfaces. This may also have contributed significantly to the activity of these electrodes.

They also found that the onset of hydrogen generation was not observable in sample Ni 1 under the applied voltages. However in all other samples tested, bubble formation was observed during chronovoltammetry at -1.4V: therefore the dynamic, changing surface area may have contributed to non-reproducibility. The production of hydrogen possible at different potentials for the various track-etched structured nickel electrodes, is compared in **Table 3.3**.

Table 3.3: *Grams of H_2/m^2/day obtained over different track etched secondary structured Ni electrodes at 1.4V [17].*

Ni structures	**H_2/m^2/day**
Ni 1	48
Ni 2	150
Ni 3	164
Ni 4	**238**
Ni 5	85
Ni 6	97
Ni flat foil	30

The author would like to express his sincere gratitude to L. Petrik, B. Bladergroen, S. Botha, V.M. Linkov and G. Gericke for their help in the realization of this investigation.

3.4 Novel Ni nanomaterials: Preparation and morphology of Ni nano-needles synthesized with asymmetric track-etched membranes

An asymmetric membrane is constituted of two or more structural planes of non-identical morphologies. It can be created by the modification of a track membrane structure. If PET membrane is treated in a plasma of non-polymerizing gases, the surfaces are etched together and the track membrane mass decreases via the emission of gaseous products. Kravets *et al*. [18] showed that the treatment of PET track membrane in a glow discharge could be used as a non-chemical method for pore etching. It was also shown that the treatment of PET and polypropylene (PP) track membranes in RF-discharge plasma in air led to the formation of track membranes with the shape of the membrane pores changed.

The pores are characterized by a large aspect ratio and a narrow size distribution [[4]:**Chapter 1**]. Meeting the increasing interest in the production of pores with opening diameters down to the nanometer scale, new etching methods have been developed by using one-side etching procedure [19, 84:**Chapter 1**]. To etch the track from one side, the irradiated foil was placed between the two chambers of a conductivity cell. One chamber of the cell was filled with the etchant while the other side of the membrane was protected by a stopping medium.

Immediately, when the etchant reaches the opposite surface of the sample, an acidic stopping solution neutralizes the NaOH etchant. The duration of the etching process was 2 hours. The small pore openings on the other side of the sample are below SEM resolution capabilities. **Figure 3.13** shows a schematic representation of an asymmetric membrane. Asymmetric track membranes with various characteristics can be produced both by varying the discharge parameters and by changing the etch time at definite discharge parameters.

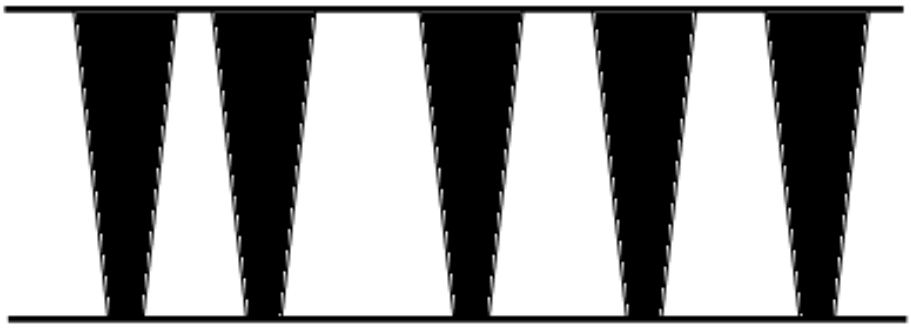

Figure 3.13: *Schematic structure of pores of a source PET track membrane with a changed pore profile.*

The preparation of asymmetrical ultra-porous track membranes was done in collaboration with the Institute of Crystallography of the Russian Academy of Science (RAS). PET membranes (23µm thick) were irradiated with high energy Kr ions at a fluence of 3 x 10^9 pores/cm^2. The surface morphology and porous parameters of this template has been investigated by SEM (as shown in **Figures 3.14**). The nanowires synthesized using this method can be as narrow as 10nm. An example of asymmetric nanowires produced in this investigation is shown in **Figures 3.15**.

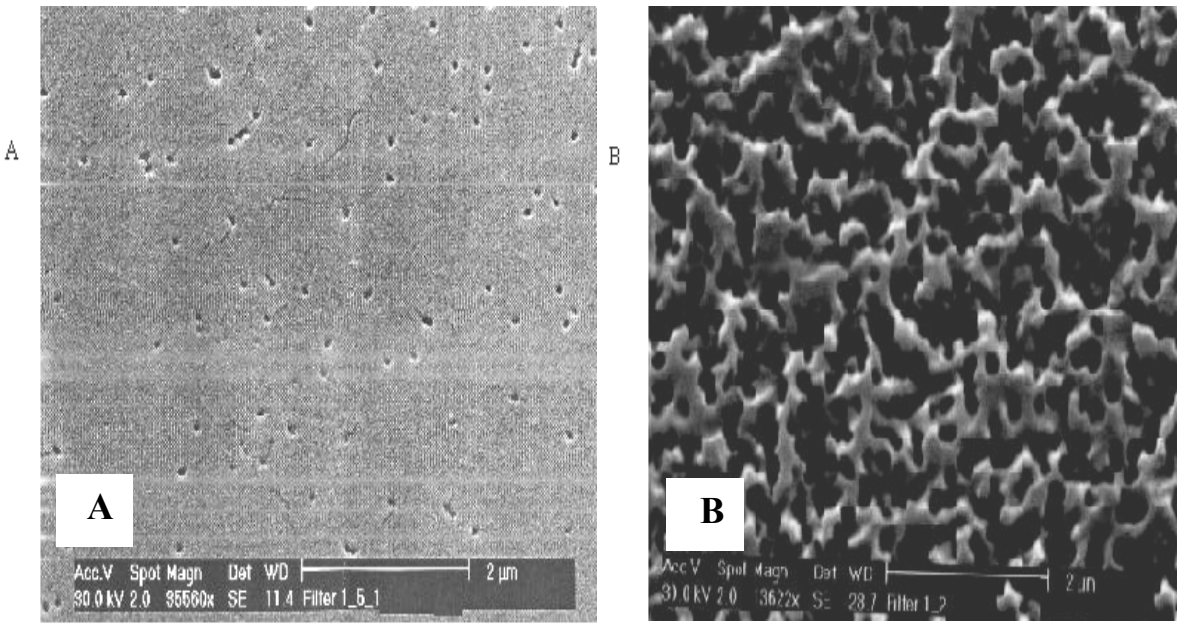

Figure 3.14: *SEM of asymmetrical track-etched membrane surface (***A***) top view selective layer of membrane, (***B***) top view of non selective/supporting layer*.

The asymmetrical membranes, most importantly, produce stable nickel nanostructured wires with a thickness less than 50nm. The creation of consolidated nanomaterials with these parameters is of particular interest for modern nanotechnology. Two varying thicknesses of asymmetrical membranes were used, namely, 23µm and 10µm. The increase in thickness of the polymeric membrane was expected to increase the catalytic activity of electrodes due to the increase in the surface area. For comparison purposes, experiments using 23µm thick microporous asymmetric templates with 0.2 and 0.4µm pore diameter were used for the preparation of nickel nanostructured electrodes.

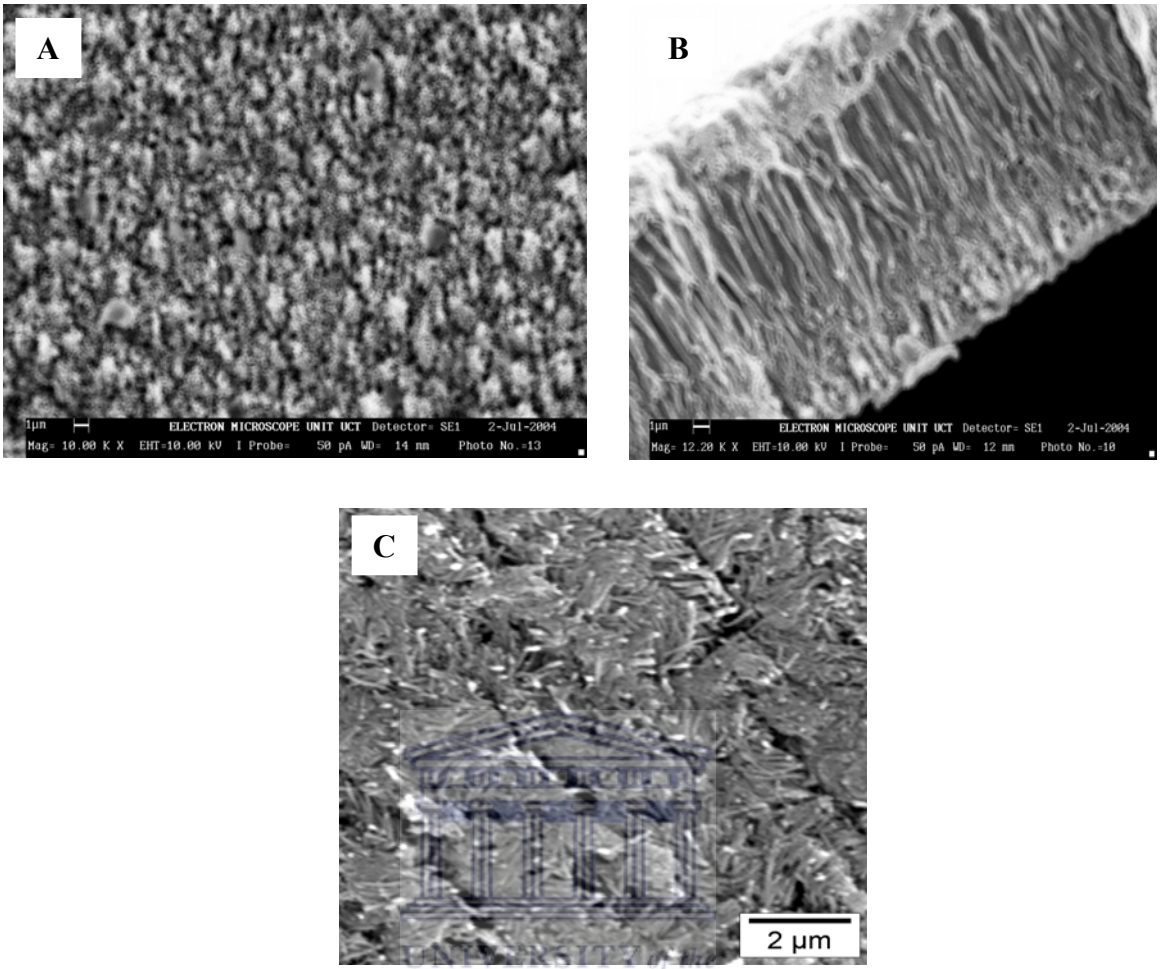

Figure 3.15: *SEM micrographs showing nickel secondary structures prepared using asymmetrical membranes.* Hard *nickel bath was used during electrodeposition. (***A***) & (***C***) shows top view and (***B***) cross-section of nickel nanowires for 25 minutes deposition time.*

The SEM images indicate that many of the wires maintain the original diameters for quite sometime after protruding from the holes, although some of them were seen to form branches. The wires perhaps maintain the same diameters outside the membrane to keep the surface energy at a minimum. The nanowires thus prepared were stable for months in terms of their physical forms and their chemical characteristics.

CV technology is a useful method which enables independent estimation of oxidation [20] as well as reduction reaction potentials and throws light on the mechanism of obtained electrodes. Furthermore, within certain limitations, it enables estimations to be made [21, 22] of various parameters such as charge capacity, coulombic efficiency, reversible potential and reversibility.

Figure 3.16 shows an electrochemical behaviour of nickel structures prepared using asymmetric membrane in *Hard* bath solution. The peaks correspond to the oxidation of Ni to α-$Ni(OH)_2$ [23, 24] and the reduction later upon potential reversal. The intensity of both the oxidation and reduction peaks were found to increase upon the increase of the nickel loading into the pores of the template membranes.

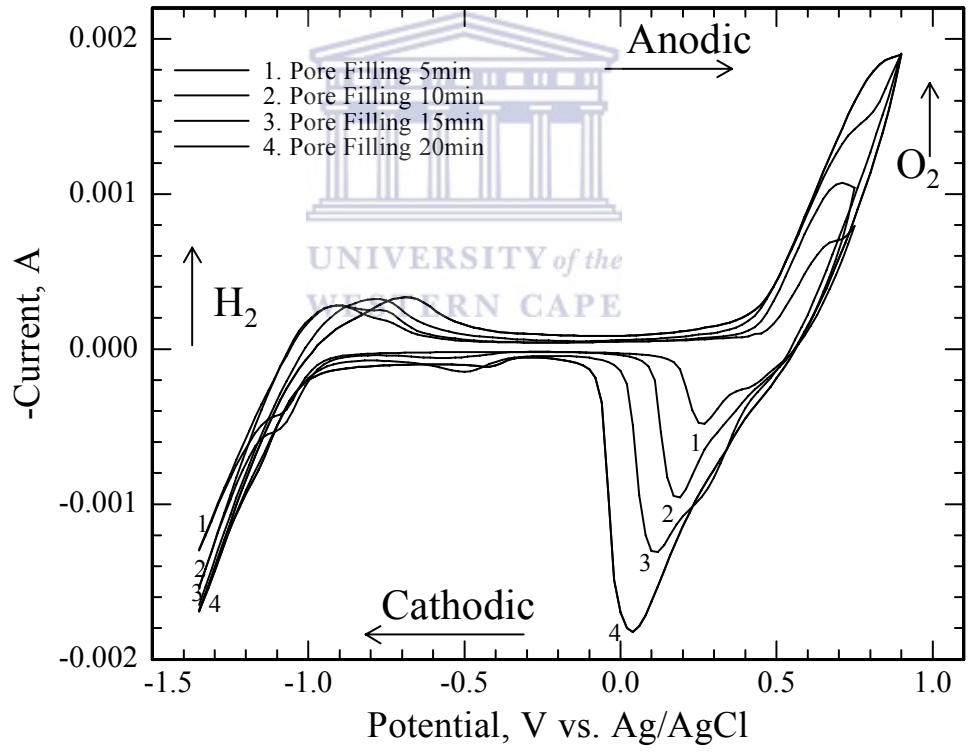

Figure 3.16: *Comparison of the electrochemical behaviour of nickel structures prepared by asymmetric membrane for 5, 10, 15 and 20 minutes in* Hard *Bath nickel plating solution. 0.1M KOH solution was used as electrolyte at a sweep rate of 8mV/s.*

3.5 The peculiarity of Ni nanomaterials obtained by the electroless deposition technique

In the next investigation, PET membranes of varying pore diameters were electroless plated via the "two-step" process (a detailed explanation is found in **section 2.2.2**). The sensitization of the PET membranes was carried out by directly immersing the polymer in an aqueous solution containing 22.5g $SnCl_2.H_2O$ and 30ml HCl. The activation mixture was prepared by dissolving 0.1g $PdCl_2$ in 2ml HCl and the volume was increased up to 500ml with de-ionized water.

The activated polymers were immersed in nickel electroless plating bath (refer to **Table 2.3**). The sensitization reduces the induction period of the Ni deposition reaction and promotes complete coverage of the surface and improves plating quality [25]. The Sn sensitizing layer enhances Pd adsorption as well as the binding strength of Pd to the surface [[2]:**Chapter 1**]. After the sensitization and activation, Pd and reduced Pd atoms exist on the surface.

Samples were prepared by using track-etched polymer membranes with pore diameter ranging from 0.03-0.1μm as template matrix. In order to increase the thickness of the supporting layer, an additional nickel film was carried out by the electrodeposition method. The opposite side of the membrane was insulated in order to avoid undesirable filling of pores. The template polymer membrane was etched in a alkaline solution to expose wires of different diameters. The electrochemical behaviour of the prepared electrodes was investigated by cyclic voltammetry in aqueous 0.1M KOH solution at room temperature. A platinum wire as counter electrode and a silver-silver chloride (Ag/AgCl) electrode as reference were used. The electroless deposition method was only used for the preparation of nanostructured nickel materials.

Figure 3.17 below shows the cyclic voltammograms of wires prepared with asymmetrical membrane, 0.05µm, 0.03µm diameter membrane and smooth nickel foil. Each electrode has one anodic and one cathodic peak, corresponding to the nickel hydroxide redox reaction. There is a pronounced difference in the behaviour of the nickel wires compared to the nickel foil. At 30mV/s sweep rate, the anodic peak appeared at 0.5, 0.4 and 0.25V for the asymmetric, 0.03µm and Ni foil, respectively and the reduction peaks appears at –0.1, 0.05 and 0.1, respectively. This behaviour indicates that with high surface area nanostructures, both the oxidation and reduction peak potentials shifts towards the positive and negative directions respectively. Steady-state voltammograms was observed for all samples after cycling continuously for 30 minutes. Both the anodic and cathodic peak currents were found to be stable with time.

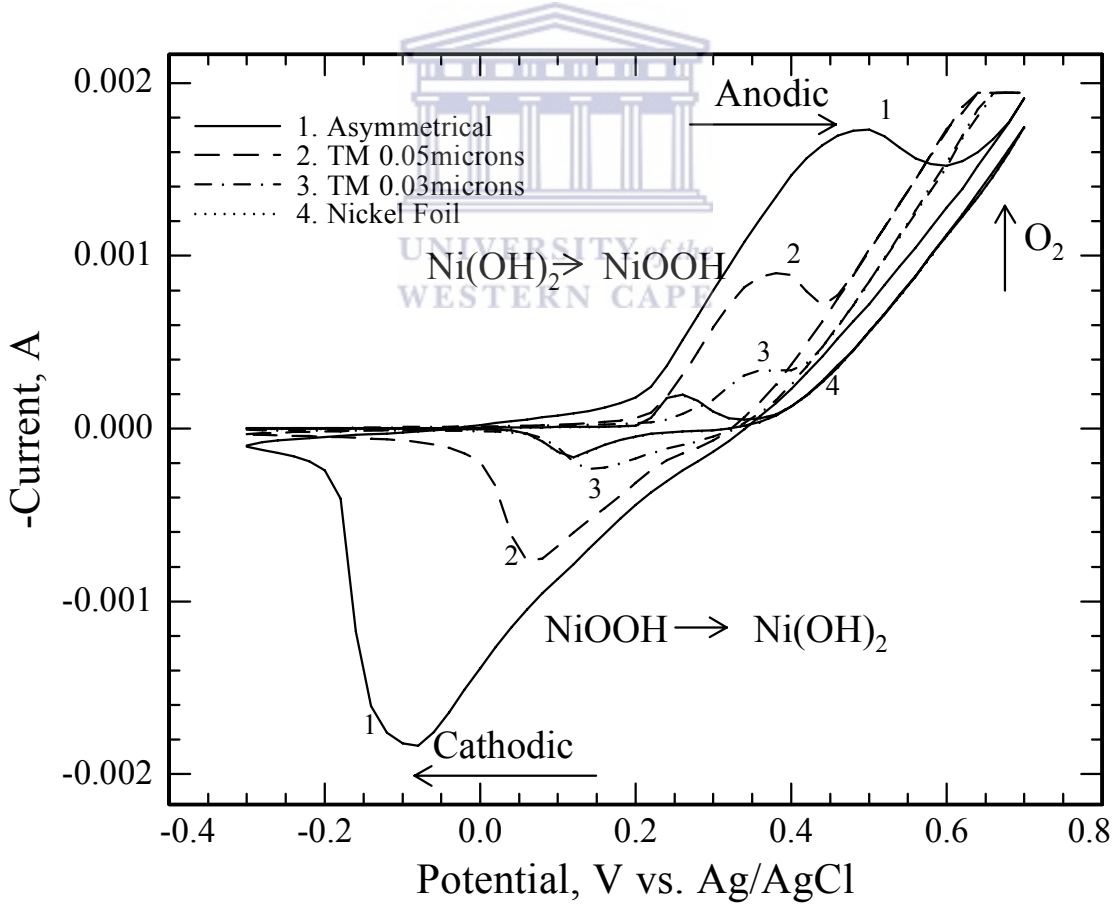

Figure 3.17: *Comparison of the electrocatalytic activity of nickel structures prepared using the electroless deposition method in 0.1M KOH electrolyte. Sweep rate 30mV/s.*

3.6 Influence of the template structure on the crystal nature of Ni micro- and nanowires

In this section, studies of the crystallographic structure of electrodeposited bulk Ni material, micro- and nanowires will be presented. **Figure 3.18** shows the XRD results of nickel structures after the dissolution of the template membrane. The diffraction peaks of Ni were clearly shown on all patterns. The X-ray diffraction patterns clearly show the characteristic reflections expected for nickel with face centered cubic (FCC) structure [25, 26]. The spectra recorded showed that the structures were crystalline. **Figure 3.19** shows a plot of Ni(111) peak intensity of the nano-, micro- and macro nickel structures versus pore diameter. The peaks recorded correspond in increasing order of 2Θ to (111), (200), (220), (311) and (222) reflections. The ratio of intensities of the XRD peaks of Ni(200) and Ni(111) planes for electrodeposited macrostructures, microstructures and nanostructures are 4.05, 4.3 and 3.92, respectively and that of Ni(111) and Ni(311) are 4.65, 3.12 and 1.92, respectively. It can be seen that there is a preferential growth of Ni(111) planes in all cases except for nickel bulk material (as shown in **Table 3.4**).

Diffraction patterns of nickel structures showed that the intensity of Ni(111) peak is larger than that of Ni(200) while the opposite results was found on the pattern of the nickel foil. In addition, the sequence of the Ni crystalline planes with respect to decreasing intensity is Ni(111) > Ni(311) > Ni(200) while the nickel foil was Ni(200) > Ni(220) > Ni(111).

The intensity of all diffraction peaks on the XRD spectra is very low (smaller than 1200), indicating that the amount of crystalline Ni within these deposits should be low. The XRD spectra of these three deposits are not significantly influenced by both anodic and cathodic polarization at very high current densities, implying their good stability in water electrolysis. The high activity of hydrogen evolution on these deposits is not only due to their catalytic activity but also attributable to their relatively high surface area.

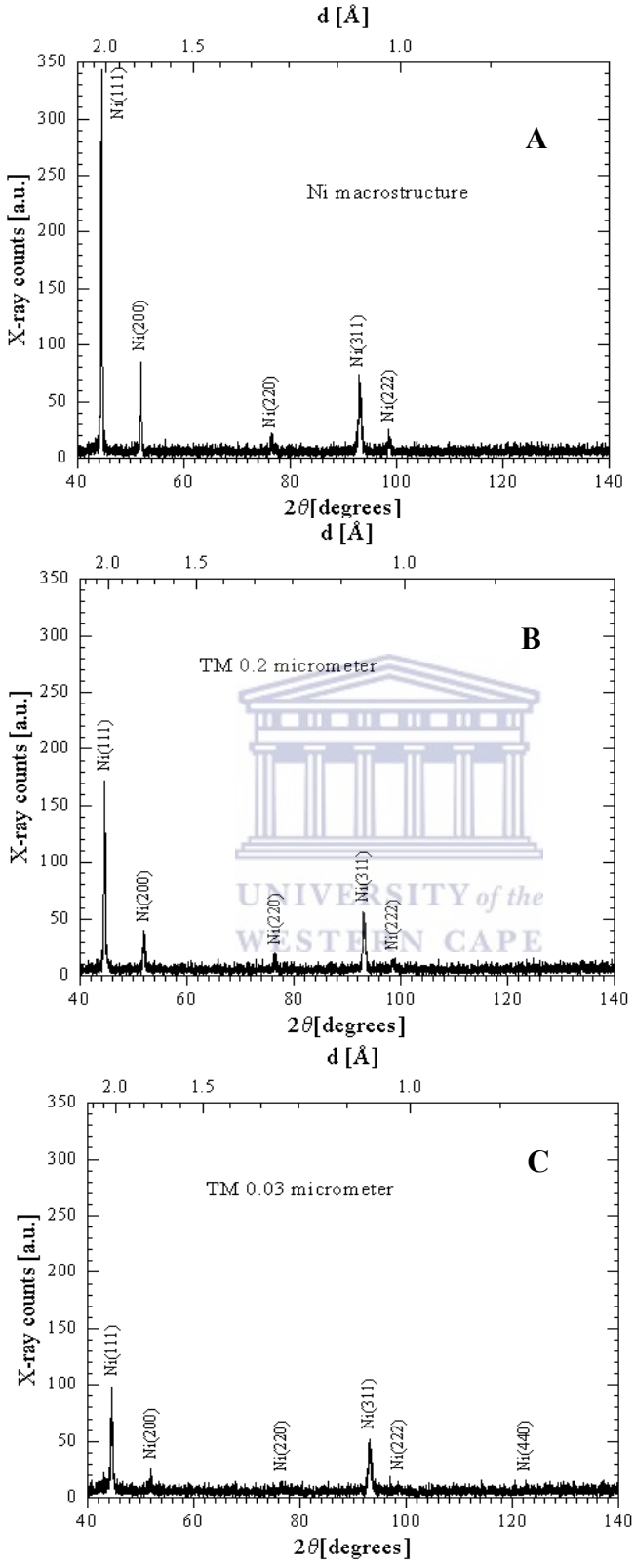

Figure 3.18: *X-ray diffraction pattern of nickel structure after the dissolution of the template membrane. Ni(111) has the highest intensity.* (**A**) *Ni macrostructure*, (**B**) *Ni microstructure and* (**C**) *Ni nanostructure*.

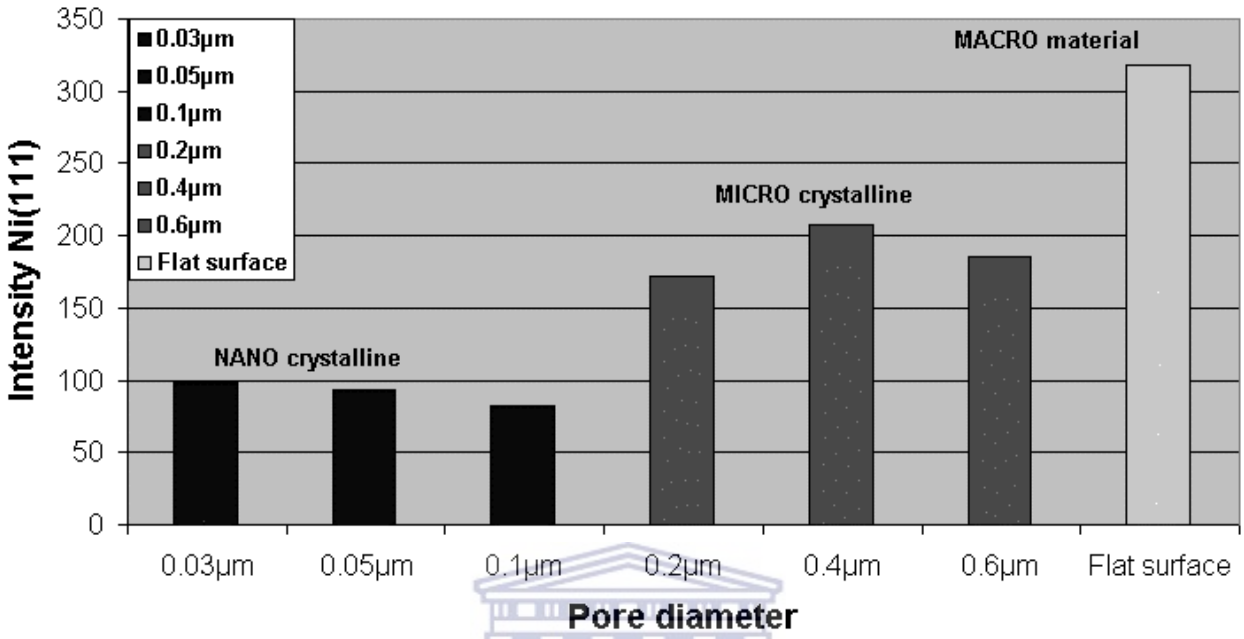

Figure 3.19: *Summary of X-ray diffraction results of Ni(111) peak Intensity of nano-, micro- and macro nickel materials versus pore diameter.*

The formation of oriented crystals on a sufficiently smooth and crystallographically indifferent substrate depends on the conditions of deposition. According to the studies of electrocrystallization, the orientation of the crystallites in deposited layers depends on the overvoltage during deposition.

Table 3.4 shows the results of X-ray analysis of nickel wires of different pore diameters. These results may be attributed to the influence of the Ni substrate on the nucleation or growth of nickel wires. The XRD phase analyses revealed that the nickel nanowires were polycrystalline in nature. It was observed that changing the pore diameter of the membrane did not affect this orientation.

The development of preferred planes in nickel deposits is a result of adsorbed hydrogen, which may be enhanced by the electrolyte temperature while pH of the solution remains constant [27]. The XRD pattern of nickel wires show varying peak

width ranging from 0.2703° up to 0.4271°, depending on the pore diameter of the wires. Nickel nanowires grown through the PET templates showed a homogeneous growth, though in a small number of pores the wires showed voids.

Table 3.4: *Effect of template pore diameter on crystallographic orientation of nickel electrodeposited from the* Hard *bath solution.*

Templates	**Crystallographic orientation (*hkl*)**			
	Relative peak intensities (I/I_{max})%			
	(111)	**(200)**	**(220)**	**(311)**
0.03µm	100	26	15	53
0.05µm	100	18	18	67
0.1µm	100	24	27	63
0.2µm	100	23	12	33
0.4µm	100	15	10	32
0.6µm	100	19	11	35
Electroplated	100	81	21	70
Vac. deposited	100	5	7	18
Nickel Foil	46	100	77	22

3.7 The effect of surface modification by Pt group metals on the electrochemical behaviour of Ni microwires

The study of the electrochemical properties of so-called nickel microstructures modified with platinum and palladium particles is the subject of this section of the thesis. The hydrogen evolution reaction (HER) is an electrochemical process that has received wide attention because of its importance in both fundamental and technological electrochemistry [28]. From a purely technological standpoint, the cost of electrolytic hydrogen is directly dependent on the voltage used to operate an electrolyzer at significant current densities [29]. The operational voltage depends on the overpotentials for the cathodic and anodic reactions and on the internal resistance of the cell [29]. Because of cost and stability considerations, very few materials can even be considered for use as anodes and cathodes in practical electrolytic cells [30].

Two properties play an important role in selecting catalytically active materials for hydrogen evolution, namely, the actual electrocatalytic effect of the material and its long-term stability. Electrode materials with catalytic properties for water electrolysis have been investigated by several authors and it was found that platinum is very effective [28-36]. Although platinum is an expensive metal, because it has an electrocatalytic effect on the formation of hydrogen at the cathode, it is the most widely used for electrolysis in industry [31].

The overpotential due to hydrogen evolution on the platinum cathode in acidic and basic medium is not as high. Pt-metal and Pt-metal oxides are either applied in the form of a thin coating on a less expensive but easily produced and shaped supporting metal. This applies generally to gas evolving electrodes or they are worked into highly dispersed forms into relatively very thin (0.1-0.5mm) porous gas diffusion electrodes [36]. Porous electrodes have a wide range of application, and are commonly used in batteries, fuel cells and electrolysis [37]. The performance of electrolytic materials

have usually been improved by either increasing the ratio between the real and the apparent surface area of an electrode or by a combination of electrocatalytic components [38]. A less common way of improving the electrocatalytic activity is by modifying the microstructures.

In this study, an attempt was made to enhance the electrochemical activity of the nickel structures for hydrogen production. This was done by modifying it with Pt group metals. Nickel microstructures were prepared by using 0.4μm pore diameter PET membrane as sacrificial membrane. After etching the polymeric membrane, the nickel microstructures were modified with Pt, Pd and Pt-Pd alloy.

A fundamental parameter that characterizes an electrode performance is the value of the current density at a given cathode potential. This value must be as small as possible in order to minimize the power consumed during water electrolysis. The aim of this work was to present a novel electrode, which has been modified with Pt and Pd by the electroless deposition method. With the data obtained, an attempt was made to determine the best cathode for the most economical electrolysis process.

3.7.1 The influence of Pt deposits on Ni microwires and on the hydrogen evolution reaction

Platinum is a versatile but expensive catalyst or material [39]. Pt is one of the best electrocatalysts for the production of hydrogen. Nickel structures were platinized by cathodizing at room temperature for times varying between 0 and 45 minutes in a solution containing 1.2mg/ml of chloroplatinic acid solution (H_2PtCl_6) in 5ml test tube. The platinized working electrode was connected to a platinum counter electrode in the electrolyte. The experiments were performed at room temperatures. During the investigation of the cathodic behaviours of platinized nickel structures against platinum as counter electrode by electrolysis, progressively increasing voltage was applied from zero volts up to 2.0V from a direct current source. Current-potential curves were obtained from electrodes arranged in this way.

Platinum distribution was determined by SEM. The Ni structures grown in the etched ion tracks, with diameter of about 0.4μm after modification are demonstrated at low magnification in **Figure 3.20**. In the tracks, Ni growth propagates only along the axes of the pores, since it is limited in the perpendicular direction by the walls of the cylindrical templates. Therefore, these structures usually take on a cylindrical shape as can be seen in the figure below.

From a comparison of the Ni and Ni-Pt micrographs of **Figure 3.20**, it must be emphasized that the Pt deposited on the microstructures by chemical reduction, appears to have a less uniform distribution. These facts affect the electrode surface area, leading to an increase of the active surface area. This is also substantiated by the stronger catalytic activity of these systems.

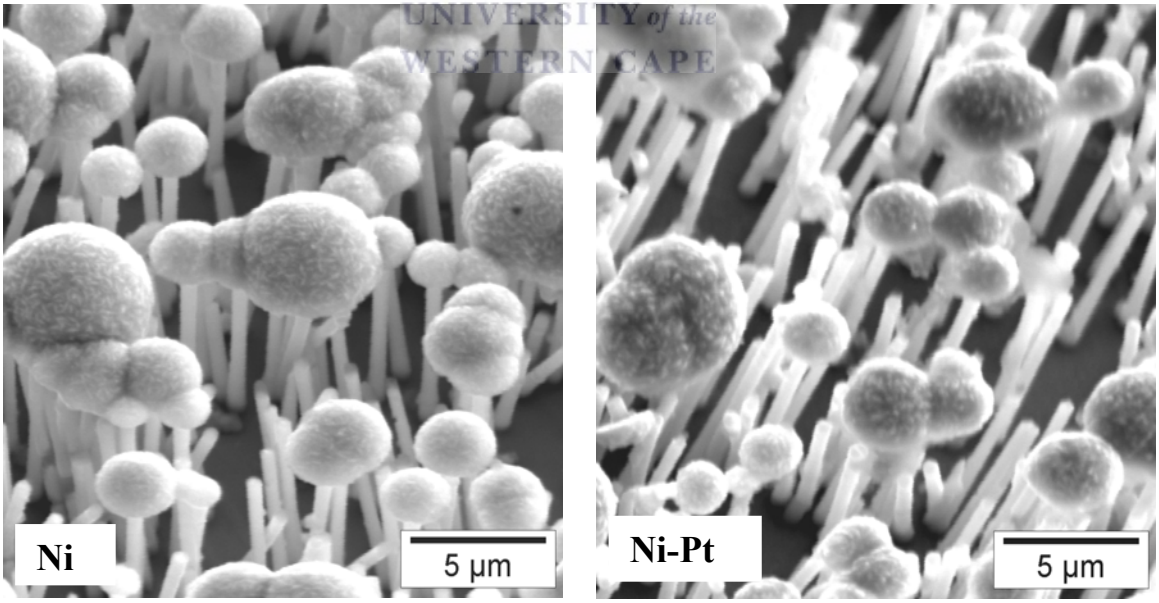

Figure 3.20: *SEM micrographs of the nickel microstructure after the dissolution of the template membrane. The structures were modified with platinum in a chloroplatinic acid solution to activate the surface area.*

Energy dispersive spectrometry (EDS) was further used in order to determine the chemical composition of the modified structures and to investigate the distribution of the elements on the electrode surface. The atomic percentage of Pt on Ni wires is shown in **Figure 3.21**. EDS data correspond to bulk particles and may differ from the surface values due to segregation. The EDS analysis of the sample resulted in a composition of 71 at.% Pt and 25 at.% Ni.

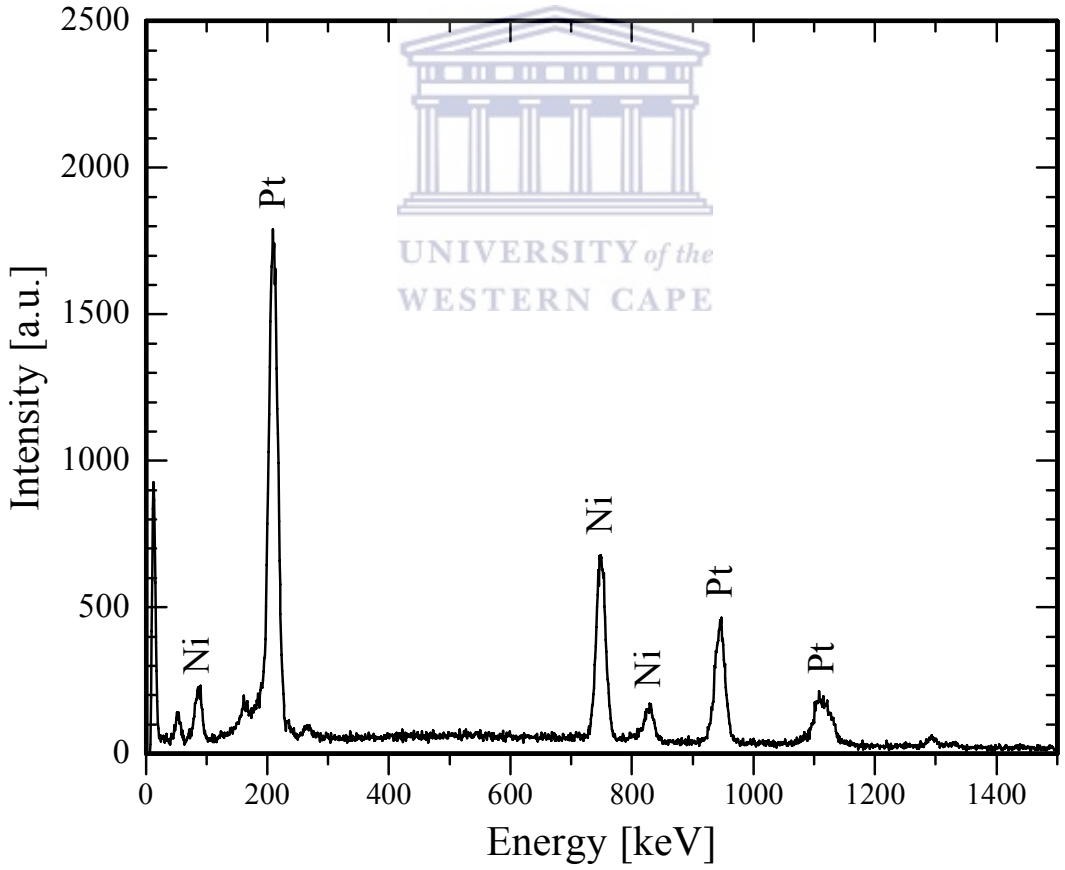

Figure 3.21: *EDS plot of nickel microstructure modified in chloroplatinic acid solution. It is evident that Pt particles exist on the surface.*

Metal nanoparticle-modified electrodes are used increasingly in many electrochemical applications owing to their extraordinary catalytic properties over bulk metal electrodes. CV measurements were performed to characterize the electrocatalytic behaviour of the Pt modified electrodes towards hydrogen reduction in 0.1M KOH. All the measurements were performed at room temperature (25±1°C). The current density was calculated on the basis of the geometric surface area of the platinized Ni microstructured electrodes.

The start of the hydrogen evolution reaction on platinized nickel structures occurs at about -1.1V while on the unmodified structures it occurs at about -1.25V, a shift of 0.15V when compared to each other. Thus, the electroless deposition of Pt nanoparticles onto Ni electrodes was found to enhance their electrocatalytic activity towards the hydrogen reduction reaction in alkaline medium (as shown in **Figure 3.22**). **Figure 3.23** shows the current-potential curves of the hydrogen reaction recorded after modifying the nickel structures with Pt after water electrolysis was started.

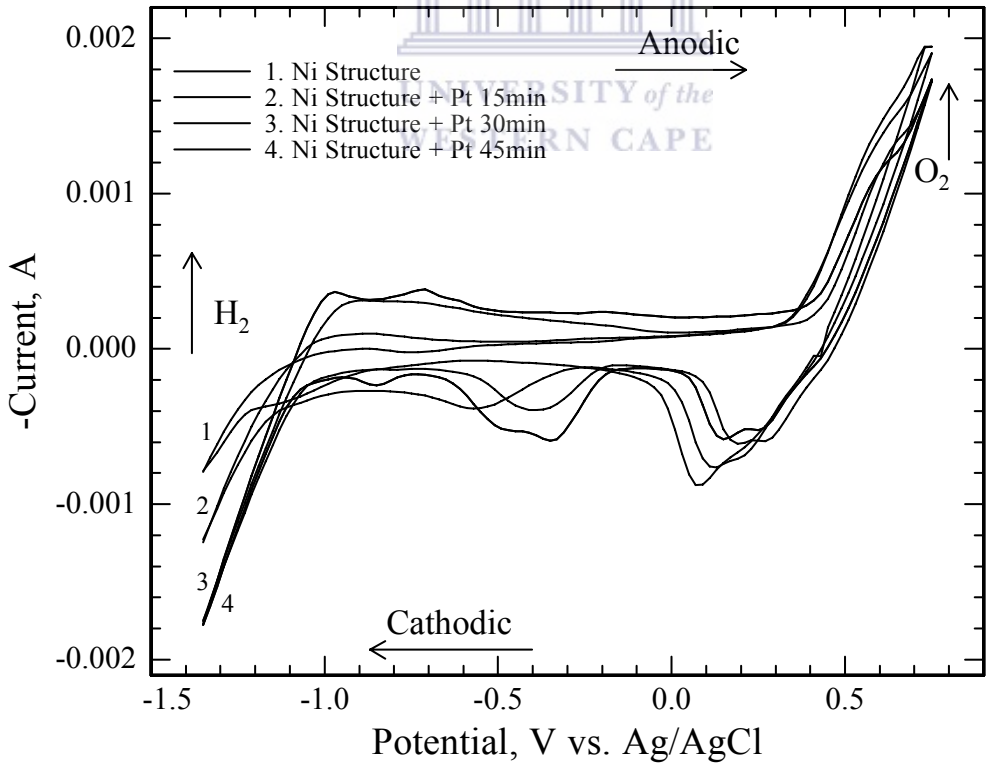

Figure 3.22: *Comparison of the electrochemical behaviour of nickel samples modified in platinum solution (1.2mg/ml in concentration). The modification was done*

for times varying between 0 and 45 minutes. 0.1M KOH solution was used as electrolyte at a sweep rate of 50mV/s.

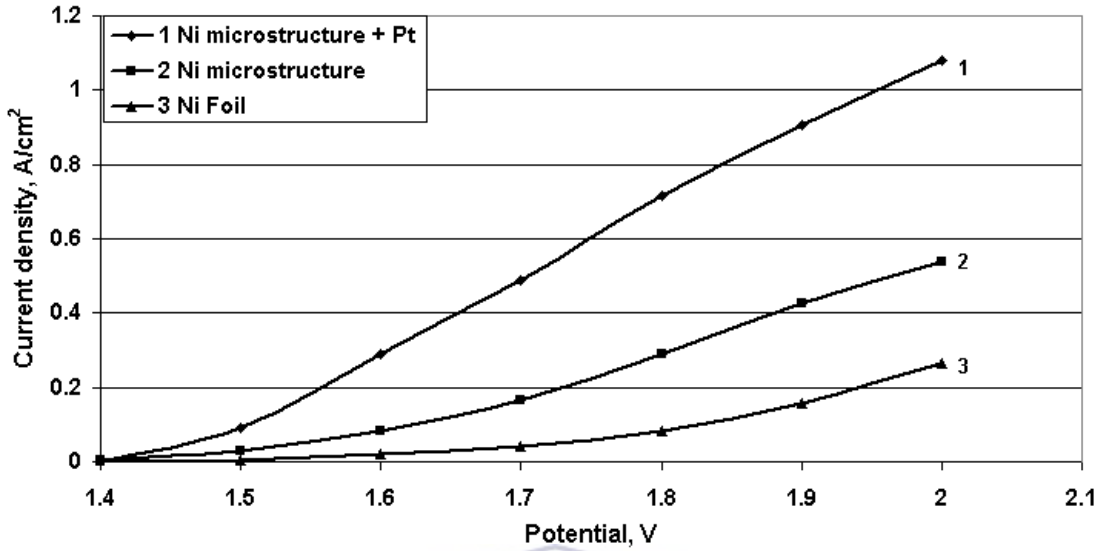

Figure 3.23: *Current-potential curves of the hydrogen evolution reaction of nickel structures after modifying with platinum.*

3.7.2 The influence of Pd deposits on Ni microwires and on the hydrogen evolution reaction

In the present study, the preparation of palladium-nickel microstructured electrodes after intermediate chemical or electrochemical reduction is investigated. Palladium, as an important noble metal, is widely recognized in heterogeneous catalysis and electroanalysis [40]. Palladium nanoparticles can be prepared by various deposition methods including chemical reduction of Pd complexes [48], ion exchange, vapour deposition, thermal evaporation in vacuum, and electrochemical deposition. It is well known that the basic properties of impregnated catalysts are strongly affected by the impregnation method, the microstructure, the surface reactivity, and the metal precursor.

The spontaneous deposition of Pd metal particles on nickel structures was carried out by immersing the structures into a solution containing $PdCl_2$. Electroless deposition was done between 0 and 60 minutes. After deposition, the Ni sample was rinsed thoroughly with de-ionized water before surface characterization. The as deposited Pd/Ni samples were subjected to SEM analysis and then made into electrodes for electrochemical investigation. SEM images showed the formation of Pd morphologies (see **Figure 3.24**).

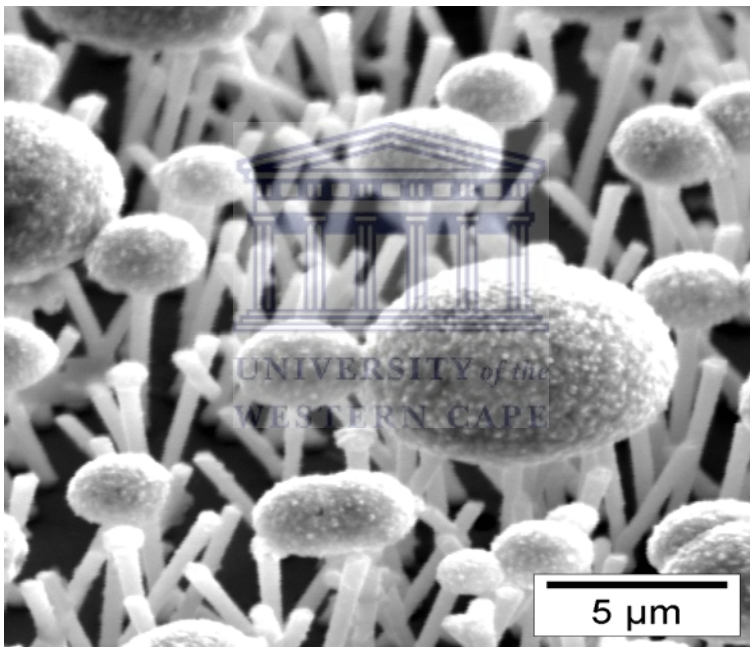

Figure 3.24: *SEM micrograph of palladium modified nickel wires.*

Figure 3.25 shows the effect of Pd-plating on the HER for Ni microstructured electrodes in 0.1M KOH electrolyte at 25°C. The electrode was insulated, except for the front Pd/Ni surface. In addition, Ni disk electrodes polished down to a smooth mirror finish were also subjected to electrochemical investigations. Their catalytic activity and selectivity is based upon the ion-metal interaction at the Ni/Pd interface. The resulting change in morphology and electron structure is responsible for the catalytic activity of the modified structures. The electrocatalytic activity for such

modified electrodes was found to be similar to or a little greater than that of Ni structures.

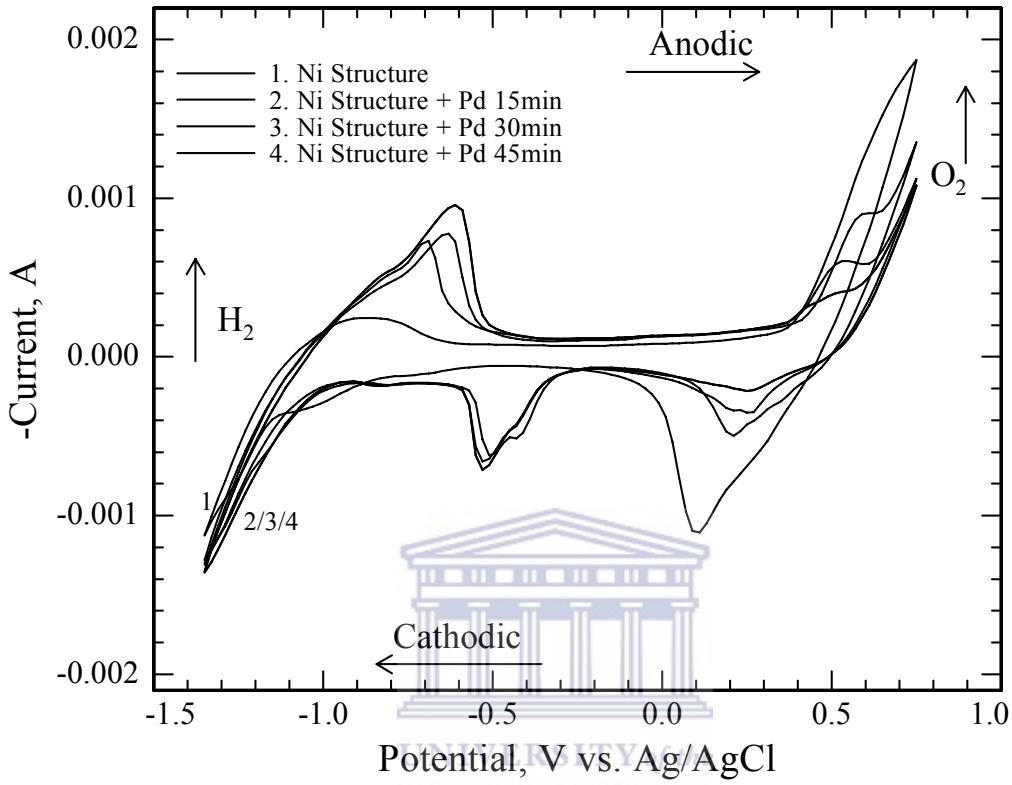

Figure 3.25: *Effect of Pd-plating on the cyclic voltammetry of Ni microstructured electrodes in 0.1M KOH electrolyte at 25°C.*

The curve in **Figure 3.25** showed that hydrogen evolution onset occurred at about -1.1V. The anodic scan showed an increasing current until the switching potential -0.6V, indicating formation of palladium oxide (PdO_x) species on the nickel wires. The cathodic peak observed at -0.5V was due to the reduction of PdO_x. The first indication of a change in the CV was the slight increase on the H_2-evolution current of the Pd-modified electrodes. In the anodic scan (-1.3V to +0.7), there was an increasing anodic current beginning at -0.4V that peaked around +0.5V and eventually decreased until the cathodic vertex potential was reached. In the reverse cathodic scans, the PdO_x reduction peak became smaller and was followed by an oxidation peak with a maximum at -0.7V. The measured Pd electro-active areas were

used to report the current densities of Pd/Ni electrodes. However, a slight increase in catalytic activity was observed on Pd/Ni in comparison with unmodified Ni structures.

3.7.3 Influence of Pt-Pd deposits on Ni microwires and on the hydrogen evolution reaction

Co-deposition of Pd and Pt ions from suitable combinations of H_2Cl_6Pt and $PdCl_2$ solutions on nickel structures, produce Pt-Pd electrodes with catalytic properties for hydrogen production. **Figure 3.26** shows a SEM micrograph of a Pd-Pt coated nickel structures.

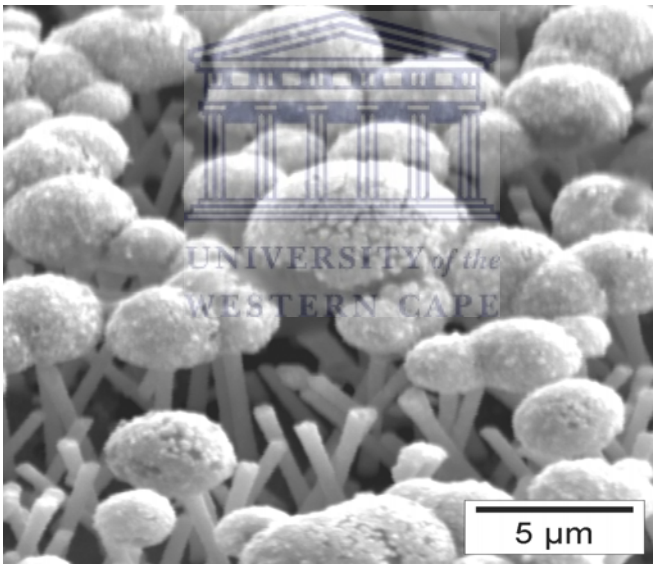

Figure 3.26: *SEM micrographs of a palladium-platinum coated nickel structure*.

The micrograph shows that Pd-Pt was uniformly deposited on the nickel structures. When a well-developed outermost Pd and Pt interface layer is formed above the Ni structures, it becomes more activated. The resulting improved performance appears to be largely due to the increase in real surface area.

In **Figure 3.27** shows voltammograms of nickel microstructures after modified with palladium and platinum particles. CV is particularly useful in some respect, and although it provides no structural data, it yields a measure (in terms of peak potential values) of the energy of the surface active states and clearly demonstrates the existence of several active surface states responses for the same metal.

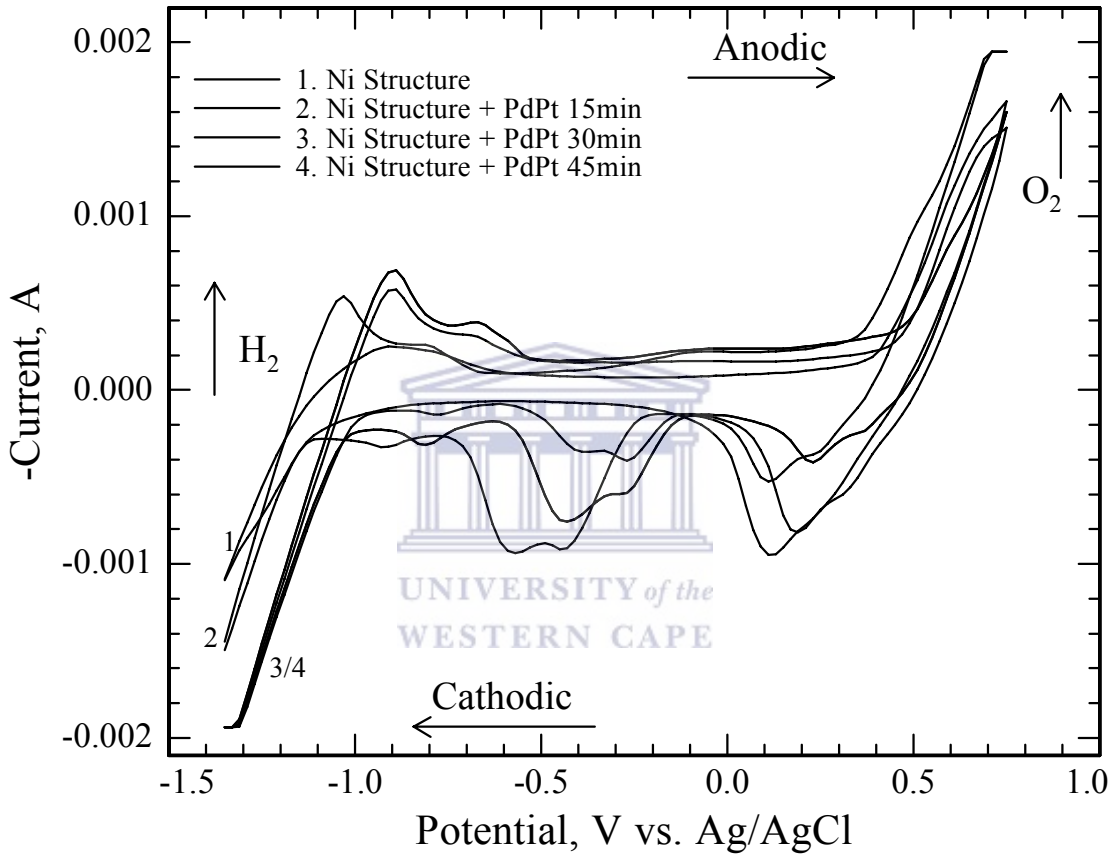

Figure 3.27: *Cyclic voltammograms obtained with nickel structures modified with palladium and platinum particles. Sweep rate 50mV/s.*

The above procedure (i.e $H_2Cl_6Pt/PdCl_2$ solution) can be employed as a method of dispersing Pt and Pd nanoparticles on Ni structures. It was shown early on that noble metals, platinum and palladium in particular, are the most active for promoting oxidation reactions, so a large effort has been focused on studying catalysts based on those elements. The cathodic peak attributed to $NiOOH/Ni(OH)_2$ was found to gradually decrease with increasing electroless deposition time.

The nickel structures were found to have highly electrocatalytic activities for hydrogen evolution, almost comparable to Pt electrodes. Electrocatalytic surfaces consisting of nanometer-sized metal particles of noble metals such as Pt and Pd embedded onto nickel structures have been shown to exhibit excellent catalytic properties. **Figure 3.28** shows cyclic voltammograms obtained from nickel structures modified with palladium, platinum and palladium-platinum particles.

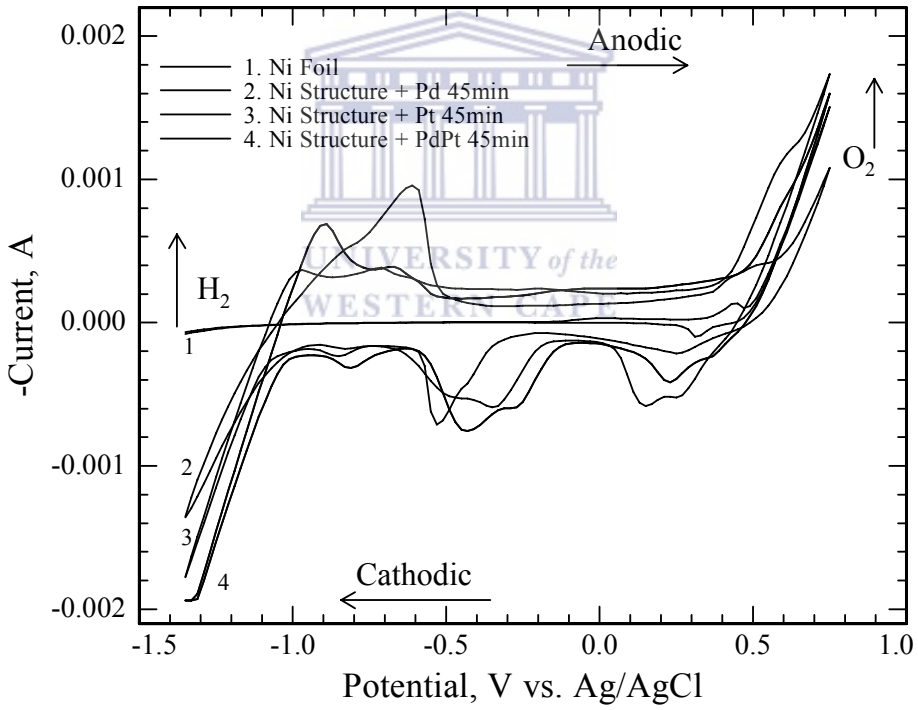

Figure 3.28: *Comparison of cyclic voltammograms obtained from nickel structures modified with platinum, palladium and palladium-platinum particles. Scan rate was 50mV/s.*

The main aim of electrochemical methods of hydrogen production is to reduce the overpotential of HER. For this purpose one is searching for new electrode materials, which lower the energetic barrier accompanying HER. During the last few decades a great step forward has been made in this field.

The chronoamperometric analyses for the hydrogen evolution reaction were conducted by the application of a series of potential steps of 100 mV amplitude for a duration of 10s between -1.4 and -2.0V in an electrochemical cell. An alkaline (40% KOH) solution at 70°C was used as an electrolyte with platinum mesh as counter electrode.

All presented results were obtained with electrodes freshly modified with platinum and palladium solutions. For electrochemical characterization, *V-i* curves were recorded (as shown in **Figure 3.29**).

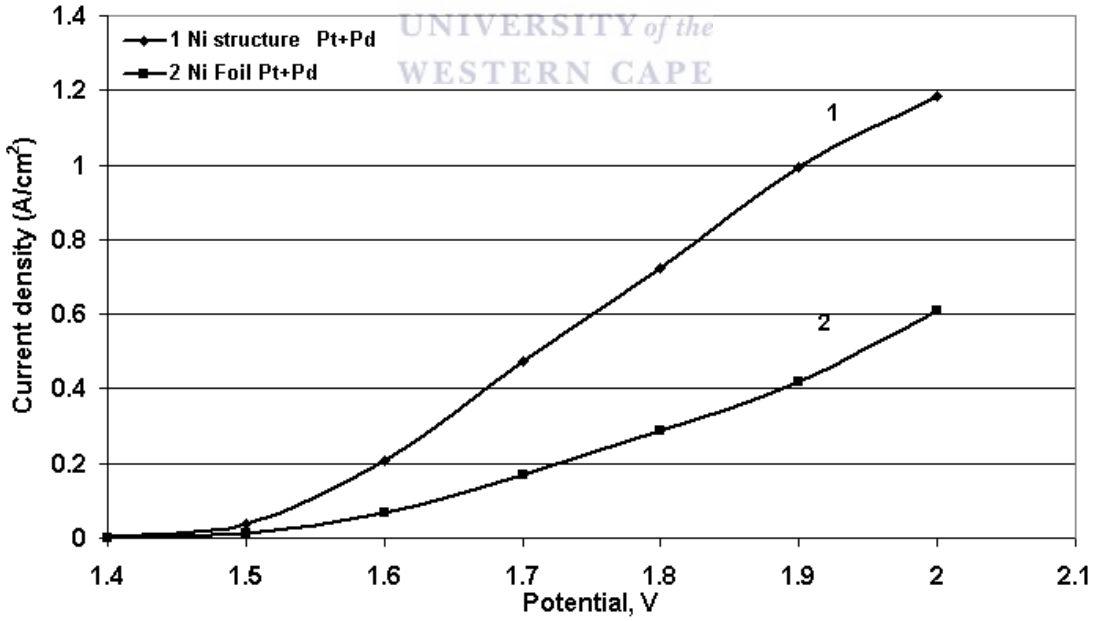

Figure 3.29: *Activity for hydrogen production for secondary structures and nickel foils after activation by Pt and Pd for 1hr each.*

Nickel microstructures modified with Pt and Pd for 1 hour each showed high activity for hydrogen production compared to Ni foil activated under the same conditions.

The current obtained with structures modified with Pt + Pd particles is much larger than in the non-modified case (as shown in **Figure 3.29**). Enhancement of cathodic activity of nickel for electrolytic hydrogen evolution has been demonstrated by the formation of Pd and Pt particles on the surface of nickel micro- and nanostructures. Thus, the catalytic activity for hydrogen evolution can be enhanced by modifying the nickel structures with platinum and palladium.

An overview of the cathode performance due to optimization and fine-tuning of individual parameters during the course of the investigation is given in **Table 3.5**. This table shows that the modified nano- and microstructured nickel is significantly more active than the Ni bulk material or Pt foil. The highest current density was obtained for microstructured nickel that was modified with Pd and Pt; with current density 475mA/cm^2 at 1.7V and 70°C.

Table 3.5: *Summary of current densities of nickel materials 'before' and 'after' activation with platinum and/or palladium at 25°C.*

Material	**Temperature °C**	**Activated with**	**Current density [A/cm^2]**	
			(at 2.0 V)	*(at 1.7 V)*
Nickel Foil	25	-	0.125	0.006
Platinum Foil	25	-	0.191	0.032
Ni –microstructure 0.4µm	25	-	0.299	0.022
Ni-nanostructure Asymmetrical	25	-	0.311	0.056
Ni –microstructure 0.4µm	25	Pt	0.44	0.038
Ni-nanostructure Asymmetrical	25	Pt	0.593	0.204
Ni –microstructure 0.4µm	25	Pd	0.299	0.022
Ni-nanostructure Asymmetrical	25	Pd	0.311	0.056
Ni –microstructure 0.4µm	25	Pt + Pd	0.739	0.242
Ni-nanostructure Asymmetrical	25	Pt + Pd	0.835	0.276
Ni –microstructure 0.4µm	70	Pt + Pd	1.2	0.475
Ni-nanostructure Asymmetrical	70	Pt + Pd	-	-

3.8 Conclusions

From the fabricated nickel structures and the study of its properties, the following general conclusions can be made:

1. Crystalline nickel micro- and nanowires were produced by electroless and electrochemical deposition in etched ion-track membranes. Their structure and morphology was characterized by Scanning Electron Microscopy and X-ray Diffraction. Electrochemical techniques were used to test the structures for electrocatalytic activity.

2. The purpose of this research was to solve a whole range of scientific and technological challenges. By ion track technology, a new type of template matrix with unique structure was fabricated. Nano- and microstructured nickel materials with sizes between 0.015 and 1μm were synthesized using different track-etched templates.

3. It was found that of all the three nickel plating electrolytes used (i.e. *Hard*, *Mirror* and *Watt*) *Hard* nickel plating bath was an optimal solution for preparation of mechanically strong and catalytically active structures. This behaviour was observed when using a 0.4μm pore diameter template and 23μm length. The microwires were found to be smooth and uniform along their length and they also exhibited faster growth.

4. Despite the obvious uniqueness of the catalytic properties of nickel nano- and microstructured materials, no evidence in the literature that the phenomenon has ever been understood and described before was seen. A significant improvement was gained in electrochemical activity for hydrogen generation by the use of enhanced surface area nickel electrodes with nanosized structures compared to smooth Ni foil electrodes. Stability was related to surface nanostructure, and the most active samples were also the most stable during

successive cycling in an electrolyte environment.

5. The experimental results showed that cyclic voltammetry is a suitable method to analyze the effect of Ni structure and the chemical composition of the cathode material on electrocatalytic activity. It was also established that materials obtained using nanosized templates had electrocatalytic activity ten times higher than bulk nickel materials. The increase in activity is proportional to an increased growth of material surface.

6. The surface activation method of nano- and microstructured nickel by nanoparticles of platinum and palladium with the purpose of further increasing the catalytic activity was developed. It was found that the Pt and Pt-Pd modified nickel structures are very suitable catalytic materials for several chemical and electrochemical reactions. The strong catalytic activity of these systems is due to the high dispersion of Pt and Pt-Pd on the nickel structures despite the minute quantities of the metal. The Pd-electroless plating on the structures had no significant effect on the current-potential relationship. Metal particle-modified electrodes can be used in many electrochemical applications owing to their extraordinary catalytic properties over bulk metal electrodes. Palladium and platinum films deposited by the electroless method onto Ni microstructures showed sharp peaks in the hydrogen region. The value recorded at room temperature (+/-25°C) under an applied potential of 1.7V in 40 wt.% KOH (i=475mA/cm^2) is amongs the highest so far reported in the literature.

7. The results obtained during this research can be used not only in electrochemistry but in a wide range of research fields. From an evaluation of the results, further research is needed to better understand the electrochemical behaviour.

3.9 References

[1] Mikael Lindeberg, *High aspect ratio microsystem fabrication by ion track lithography*, Ph. D. Dissertation (**2003**).

[2] I.Z. Rahman, K.M. Razeeb, Md. Kamruzzaman, Marina Serantoni, *Journal of Materials Processing Technology* 153-154, (**2004**) 811.

[3] G.B. Khomutov, V.V. Kislov, M.N. Antipina, R.V. Gainutdinov, S.P. Gubin, A.Yu. Obydenov , S.A. Pavlov , A.A. Rakhnyanskaya , A.N. Sergeev-Cherenkov, E.S. Soldatov, D.B. Suyatin , A.L. Tolstikhina , A.S. Trifonov and T.V. Yurova, *Microelectronic Engineering* 69, (**2003**) 373.

[4] C. Schoenenberger, B.M.I. van der Zande, L.G.J. Fokkink, M. Henny, C. Schmid, M. Krueger, A. Bachtold, A. Huber, H. Birk and U. Staufer, *Journal of Physical Chemistry* B101, (**1997**) 5497.

[5] E. Ferain and R. Legras, *Nuclear Instruments and Methods in Physics Research* B174, (**2001**) 116.

[6] M.F. Kibria and M.SH. Mridha, *International Journal of Hydrogen Energy* 21, (**1996**) 179.

[7] Dragica Lj. Stojic, Bozidar D. Cekic, Aleksandar D. Maksic, Milica P. Marceta Kaninski and Scepan S. Miljanic, *International Journal of Hydrogen Energy* 30, (**2005**) 21.

[8] A.C.D. Angelo, E.R. Gonzalez and L.A. Avaca, *International Journal of Hydrogen Energy* 16, (**1991**) 1.

[9] I. Arulraj and D.C. Tribedi, *International Journal of Hydrogen Energy* 14, (**1989**) 893.

[10] D.D. MacDonald, B.G. Pound and S.J. Lenhart, *Journal of Power Sources* 29, (**1990**) 477.

[11] J.L. Weininger, in R.G. Gunther and S. Gross (**eds**.), *Journal of the Electrochemical Society*, 82-84 (**1982**) 1.

[12] Chi-Chang Hu and Yau-Ruen Wu, *Materials Chemistry and Physics* 82, (**2003**) 588.

[13] C.-C. Hu, C.-Y. Lin and T.-C. Wen, *Materials Chemistry and Physics* 44, (**1996**) 233.

[14] Y.-S. Lee, C.-C. Hu and T.-C. Wen, *Journal of the Electrochemical Society* 143, (**1996**) 1218.

[15] T.-C. Wen, C.-C. Hu and Y.-J. Li, *Journal of the Electrochemical Society* 140, (**1993**) 2554.

[16] H. Cheng, K. Scott and C. Ramshaw, *Journal of the Electrochemical Society* 149(11), (**2002**) D172.

[17] L. Petrik, B. Bladergroen, S. Botha, V.M. Linkov and G. Gericke, *Nanostructured catalysts and membrane reactors for electrosynthesis*, Eskom Project Report, **2002**.

[18] Lyubov I. Kravets, Serguei N. Dmitriev, Vladimir V. Sleptsov and Vera M. Elinson, *Desalination* 144, (**2002**) 27.

[19] P. Apel, Y.E. Korchev, Z. Siwy, R. Spohr, M. Yoshida, *Nuclear Instruments and Methods in Physics Research* B184, (**2001**) 337.

[20] Xianyou Wang, Jie Yan, Huatang Yuan, Zhen Zhou, Deying Song, Yunshi Zhang and Ligu Zhu, *Journal of Power Sources* 72, (**1998**) 221.

[21] I.-W. Lyo and P. Avouris, *Science* 253, (**1991**) 173.

[22] C.J.A. Monty, *High Temperature Chemistry Processes* 3, (**1994**) 467.

[23] Ian J. Brown and Sotiris Sotiropoulos, *Electrochimica Acta* 46, (**2001**) 2711.

[24] S.A.S. Machado and L.A. Avaca, *Electrochimica Acta* 39 (10), (**1994**) 1385.

[25] V. Ganesh, V. Lakshminarayanan, *Electrochimica Acta* 49, (**2004**) 3561.

[26] C. Hammond, *The Basics of Crystallography and Diffraction*, Oxford University Press, Oxford, **1997**.

[27] M.J. Giz, S.C. Bento and E.R. Gonzalez, *International Journal of Hydrogen Energy* 25, (**2000**) 621.

[28] S. Trasatti, *Electrochimica Acta* 36, (**1991**) 225.

[29] M.J. De Giz, G. Tremiliosi-Filho and E.R. Gonzalez, *Electrochimica Acta* 39, (**1994**) 1775.

[30] Birgul Yazici, *Turkish Journal of Chemistry* 23, (**1999**) 301.

[31] D.J. Walton, L.D. Burke and M.M. Murphy, *Electrochimica Acta* 41, (**1996**) 2747.

[32] R.M.Q. Mello and E.A. Ticianelli, *Electrochimica Acta* 42, (**1997**) 1031.

[33] E.E. Farndon and D. Pletcher, *Electrochimica Acta* 42, (**1997**) 1281.

[34] J.H. Ye and P.S. Fedkiw, *Electrochimica Acta* 41, (**1996**) 221.

[35] N.V. Korovin, *Electrochimica Acta* 39, (**1994**) 1503.

[36] H. Wendy, *Electrochimica Acta* 39, (**1994**) 1749.

[37] G. Lindbergh, *Electrochimica Acta* 42, (**1997**) 1239.

[38] F.C. Crnkovic, S.A.S. Machado and L.A. Avaca, *International Journal of Hydrogen Energy* 29, (**2004**) 249.

[39] Ning Chi, Kwong-Yu Chan and David Lee Phillips, *Catalysis Letters* 71(1-2), (**2001**) 21.

[40] Dao-Jun Guo and Hu-Lin Li, *Journal of Colloid and Interface Science* 286, (**2005**) 274.

4 OVERALL CONCLUSIONS AND FUTURE RESEARCH DIRECTIONS

In the previous chapter the research results were discussed. In the final chapter of this thesis, the discussion focuses on the main conclusions, recommendations and proposals for future research.

Micro- and nanomaterials consist of an emerging subdiscipline of chemical and material science that deals with the development of methods for synthesizing nanoscopic particles of a desired material and with specific characterization of the properties of the obtained nanomaterial. Nanomaterials have a wide range of possible commercial and technological applications, including uses in chemistry, physics, electronics, optics, materials and biomedical sciences.

The template method is a simple and powerful process for the synthesis of micro and nanomaterials. Polymer membranes with cylindrical pores were created by bombardment with heavy-ion beams followed by chemical etching. Stacks of PET foils, of thickness 10 – 30μm, were irradiated with swift heavy ions. Fluences between 10^6 and 10^9 ions/cm^2 were used. The energetic ion beams have established themselves as an indispensable tool for the production of track-etched membranes. The technology can be applied directly to most polymers and, via the replication technique, to a wide variety of materials, including metals. Production of track-etch membranes stands out among other applications of swift heavy ions. In a chemical etching process, the latent tracks of the ions were enlarged, in an aqueous alkaline solution, to pores with diameters between 50 and 400nm. Pores larger that 100nm exhibited cylindrical geometry. In order to produce cylindrical wires with diameters as small as several nanometers, like asymmetric membrane, thinner membranes have to be employed and eventually sensitization of the ion tracks by exposure to UV-light was performed before etching.

It was demonstrated that metallic microstructures can be prepared using electrochemical deposition. Electrodeposition method is capable of producing high-

quality micro- and nanowires with desirable features, including wires with reproducible size. Usually there are many variable parameters that can be used to tune the properties of nanowires, such as material, crystallinity, structure etc. Galvanostatic and potentiostatic deposition of nickel in pores with large, several hundred nanometers, and small, several ten nanometers, diameter pores have been investigated using a two-electrode electrochemical cell. Results of systematic study aimed at determination of the optimal deposition parametes, overvoltage, temperature and electrolyte solution, required for uniform and stable nickel structures growth were presented.

In this study the feasibility of using nickel wires prepared by electroless and electrochemical deposition as cathode for the hydrogen evolution reaction in alkaline water solutions was studied. Electrocalytic process on nickel electrodes, as surveyed using electrochemical techniques, almost invariable commence and terminate at reasonable well-defined potentials within the region. The resulting materials showed high current density values for the HER in concentrated basic solutions and it was shown that its performance could be further improved by increasing the surface area or modification. It was shown that increasing the temperature increases the current density at the exit face of the electrodes. The Ni structures studied possessed very good stability to potential cycling conditions. The structural composition and surface morphology was investigated using X-ray diffraction (XRD) and scanning electron microscopy (SEM), respectively. The XRD analysis revealed that all Ni structures were crystalline.

It was established that the structure of the template significantly influences the crystallinity of obtained materials. The crystalline state of the structures showed a definite influence on the catalytic activity in the electrochemical reduction test reactions. The sequence of the Ni crystalline planes with respect to decreasing intensity is Ni(111) > Ni(311) > Ni(200) while the nickel foil was Ni(200) > Ni(220) > Ni(111). The high activity for hydrogen evolution on these deposits is not only due to their catalytic activity but also attributed to their relatively high surface area.

Co-deposition of Pt and Pd ions from suitable combinations of H_2Cl_6Pt and $PdCl_2$ solutions on nickel microstructures, produce Pt-Pd electrodes with catalytic

properties for hydrogen production. It was found that the Pt and Pd + Pt modified nickel structures are very suitable catalytic materials for several chemical and electrochemical reaction. The strong catalytic activity of these systems is due to the high dispersion of Pt and Pd-Pt on the nickel structures despite the minute quantities of the metal. The Pd-electroless plating on the structures had no significant effect on the current-potential relationship. Hydrogen evolution reaction from Pt and Pd-Pt alloy modified nickel structures showed that the electrocatalytic activity of these electrodes was significantly improved. This suggests that Ni microwires modified with Pd-Pt alloy can be used in place of the Pt electrode in alkaline water electrolysis since it has similar characteristics to the platinum electrode.

The enhanced HER electrocatalytic activity observed on these electrodes was attributed to their chemical composition. Metal particle-modified electrodes can be used in many electrochemical applications owing to their extraordinary catalytic properties over bulk metal electrodes. Energy dispersive spectrometry was further used in order to determine the chemical composition of the modified structure and to investigate the distribution of the elements on the electrode surface. The spectra showed the characteristic peaks for Ni and Pt elements.

In a novel process, the nickel nanostructures were prepared from asymmetric polymers, a low cost track-etch membrane. From the chronoamperometric studies, current-voltage characteristics and measurements of the H_2 evolution voltage, it is obvious that electrodes with asymmetrical structures yielded high current densties.

Future research directions

Based on the analysis and conclusions of this study, a number of suggestions regarding priorities for future research directions and areas of investigation are made:

1. The template method is proving to be a powerful approach for preparing nanomaterials. From a fundamental point of view, our interest is to produce nanostrucutures with even smaller diameter in order to explore more

thoroughly the effects of size on the properties of materials. In addition to that, we want to use the template approach to prepare composite nanomaterials and also develope new ways to do template synthesis, so that tubules and fibrils composed of other types of materials can be prepared.

2. Our intention is also to push the track-etching technology further, mainly to produce templates which are more resistant to chemicals and useable under high temperature conditions, and also to extend the possibilities offered by the patterning process. We also intend to extend the existing laboratory-scale technology and fabricate more free standing or supported track-etch templates.

3. Several intermetallic combinations of transition metals wires, like Hf_2Fe, Zr-Pt, Nb-Pd(I), Pd-Ta, Nb-Pd(II) and Ti-Pt, will be used as cathode materials in the electrolytic evolution of hydrogen from alkaline aqueous solutions. We also intended to develop new types of composite consolidated nanomaterials using Ni-Co, Ni-Ti, Ni-Cu alloys as base materials and to investigate the influence of dopants on changes of electrochemical properties of nickel nanomaterials.